

The Pennsylvania State University
The Graduate School

**EVALUATION OF QUANTUM CORRELATIONS FOR USE IN
QUANTUM RADAR AND QUANTUM COMMUNICATION SYSTEMS**

A Dissertation in
Electrical Engineering
by
Rory Howell

© 2023 Rory Howell

Submitted in Partial Fulfillment
of the Requirements
for the Degree of

Doctor of Philosophy

August 2023

The dissertation of Rory Bowell was reviewed and approved by the following:

Ram Narayanan
Professor of Electrical Engineering
Dissertation Advisor
Chair of Committee

Matthew Brandsema
Assistant Research Professor
Special Member

Sahin Ozdemir
Professor of Engineering Science and Mechanics

Timothy Kane
Professor of Electrical Engineering

Xingjie Ni
Professor of Electrical Engineering

Stephen Howell
Chief Scientist, Naval Surface Warfare Center - Crane Division
Special Member

Jonathan Dilger
Command Chief Scientist, Naval Surface Warfare Center - Crane Division
Special Member

Madhavan Swaminathan
Professor of Electrical Engineering
Department Head of Electrical Engineering

Abstract

Classical technologies have been used for decades in the radar and communication applications. While it is understood that classical radar and communication are functional, we are approaching the limits to which they can be improved. As technology improvements bring us close to these limits, it is necessary to utilize new approaches to stop counter technologies from deeming it irrelevant. One of the solutions that has been proposed to this problem is to use quantum correlations to improve the performance of classical systems. Unlike classical systems, quantum systems have the ability to correlate at the photon level due to the ability to generate two photons at the same time. This ability to correlate waveforms at a photon level has been shown to have many dB of improvement in the low signal-to-noise ratio regime over classical sensing systems.

This dissertation will analyze two types of quantum radar systems, bipartite and tripartite. It will also explore the various correlation coefficients for different types of quantum radar measurement schemes. For the bipartite system it will explore methods such as: (i) immediate detection of the idler photon events to be used in post-processing correlation with the signal photon events, (ii) immediate detection of the idler electric field to be used in post-processing correlation with the signal electric field, (iii) immediate detection of the idler quadratures to be used in post-processing correlation with the signal quadratures. The thesis will also attempt to solve a tripartite correlation where two lasers are used to create two signal photons and an idler photon. This system will be explored with basic electric field measurements and a derivation of the photon counting measurement. The showcased results compare the performance of these different methodologies for various environmental scenarios. This work is important at developing the fundamentals behind quantum technologies that require covariance measurements and will permit more accurate selection of the appropriate measurement styles for individual systems

Table of Contents

List of Figures	vi
List of Symbols	vii
Acknowledgments	ix
Chapter 1	
Introduction	1
1.1 A Need for Quantum Radar	3
1.2 A Need to Explore Alternate Quantum States	4
1.3 A Need for a Measurement System Comparison	4
1.4 The Difficulties of Quantum Radar	5
1.4.1 Detection Theory and Counting Statistics for Optical Systems . .	6
1.4.2 Jitter, Dark Count, Spatial Coherence, and Signal-Dependent Noise	7
1.5 Outline	8
Chapter 2	
Derivation of Bipartite Correlations	9
2.1 Introduction	9
2.2 Electric Field Covariance	10
2.3 Number Operator Covariance	16
2.4 Electric Field Quadrature Covariance	18
2.5 Analysis	19
2.6 Conclusion	22
Chapter 3	
Analysis of Tripartite Electric Field Correlation	24
3.1 Introduction	24
3.2 Tripartite Derivation	26
3.2.1 Wave function derivation in terms of mean photon number per mode	26
3.2.2 Covariance Matrix	28
3.3 Analysis	37
3.4 Conclusion	38

Chapter 4	
Derivation of the Tripartite Number Operator Correlation	40
4.1 Introduction	40
4.2 Derivation	40
4.3 Conclusion	57
Chapter 5	
Conclusions and Future Work	58
5.1 Future Work	59
Appendix A	
Evaluating the Fock State Basis of the Tripartite State	60
A.1 Electric Field Operator	60
A.2 Number Operator	75
Appendix B	
MATLAB Code	90
B.1 Tripartite Electric Field Operator Simulation	90
B.2 Tripartite Number Operator Simulation	93
B.3 Detector Function Simulation	95
Bibliography	97

List of Figures

1.1	The purpose of this image is to show that a beam splitter imparts a random 50:50 chance for each photon passing through it to pass into 1 of the 2 arms. This causes some of the photons go one direction, and some of them go another, which causes the two waveforms to be different at the single photon level. An SPDC source creates two truly identical streams.	2
2.1	The general experimental setup for the measurement schemes discussed. In all cases, the idler photon is measured immediately and correlated with the returning signal photon at a later point in time. The detectors can vary between single photon counters and electric field sensors.	10
2.2	Correlation coefficient of the various methods for Scenario 1. ($\kappa=.7, N_B=10$)	21
2.3	Correlation coefficient of the various methods for Scenario 2. ($\kappa=.1, N_B=10$)	22
2.4	Correlation coefficient for low N_s for scenario 1	23
3.1	Basic setup for tripartite system with both signals staying together and the idler being immediately detected. This setup is valid for both the electric field measurement and the photon counting measurement.	25
3.2	Correlations of the three path combinations in terms of r_1 and $r_2, N_B = 10$.	37
3.3	Correlations for for the tripartite system using the detector function at various transmissivities, $N_B = 10$	38
3.4	Correlations for the tripartite system when $r_1 = r_2$ versus the bipartite system, $N_B=10$	39

List of Symbols

N_s	The mean photon number per mode of the signal
N_B	The mean photon number per mode of the background noise
N_T	The mean photon number per mode of the thermal noise
I	Intensity of a laser
A	Cross-sectional area of a laser
\hbar	Planck's constant divided by 2π
ω	Angular frequency of the laser
N	Average number of counts for a detector
Φ	Photon flux
η	Quantum efficiency of a detector
T	Time
\mathcal{R}	Average count rate of a detector
P	Laser power
L	Length
c	Speed of light
\bar{n}	Average amount of photons in a section of light
$\mathcal{P}(n)$	Probability of obtaining n photons
\hat{a}	Annihilation operator
\hat{a}^\dagger	Creation operator
\mathbf{k}	Wave vector

χ	Phase
$\hat{\epsilon}_k$	Unit polarization vector
ν_k	Frequency of mode \mathbf{k}
V	Quantization Volume
Ψ	Wavefunction
ρ	Density Matrix
\hat{O}	General operator
\hat{E}	Electric Field Operator
\hat{N}	Number Operator
r_{xy}	Correlation Coefficient
κ	Transmissivity
r	Squeezing factor
r_1	Squeezing factor of laser 1
r_2	Squeezing factor of laser 2
cov	Covariance

Acknowledgments

I would first like to thank my thesis advisor, Professor Ram Narayanan, for his patience and his invaluable advice throughout my studies. I would also like to extend special thanks to Dr. Matthew Brandsema for his willingness to share his knowledge and experiences with me. The tutelage of you two has allowed me to have great success and without your support I would have nowhere near the abilities I have today. I now would like to thank my core committee members, Professors Sahin Ozdemir, Timothy Kane, and Xingjie Ni for reviewing my dissertation and giving me observations that greatly improved my work. I would also like to extend thanks to the two final members of my committee Dr. Stephen Howell and Dr. Jonathan Dilger of NSWC Crane, the external work I completed in Indiana has given me additional experience that I would not have been able to obtain otherwise.

This material is based upon work supported by the Naval Surface Warfare Center - Crane Division NEEC Grant under Award No. N00174-19-1-0007.

Any opinions, findings, and conclusions or recommendations expressed in this publication are those of the author and do not necessarily reflect the views of the Naval Surface Warfare Center - Crane Division.

I would also like to thank my colleague, Bilal Ahmed, for without him the lab would not have been nearly as enjoyable or successful.

I would finally like to thank my family, my friends, and my former teachers. It took a lot of support and patience to get to here, and without the help of the many Good People in my life, I would not have been able to make it through my academic journey and become the engineer I am today.

Chapter 1 | Introduction

Classical radar systems have been extensively employed since the early 20th century for detection, targeting, and meteorology with the addition of laser radar systems (LIDAR) in the early 1960's. With the unceasing technological upgrades over the past 100 years, new radar technologies have continued to outperform their precursors. However, current technologies are approaching the limit that they can not overcome.

With the search for a way to bypass these limits, new technologies need to be explored. Much like in computing and communication systems, the unique properties of quantum mechanics drew the eye of researchers and led to what is known as quantum radar. Quantum radar uses quantum effects such as spontaneous parametric down conversion (SPDC) to create two low frequency photons from a single high frequency photon. There are a few methods to determine if the signal photon has hit the target. The first is to count the photons received from the idler and the signal paths, this is called quantum illumination. [1] Another method I, and in future work my colleagues, seek to explore is to measure the signal and idler using balanced homodyne detection to determine the IQ data and determine correlations from this data.

Quantum systems have been shown to enhance the performance of both radar and communication by improving the ability to discern weak received signals from the noise or providing a secure propagation channel [2-9]. While there are many useful properties intrinsic to quantum mechanics, the main ability to assist with this performance improvement is through quantum entanglement. [10] This benefit of using down converted photons over a normal LIDAR waveform is that the down converted photons will be discernible due to the waves identical binary waveform. [4,11] With these binary waveforms, a time correlation is able to be done to determine whether what was received by the detector is the sent signal or thermal noise. Figure (1.1) is shown to give a better understanding of how the photon waveforms enhance sensing. One can see that when

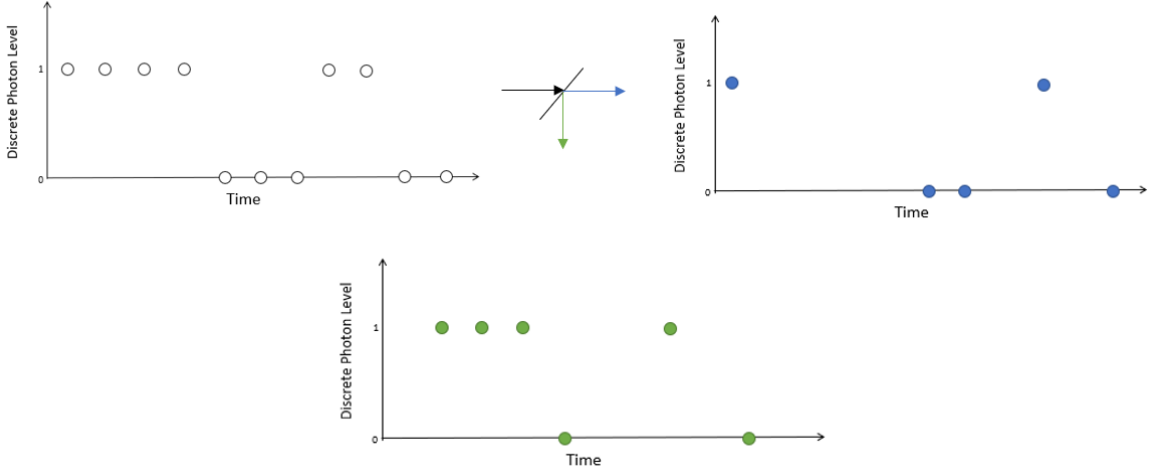


Figure 1.1. The purpose of this image is to show that a beam splitter imparts a random 50:50 chance for each photon passing through it to pass into 1 of the 2 arms. This causes some of the photons go one direction, and some of them go another, which causes the two waveforms to be different at the single photon level. An SPDC source creates two truly identical streams.

using a beamsplitter a random 50:50 chance is imparted on each photon that passes through the beamsplitter. These photons will have an equal chance of going to one of two arms, causing the photon waveform to be random and unequal. This is in comparison to an SPDC source which creates two truly identical photon waveforms.

One detection scheme who's correlation coefficient has been explored is the optical parametric amplifier (OPA) where upon return a non-linear crystal is used to combine the signal and idler with a quantum covariance of $\sqrt{N_s(N_s + 1)}$, where N_s is the mean photon number per mode of the signal. [12] This method is referred to here as an analog method and requires a delay line in the idler branch to allow the signal photon and idler photon to interact in the non-linear medium (OPA) to obtain the correlation. This correlation has been physically realized on the lab bench, but its viability outside a lab environment due to the delay line may be low due to the unknown nature of the length and the ability to generate a delay line long enough to math the signal.

Other detection schemes have been shown to work in the lab environment, but the correlation for these experiments are still unknown. [13] The two-mode squeezing radar creates entangled paths in the microwave regime using a Josephson parametric amplifier and is shown to have a significant gain over a normal two-mode noise radar. After getting passed between two horn antennas, the electric field of the signal is measured and is then correlated with the immediately captured electric field measurement of the idler path. This scheme can also be used in the optical regime through the use of balanced homodyne

detection. Using this detection scheme, one can take many measurements and determine the quadrature measurements of the quantum system. The reason that one must take many measurements is due to the uncertainty principle between the phase of the electric of the photon number where to know the phase of the electric field, the amount of photons that are being measured is unknown. Using these quadrature measurements, the bulk electric field measurement can be calculated by moving from phase space to the metric space, but it would probably be wiser to just use the quadrature measurements.

While many quantum radar systems have been shown to work in the lab, the specific correlation coefficients of many of these methods have not been calculated. Without an understanding of the maximum limit on the correlations, the ability to determine the effectiveness of the lab setups is not possible.

1.1 A Need for Quantum Radar

The need for quantum radar is due to its increased enhancement in the low signal-to-noise ratio regime. Now, one might theorize that using a coherent beam and a beamsplitter that similar results can be obtained. To explore this theory, I will follow the mathematics of Ref. [11]. Where we start with the coherent state written as a displaced vacuum:

$$|\alpha\rangle e^{\alpha\hat{a}_c^\dagger - \alpha^*\hat{a}_c} |0\rangle = \hat{D}(\alpha) |0\rangle \quad (1.1)$$

where we use the beamsplitter relations:

$$\hat{a}_i = \frac{\hat{a}_0 + i\hat{a}_c}{\sqrt{2}}, \hat{a}_c = \frac{i\hat{a}_0 + \hat{a}_c}{\sqrt{2}} \quad (1.2)$$

Which are inverted:

$$\hat{a}_0 = \frac{\hat{a}_i - i\hat{a}_s}{\sqrt{2}}, \hat{a}_c = \frac{-i\hat{a}_i + \hat{a}_s}{\sqrt{2}} \quad (1.3)$$

Substituting these values into the displaced vacuum and simplifying:

$$e^{\beta_2\hat{a}_i^\dagger - \beta_2^*\hat{a}_i} e^{\beta_1\hat{a}_s^\dagger + \beta_1^*\hat{a}_s} e^{2\beta_1^*\hat{a}_s} = \hat{D}_i(\beta_2)\hat{D}(\beta_1) |0, 0\rangle \quad (1.4)$$

where $\beta_1 = \frac{\alpha}{\sqrt{2}}$ and $\beta_2 = \frac{i\alpha}{\sqrt{2}}$. From this we can see that each of the outputs from the beamsplitter are a coherent state with a different displacement.

Now we use this wave function to determine the covariance between the two branches.

$$Cov(\hat{A}, \hat{B}) = \frac{1}{2} \langle \{\hat{A}, \hat{B}\} \rangle - \langle \hat{A} \rangle \langle \hat{B} \rangle \quad (1.5)$$

where $\hat{A} = \hat{a}_i^\dagger \hat{a}_i$ and $\hat{B} = \hat{a}_s^\dagger \hat{a}_s$. From this we can calculate both terms and see that $\frac{1}{2} \langle \{\hat{A}, \hat{B}\} \rangle = \langle \hat{A} \rangle \langle \hat{B} \rangle$ and the covariance is zero.

This shows that to use photon level correlations for radar and communication systems, that the photons for both paths need to be generated at the same time. Without this simultaneous generation, the correlations for the idler and signal path will be zero and it will be impossible to differentiate the signal path in a high noise environment. Due to this we are also able to immediately detect the idler due to doing a waveform comparison that does not require entanglement to be maintained.

1.2 A Need to Explore Alternate Quantum States

Currently, research is focused on bipartite states. These states are typically generated with down conversion where a single photon is split into two, lower energy photons. While these states have been shown to be effective for use in quantum radar, the current technology and materials are not able to generate down converted photons at a high rate. This is problematic because while quantum systems have been shown to work in the best in the low SNR regime, the photon generation is not enough to get discernible returns over long distances in atmosphere. While the analysis given in this paper is only looking at the theoretical limits of the technology, the exploration of shorter term technologies can also be explored in the same way as the bipartite states.

For this I propose a tripartite system that uses ^{85}Rb atomic vapor to create three entangled photons using four wave mixing [14]. With this system, two lasers are used, doubling the initial photons put into the system and also doubling the chance of the nonlinear effect occurring. With this analysis, I hope to determine the viability of npartite systems currently and if they are able to make up the current shortcomings of the bipartite technology.

1.3 A Need for a Measurement System Comparison

In current experiments, there are many ways to determine the correlation between the signal and idler beams. These ways include photon counting, quadrature measurements,

optical parametric amplifiers, and electric field measurements [2, 7, 8, 15]. While all of these have shown an improvement over the classical system, which of these technologies is the best has not been determined. Currently there only exists a calculation on the optical parametric amplifier method, which requires the use of a delay line limiting its ability for long range sensing [12].

The lack of a known comparison between the current state-of-the-art approaches to measurements in the quantum radar space necessitates the calculation, analysis, and comparison of these measurement types. The purpose of this dissertation is to remove confusion of the best method for detection and ranging using down converted photons for immediate idler detector strategies.

1.4 The Difficulties of Quantum Radar

Quantum radar has had many critics speak out against the technology due to the claims of performance versus the current outcomes of the research. Current research relies on the assumption that technology will be created that generates down converted photons at a higher rate and also that is able to detect single photons events and distinguish these events from noise accurately.

While there have been many critics, recent experiments in both the optical and microwave regime have shown that quantum radar has viability for low-power sensing is available. One such experiment uses a dilution refrigerator to allow a superconducting Josephson Parametric Amplifier to generate entangled microwaves. In this experiment, normal horn antennas are used to transmit these waves into free space and are their electric field is measured. With this the quantum advantage was shown [16]. Another experiment showcased entanglement-enhanced sensing that outperformed current classical technologies in multiple areas [17]. Another experiment showcased that when using a fiber setup, optical parametric amplifiers are able to obtain the correlation that has been calculated [12, 15, 18]. These experiments showcase that quantum radar technology is viable in the lab currently and will be able to provide an advantage when the technological advancement happens. The purpose of this dissertation is to give the basis of knowledge for this future technology, so that when the technology is viable, the information is already there.

1.4.1 Detection Theory and Counting Statistics for Optical Systems

This section looks to establish how detection efficiency effects classic and quantum radar systems. This is imperative because understanding how optical detection occurs starts to bring forth the importance of using quantum sources to assist with detection and ranging. This will follow Ref. [19]. The section will only touch on the major portions of detection theory and counting statistics, for a more thorough understanding of this concept please read the resource.

The basis of all photon counting statistics is photon flux:

$$\Phi = \frac{IA}{\hbar\omega} = \frac{P}{\hbar\omega} \text{photons}^{-1} \quad (1.6)$$

where A is the cross sectional area of the detection surface, I is the intensity, and P is the power in watts. Photon flux is a description of the number of photons in a second on an area. With this photon flux and the quantum efficiency, η , (the ratio of the photons counted to the total number of photons that hit the area) we are able to determine the average number of counts:

$$N(T) = \eta\Phi T = \frac{\eta PT}{\hbar\omega} \quad (1.7)$$

where T is the period. It is found the average count rate is:

$$\mathcal{R} = \frac{N}{T} = \eta\Phi = \frac{\eta P}{\hbar\omega} \text{ counts s}^{-1} \quad (1.8)$$

While that tells us the average amount of photons we will obtain when sensing when using coherent light, the reality is that different sections of the beam will contain different amounts of photons. This requires the beam to be broken up into segments and a probability distribution to be created to determine the likelihood of each photon count. To do this we find the average amount of photons in a section of length L .

$$\bar{n} = \frac{\Phi L}{c} \quad (1.9)$$

where to determine the probability of obtaining n photons in that length of laser, we find that the probability is a Poisson distribution:

$$\mathcal{P}(n) = \frac{\bar{n}^n}{n!} e^{-\bar{n}}, \quad n = 0, 1, 2, \dots \quad (1.10)$$

Which matches a Poisson process as these processes generally refer to random events

that can only generate whole numbers. Now there are three different classification of Poisson light. Super-Poisson where $\Delta n > \sqrt{\bar{n}}$, Poisson where $\Delta n = \sqrt{\bar{n}}$, and sub-Poisson where $\Delta n < \sqrt{\bar{n}}$, where Δn is the photon number variance.

With this in mind, we look at the quantum theory of photodetection and the relationship between the variance in photocount number and the amount of photons hitting the detector:

$$(\Delta N)^2 = \eta^2(\Delta n)^2 + \eta(1 - \eta)\bar{n} \quad (1.11)$$

where we can see with that if $\Delta N = \Delta n$ that the photocount is perfectly reproduced. This dissertation will focus on when the quantum efficiency is perfect ($\eta = 1$):

$$(\Delta N)^2 = (\Delta n)^2 \quad (1.12)$$

where we can see that for our sources, the variance in the amount of photons detected is equivalent to the variance of the photons sent where for a Poisson process is equal to $\sqrt{\bar{n}}$.

In the non-ideal cases, the mean photon number in a length of laser should be very low due quantum radar focusing on the low power regime. It should also be noted that since this variance is low, the occurrence of an error due to timing jitter is much more likely to occur. Due to this the variance in quantum radar experiments should be negligible.

It should also be noted that while the overall creation of the photons from the pump beam is a Poisson distribution, the immediate capture of the idler heralds the signal and the Poisson distribution of the pump beam gives the randomization of the photon waveform.

1.4.2 Jitter, Dark Count, Spatial Coherence, and Signal-Dependent Noise

Other issues that could effect the correlations of the quantum radar systems is jitter and dark count. Dark count is the amount of photons detected by the sensor without any signal being reflected into the sensor. Dark count can be reduced in a multitude of ways, such as cooling the sensor. For dark count, what is important is measuring it to have a baseline of what amount of counts is signal versus noise.

Timing jitter is just the uncertainty of when the photon detection occurred. Jitter cannot be fixed as its a symptom of using hardware to measure the photons, however with the ability to compare the waveforms of the signal and idler some error correction should be able to be done.

This thesis will also not discuss spatial coherence because the discussed system will have high spatial coherence as that is a property of laser light. It also would not have an effect if there was not high spatial coherence because the system is only worried about the heralded photons returning.

It should also be noted that signal-dependent noise will have an effect on the system such as bullet photons. This will not be covered in this thesis as it is just a initial exploration of the maximums of a quantum correlation system using a generalized noise variable to allow for a clearer understanding of the system.

1.5 Outline

This dissertation is outlined as follows: First, the correlations for the bipartite state is derived and simulated. This is for three separate measurement styles: electric field measurement, electric field quadrature measurement, and photon counting. Following this, an analysis of the tripartite state will be done. This includes a full derivation of the covariance matrix and an in-depth simulation of the correlation factors. In this section, a detector function will also be described that will allow for a direct comparison to the bipartite system. Then the tripartite system will be again derived, but this time with the number operator. Finally, future work on this topic will be discussed.

Chapter 2 | Derivation of Bipartite Correlations

2.1 Introduction

Bipartite quantum radar has been a topic of discussion in research [16, 20], but a direct comparison between the photon counting measurements and the electric field measurement has not been evaluated. This chapter seeks to explain the theoretical basis of current research. Namely, using quadrature measurements while also counting photons and correlating them later. We seek to compare the correlation performance of these new techniques. A general setup for one of these systems is seen in Figure (2.1) More specifically, there has been recent work showcasing a quantum advantage using classical measurements of electric field quadratures [13, 16] and by immediately detecting the idler photon counts and correlating later with the signal counts [21]. These methodologies are very similar to classical noise radar techniques done in the past [22]. The goal of this paper is to analyze the correlation performance of these type of systems and determine which method performs the best for a given situation. It is important to note that the calculations performed in this paper represent overall correlations from large data sets consisting of separate and time-separated measurements of the signal and idler streams. Indeed, electric field measurements necessarily involve many photon measurements due to the inability to simultaneously measure the photon number and electric field with arbitrary precision because of the operators not being commutable. Here, we mathematically evaluate a two-mode squeezed vacuum acted on by the number operator (photon counting), the electric field operator (electric field measurement), and the electric field quadrature [23]. In our evaluation, we solve for all parts of the covariance matrix and determine the covariance between the signal and idler beams for each system [13, 24]. Additionally, we show a comparison between the photon counting and electric field temporal covariance. This chapter is structured as follows. Section

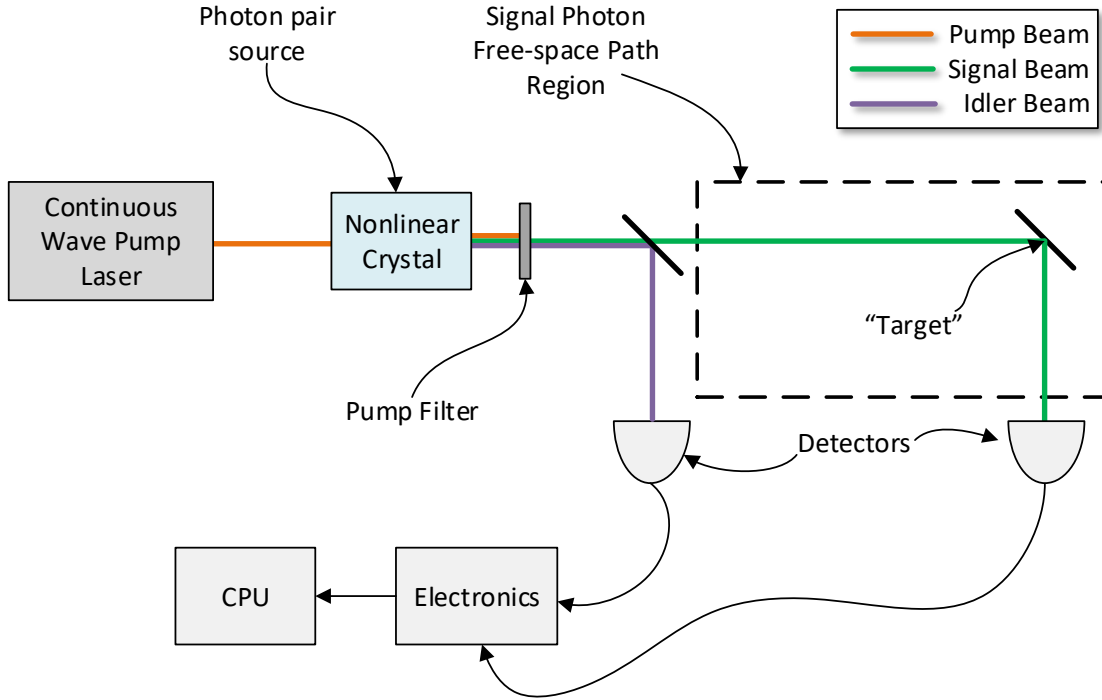


Figure 2.1. The general experimental setup for the measurement schemes discussed. In all cases, the idler photon is measured immediately and correlated with the returning signal photon at a later point in time. The detectors can vary between single photon counters and electric field sensors.

2.2 develops the mathematics associated with the electric field covariance. In Section 2.3, we develop the theory leading to the number operator covariance and compare the results with the electric field covariance. Section 2.4 analytically formulates the electric field quadrature covariance. In Section 2.5 a detailed analysis is presented of all three covariance results for different operational scenarios. Conclusions are presented in Section 2.6. It must be stated that this is looking to obtain the maximum limit of this technology and therefore perfect reflection and a perfect quantum detector is assumed.

2.2 Electric Field Covariance

The electric field operator refers to the bulk measurement of the electric fields of the signal and idler streams of photons. The correlation between the signal and immediately detected idler would be found using a digitizer in the microwave regime or could be

derived from the phase measurements in the optical regime. We begin with the electric field operator defined by [25]:

$$E(r, t) = \sum_{\mathbf{k}} \hat{\epsilon}_{\mathbf{k}} \mathcal{E}_{\mathbf{k}} \hat{a}_{\mathbf{k}} e^{-i\chi} + \hat{\epsilon}_{\mathbf{k}} \mathcal{E}_{\mathbf{k}} \hat{a}_{\mathbf{k}}^{\dagger} e^{i\chi} \quad (2.1)$$

where $\hat{a}_{\mathbf{k}}$ is the creation operator for the frequency mode, \mathbf{k} , and χ is the phase (which we can suppress by assuming that the signal and idler are aligned in time and space via post processing), $\hat{\epsilon}_{\mathbf{k}}$ is a unit polarization vector, and

$$\mathcal{E}_{\mathbf{k}} = \left(\frac{\hbar \nu_{\mathbf{k}}}{2\epsilon_0 V} \right)^{\frac{1}{2}} \quad (2.2)$$

where \hbar is Planck's constant divided by 2π , $\nu_{\mathbf{k}}$ is the frequency associated with the momentum mode \mathbf{k} , ϵ_0 is the permittivity of free space, and V is the quantization volume. $\mathcal{E}_{\mathbf{k}}$ will be suppressed since it will be canceled in the final correlation calculations due to the fact these correlations are normalized. This will allow for greater calculation simplicity and easier to understand solutions. The integral formalism is also not required for the solution as we assume the field is approximately monochromatic (a single momentum mode) where future work will look at a full band signal. For an aligned signal and idler measurement with a linear polarization, Equation (1) reduces to:

$$\hat{E} = \hat{a} + \hat{a}^{\dagger} \quad (2.3)$$

We now begin with with a two-mode squeezed state:

$$|\psi\rangle = \gamma \sum_{n=0}^{\infty} \beta^n |n, n\rangle_{i,s} \quad (2.4)$$

where i and s stand for *idler* and *signal* respectively, $\gamma = \sqrt{\frac{1}{N_s+1}}$, $\beta = \sqrt{\frac{N_s}{N_s+1}}$, and N_s is the mean photon number per mode. This state is entangled and is the output of a continuous-wave pumped spontaneous parametric down-conversion (SPDC) source. To find the covariance between the signal and idler, we need to derive the electric field covariance matrix. It should be noted that the physically realizable version of this state is a tensor product between Equation (2.4) and the thermal noise state. Formally, this calculation is done with a density matrix approach, as a density matrix fully describes a physical system's quantum state, including its statistical mixture with surrounding systems by including all possible projectors the system can collapse into, and their

associated probabilities [26, 27]. We first define the density matrix for the two-mode squeezed vacuum state:

$$\rho_{TMSV} = |\Psi\rangle\langle\Psi| \frac{1}{N_s + 1} \sum_{m=0}^{\infty} \sum_{n=0}^{\infty} \left(\frac{N_s}{N_s + 1}\right)^{\frac{n+m}{2}} |n, n\rangle\langle m, m| \quad (2.5)$$

and the density matrix for the noise state [26]:

$$\rho_T = \frac{1}{N_T + 1} \sum_{i=0}^{\infty} \left(\frac{N_T}{N_T + 1}\right)^i |i\rangle\langle i| \quad (2.6)$$

where $N_T = \frac{1}{1-\kappa} N_B$ and N_B is the mean photon number per mode in the noise path [12]. The return density matrix will be a tensor product between these two matrices:

$$\begin{aligned} \rho_{return} &= \rho_{TMSV} \otimes \rho_T \quad (2.7) \\ &= \frac{1}{N_T + 1} \frac{1}{N_s + 1} \sum_{n=0}^{\infty} \sum_{m=0}^{\infty} \sum_{i=0}^{\infty} \left(\frac{N_s}{N_s + 1}\right)^{\frac{n+m}{2}} \\ &\quad \times \left(\frac{N_T}{N_T + 1}\right)^i |n, n, i\rangle\langle m, m, i| \end{aligned}$$

This can be used to find the expectation value of an arbitrary operator, \hat{O} , by taking the trace of this density matrix with the operator applied to it.

$$\begin{aligned} \langle\hat{O}\rangle &= tr(\rho_{return}\hat{O}) \quad (2.8) \\ &= \langle m, m, j| \frac{1}{N_T + 1} \frac{1}{N_s + 1} \sum_{n=0}^{\infty} \sum_{m=0}^{\infty} \sum_{i=0}^{\infty} \left(\frac{N_s}{N_s + 1}\right)^{\frac{n+m}{2}} \\ &\quad \times \left(\frac{N_T}{N_T + 1}\right)^i |n, n, i\rangle\langle m, m, i| \hat{O} |m, m, j\rangle \quad (2.9) \end{aligned}$$

This formalism is only required when dealing with modes that include appreciable thermal noise contributions, \hat{a}_B , this is due to the complete separation of the ensembles between the noise and signal/idler modes. Therefore, for situations which have insignificant thermal background noise contributions, such as quantities involving the stored idler stream in the transceiver, we perform equivalent, but simpler in operation, state calculations. Having determined the approach for performing the calculations, simplifications will be introduced. First, the quantum covariance is defined as [28]:

$$\text{Cov}(\hat{A}, \hat{B}) = \frac{1}{2} (\langle\{\hat{A}, \hat{B}\}\rangle - \langle\hat{A}\rangle\langle\hat{B}\rangle) \quad (2.10)$$

For monochromatic fields, since the electric field operators between modes are commutative, i.e.:

$$[\hat{E}_1, \hat{E}_2] = \hat{E}_1 \hat{E}_2 - \hat{E}_2 \hat{E}_1 = 0 \quad (2.11)$$

this allows us to set $\langle \hat{E}_1 \hat{E}_2 \rangle = \langle \hat{E}_2 \hat{E}_1 \rangle$, thereby simplifying future calculations. It also allows the quantum covariance shown in Equation (2.10) to be equivalent to the classical covariance $\langle AB \rangle - \langle A \rangle \langle B \rangle$. The state shown in Equation (4) is a zero mean Gaussian state; therefore the covariance reduces to $\langle AB \rangle$. Consequently, we find the covariance matrix to be:

$$V = \begin{pmatrix} \langle \hat{E}_s^2 \rangle & \langle \hat{E}_s \hat{E}_i \rangle \\ \langle \hat{E}_i \hat{E}_s \rangle & \langle \hat{E}_i^2 \rangle \end{pmatrix} \quad (2.12)$$

We now begin the calculations of the expectation values beginning with the idler mode:

$$E_i^2 = \hat{a}_i^2 + \hat{a}_i^{\dagger 2} + \hat{a}_i \hat{a}_i^\dagger + \hat{a}_i^\dagger \hat{a}_i. \quad (2.13)$$

Due to the orthogonality of the Fock state basis, we can determine the terms in the sum:

$$\langle \psi | \hat{a}_i \hat{a}_i^\dagger | \psi \rangle = \gamma^2 \sum_{n=0}^{\infty} \sum_{m=0}^{\infty} \beta^{n+m} \langle m', n' | \hat{a}_i^2 + \hat{a}_i^{\dagger 2} + \hat{a}_i \hat{a}_i^\dagger + \hat{a}_i^\dagger \hat{a}_i | m, n \rangle \quad (2.14)$$

which do not go to zero, starting with \hat{a}_i^2 .

$$\begin{aligned} \langle m', n' | E_i^2 | m, n \rangle &= \sqrt{n(n-1)} \langle m', n' | m-2, n \rangle \\ m' &= m-2 \\ n' &= n \\ \therefore \langle m', n' | \hat{a}_i^2 | m, n \rangle &= 0 \end{aligned} \quad (2.15)$$

Now, we do the same for $\hat{a}_i^{\dagger 2}$:

$$\begin{aligned} \langle m', n' | \hat{a}_i^{\dagger 2} | m, n \rangle &= \sqrt{(n+1)(n+2)} \langle m', n' | m+2, n \rangle \\ m' &= m+2 \\ n' &= n \end{aligned}$$

$$\therefore \langle m', n' | \hat{a}_i^{\dagger 2} | m, n \rangle = 0 \quad (2.16)$$

Next, we check $\hat{a}_i \hat{a}_i^\dagger$:

$$\begin{aligned} \langle m', n' | \hat{a}_i \hat{a}_i^\dagger | m, n \rangle &= (n+1) \langle m', n' | m, n \rangle \\ m' &= m \\ n' &= n \end{aligned} \quad (2.17)$$

Due to the orthogonality of the Fock state basis, we can determine that the matrix elements associated with the \hat{a}_i^2 and $\hat{a}_i^{\dagger 2}$ in the following sum:

$$\langle \psi | \hat{E}_i^2 | \psi \rangle \quad (2.18)$$

$$= \gamma^2 \sum_{n=0}^{\infty} \sum_{m=0}^{\infty} \beta^{n+m} \langle m, m | \hat{a}_i^2 + \hat{a}_i^{\dagger 2} + \hat{a}_i \hat{a}_i^\dagger + \hat{a}_i^\dagger \hat{a}_i | n, n \rangle \quad (2.19)$$

to be zero, leaving only the cross terms. The first cross term can be found in the following manner:

$$\begin{aligned} \langle \psi | \hat{a}_i \hat{a}_i^\dagger | \psi \rangle &= \gamma^2 \sum_{n=0}^{\infty} \sum_{m=0}^{\infty} \beta^{n+m} \langle m, m | \hat{a}_i \hat{a}_i^\dagger | n, n \rangle \\ &= \gamma^2 \sum_n \left(\frac{N_s}{N_s+1} \right)^n n + \gamma^2 \sum_n \left(\frac{N_s}{N_s+1} \right)^n \end{aligned} \quad (2.20)$$

To evaluate this, we use the identity:

$$\sum_n x^n n = \frac{x}{(1-x)^2} \quad (2.21)$$

To find:

$$\begin{aligned} \gamma^2 \sum_n \left(\frac{N_s}{N_s+1} \right)^n n &= \frac{1}{N_s+1} \frac{\frac{N_s}{N_s+1}}{\left(1 - \frac{N_s}{N_s+1}\right)^2} \\ &= N_s \end{aligned} \quad (2.22)$$

and:

$$\frac{1}{N_s + 1} \sum_n \left(\frac{N_s}{N_s + 1} \right)^n = 1 \quad (2.23)$$

where we have used the standard geometric series summation formula in Equation (2.23). Thus for $\langle \hat{a}_i \hat{a}_i^\dagger \rangle$ we obtain $N_s + 1$.

Following similar steps, the second cross term is found to be: $\langle \psi | \hat{a}_i^\dagger \hat{a}_i | \psi \rangle = N_s$. Combining all terms, we obtain:

$$\langle E_i^2 \rangle = 2N_s + 1 \quad (2.24)$$

For the correlation terms in the returned signal path, we have to additionally calculate the contribution of the noise added by the free space channel. This is done by defining \hat{a}_R , where \hat{a}_R equals

$$\hat{a}_R = \sqrt{\kappa} \hat{a}_s + \sqrt{1 - \kappa} \hat{a}_B \quad (2.25)$$

where κ is the transmissivity in the signal path and \hat{a}_B is the thermal noise mode. We then use this to calculate the electric field in the returned mode, $\langle E_R^2 \rangle$. These modes contain a mean photon number of $\frac{N_B}{1 - \kappa}$.

$$\hat{E}_R = \hat{a}_R + \hat{a}_R^\dagger = \sqrt{\kappa}(\hat{a}_s + \hat{a}_s^\dagger) + \sqrt{1 - \kappa}(\hat{a}_B + \hat{a}_B^\dagger)$$

Following a similar procedure to E_i^2 , we find that the non-zero terms of E_R^2 are:

$$\hat{E}_R^2 = \kappa[\hat{a}_s \hat{a}_s^\dagger + \hat{a}_s^\dagger \hat{a}_s] + (1 - \kappa)[\hat{a}_B \hat{a}_B^\dagger + \hat{a}_B^\dagger \hat{a}_B]. \quad (2.26)$$

Where the expectation value is evaluated and it is found to be:

$$\langle \hat{E}_R^2 \rangle = 2\kappa N_s + 2N_B + 1 \quad (2.27)$$

We note that if there exists no noise in the channel, i.e. $N_B = 0$, and perfect transmission, i.e. $\kappa = 1$, then Equation (2.27) reduces to Equation (2.24). Next, we calculate the covariance terms, which are of more importance for radar purposes as they quantify the correlation between the returned and idler photons. More explicitly, we calculate $\langle E_R E_i \rangle$ where: $E_R E_i = \hat{a}_R \hat{a}_i + \hat{a}_R^\dagger \hat{a}_i^\dagger + \hat{a}_R \hat{a}_i^\dagger + \hat{a}_R^\dagger \hat{a}_i$. In a similar manner to previous

calculations, we begin by using the orthogonality Fock States to recognize that $\langle a_R a_i^\dagger \rangle$ and $\langle a_R^\dagger a_i \rangle$ are equal to 0. Using similar steps as previous calculations it is determined the cross-correlation term is $\langle \hat{E}_R \hat{E}_i \rangle = 2\sqrt{\kappa N_s(N_s + 1)}$, which finally yields the full covariance matrix for the electric field:

$$\begin{pmatrix} 2\kappa N_s + 2N_B + 1 & 2\sqrt{\kappa N_s(N_s + 1)} \\ 2\sqrt{\kappa N_s(N_s + 1)} & 2N_s + 1 \end{pmatrix} \quad (2.28)$$

Note how the covariance terms shown here are identical (up to a factor of 2) to those of the OPA and phase conjugate receiver implementations [18]. Recall that in our case, these off-diagonal terms arise from taking two separate electric field measurements, and correlating the stored data. This is significant because it provides mathematical justification that using a delay line and performing a joint measurement of the signal and idler modes is identical to immediately detecting the idler mode and correlating with later receiver signal modes. This validates the procedures of recent experiments [16, 29]. This result is due entirely to the fact that entanglement is destroyed, and a joint measurement no longer is useful in obtaining a quantum benefit. This does not however mean that the OPA or phase conjugate method should be abandoned. Using this analog method to correlate is useful since it is difficult to measure low power photon events of a realistic noisy signal.

2.3 Number Operator Covariance

The number operator refers to photon counting experiments. This can be used in a quantum radar system by immediately counting the photons of the idler beam and using post processing to correlate this binary waveform with the signal beam after it has returned [4, 30]. We begin this calculation by defining the number operator:

$$\hat{N} = \hat{a}^\dagger \hat{a} \quad (2.29)$$

Similarly to the electric field derivation, we use the two-mode squeezed state that is defined in Equation (2.4). Much like the electric field operator, the number operator is also commutative:

$$[\hat{N}_1, \hat{N}_2] = \hat{N}_1 \hat{N}_2 - \hat{N}_2 \hat{N}_1 = 0 \quad (2.30)$$

which allows $\langle \hat{N}_1 \hat{N}_2 \rangle = \langle \hat{N}_2 \hat{N}_1 \rangle$. Due to this and the number operator producing a non-zero mean, the covariance matrix for the number operator is given by:

$$V = \begin{pmatrix} \langle \hat{N}_s^2 \rangle - \langle \hat{N}_s \rangle \langle \hat{N}_s \rangle & \langle \hat{N}_R \hat{N}_i \rangle - \langle \hat{N}_R \rangle \langle \hat{N}_i \rangle \\ \langle \hat{N}_i \hat{N}_R \rangle - \langle \hat{N}_i \rangle \langle \hat{N}_R \rangle & \langle \hat{N}_i^2 \rangle - \langle \hat{N}_i \rangle \langle \hat{N}_i \rangle \end{pmatrix} \quad (2.31)$$

Now we begin the calculations for the expectation value of the idler mode:

$$\langle \hat{N}_i^2 \rangle - \langle \hat{N}_i \rangle \langle \hat{N}_i \rangle \quad (2.32)$$

where we first define:

$$\hat{N}_i^2 = \hat{a}_i^\dagger \hat{a}_i \hat{a}_i^\dagger \hat{a}_i \quad (2.33)$$

This term can be seen to be non-zero due to the orthogonality of the Fock State basis, therefore it can be applied to the two-mode squeezed vacuum state:

$$\begin{aligned} \langle \psi | \hat{N}_i^2 | \psi \rangle &= \gamma^2 \sum_{n=0}^{\infty} \sum_{m=0}^{\infty} \beta^{n+m} \langle m, m | \hat{a}_i^\dagger \hat{a}_i \hat{a}_i^\dagger \hat{a}_i | n, n \rangle \\ &= \gamma^2 \sum_n \left(\frac{N_s}{N_s + 1} \right)^n n^2 \end{aligned} \quad (2.34)$$

Using the identity $\sum_{n=0}^{\infty} x^n n^2 = -\frac{x(1+x)}{(x-1)^3}$, we obtain:

$$\langle \hat{N}_i^2 \rangle = -\gamma^2 \frac{\beta(1+\beta)}{(\beta-1)^3} = N_s(1+2N_s) \quad (2.35)$$

It can also be seen that $\hat{N}_i = \hat{a}_i^\dagger \hat{a}_i$, where the expectation value was already calculated in the previous section to be N_s , therefore:

$$\langle \hat{N}_i^2 \rangle - \langle \hat{N}_i \rangle \langle \hat{N}_i \rangle = N_s(1+N_s) \quad (2.36)$$

Next, the signal variance is evaluated and determined to be:

$$\langle \hat{N}_R^2 \rangle - \langle \hat{N}_R \rangle \langle \hat{N}_R \rangle = \kappa^2 N_s(1+N_s) + N_B(1-\kappa+N_B) \quad (2.37)$$

and the cross-correlation terms expectation values are found to be:

$$\langle \hat{N}_s \hat{N}_i \rangle - \langle \hat{N}_s \rangle \langle \hat{N}_i \rangle = \kappa N_s (1 + N_s) \quad (2.38)$$

This gives the full covariance matrix for the number operator:

$$V = \begin{pmatrix} \kappa^2 N_s (1 + N_s) + N_B (1 - \kappa + N_B) & \kappa N_s (1 + N_s) \\ \kappa N_s (1 + N_s) & N_s (1 + N_s) \end{pmatrix} \quad (2.39)$$

It is again seen that when the transmissivity is perfect ($\kappa = 1$) and the system is noiseless ($N_B = 0$), then the on-diagonal terms are equal. Finally, it should be noted that the cross correlation term for the number operator matches the covariance of the electric field operator, except they are squared due to the quadratic nature in the field mode of the number operator while the electric field operator is linear. In regards to comparing to other systems, it can be problematic to directly compare covariances. It is more appropriate to normalize the covariance to produce the correlation coefficients. This is done by simply dividing each covariance term by the product of the variances. This will be done in Section 2.5.

2.4 Electric Field Quadrature Covariance

As a method to give a more direct comparison to some of the other research that has been conducted in the field [13, 16], we also discuss the electric field quadrature measurements. To do this, we first define the covariance matrix:

$$V = \begin{pmatrix} \{\hat{I}_i, \hat{I}_i\} & \{\hat{I}_i, \hat{Q}_i\} & \{\hat{I}_i, \hat{I}_R\} & \{\hat{I}_i, \hat{Q}_R\} \\ \{\hat{Q}_i, \hat{I}_i\} & \{\hat{Q}_i, \hat{Q}_i\} & \{\hat{Q}_i, \hat{I}_R\} & \{\hat{Q}_i, \hat{Q}_R\} \\ \{\hat{I}_R, \hat{I}_i\} & \{\hat{I}_R, \hat{Q}_i\} & \{\hat{I}_R, \hat{I}_R\} & \{\hat{I}_R, \hat{Q}_R\} \\ \{\hat{Q}_R, \hat{I}_i\} & \{\hat{Q}_R, \hat{Q}_i\} & \{\hat{Q}_R, \hat{I}_R\} & \{\hat{Q}_R, \hat{Q}_R\} \end{pmatrix} \quad (2.40)$$

where $\{\cdot, \cdot\}$ represents the anti-commutator, $I = \frac{1}{2}(\hat{a}^\dagger + \hat{a})$, and $Q = \frac{i}{2}(\hat{a}^\dagger - \hat{a})$ and the subscripts refer to the idler or return path. As done in previous sections, non-zero terms are determined due to the orthogonality of the Fock state basis which is shown in Equation (2.41). It can be noted that all of these terms have been calculated in previous

$$V = \frac{1}{2} \begin{pmatrix} \frac{1}{4}(\hat{a}_i^\dagger \hat{a}_i + \hat{a}_i \hat{a}_i^\dagger) & \frac{i}{4}(\hat{a}_i \hat{a}_i^\dagger - \hat{a}_i^\dagger \hat{a}_i) & \frac{1}{4}(\hat{a}_i^\dagger \hat{a}_R^\dagger + \hat{a}_i \hat{a}_R) & \frac{i}{4}(\hat{a}_i^\dagger \hat{a}_R^\dagger - \hat{a}_i \hat{a}_R) \\ +\frac{1}{4}(\hat{a}_i \hat{a}_i^\dagger + \hat{a}_i^\dagger \hat{a}_i) & +\frac{i}{4}(\hat{a}_i^\dagger \hat{a}_i - \hat{a}_i \hat{a}_i^\dagger) & +\frac{1}{4}(\hat{a}_i^\dagger \hat{a}_R^\dagger + \hat{a}_i \hat{a}_R) & +\frac{i}{4}(\hat{a}_i^\dagger \hat{a}_R^\dagger - \hat{a}_i \hat{a}_R) \\ \frac{i}{4}(\hat{a}_i^\dagger \hat{a}_i - \hat{a}_i \hat{a}_i^\dagger) & \frac{1}{4}(\hat{a}_i^\dagger \hat{a}_i + \hat{a}_i \hat{a}_i^\dagger) & \frac{i}{4}(\hat{a}_i^\dagger \hat{a}_R^\dagger - \hat{a}_i \hat{a}_R) & -\frac{1}{4}(\hat{a}_i^\dagger \hat{a}_R^\dagger + \hat{a}_i \hat{a}_R) \\ +\frac{i}{4}(\hat{a}_i \hat{a}_i^\dagger - \hat{a}_i^\dagger \hat{a}_i) & +\frac{1}{4}(\hat{a}_i^\dagger \hat{a}_i + \hat{a}_i \hat{a}_i^\dagger) & +\frac{i}{4}(\hat{a}_i^\dagger \hat{a}_R^\dagger - \hat{a}_i \hat{a}_R) & +-\frac{1}{4}(\hat{a}_i^\dagger \hat{a}_R^\dagger + \hat{a}_i \hat{a}_R) \\ \frac{1}{4}(\hat{a}_i^\dagger \hat{a}_R^\dagger + \hat{a}_i \hat{a}_R) & \frac{i}{4}(\hat{a}_i^\dagger \hat{a}_R^\dagger + \hat{a}_i \hat{a}_R) & \frac{1}{4}(\hat{a}_R^\dagger \hat{a}_R + \hat{a}_R \hat{a}_R^\dagger) & \frac{i}{4}(\hat{a}_R \hat{a}_R^\dagger - \hat{a}_R^\dagger \hat{a}_R) \\ +\frac{1}{4}(\hat{a}_i^\dagger \hat{a}_i^\dagger + \hat{a}_i \hat{a}_R) & +\frac{i}{4}(\hat{a}_i^\dagger \hat{a}_R^\dagger - \hat{a}_i \hat{a}_R) & +\frac{1}{4}(\hat{a}_R^\dagger \hat{a}_R + \hat{a}_R \hat{a}_R^\dagger) & +\frac{i}{4}(\hat{a}_R^\dagger \hat{a}_R - \hat{a}_R \hat{a}_R^\dagger) \\ \frac{i}{4}(\hat{a}_i^\dagger \hat{a}_R^\dagger - \hat{a}_i \hat{a}_R) & -\frac{1}{4}(\hat{a}_i^\dagger \hat{a}_R^\dagger + \hat{a}_i \hat{a}_R) & \frac{i}{4}(\hat{a}_R^\dagger \hat{a}_R - \hat{a}_R \hat{a}_R^\dagger) & \frac{1}{4}(\hat{a}_R^\dagger \hat{a}_R + \hat{a}_R \hat{a}_R^\dagger) \\ +\frac{i}{4}(\hat{a}_i^\dagger \hat{a}_i^\dagger - \hat{a}_i \hat{a}_R) & -\frac{1}{4}(\hat{a}_i^\dagger \hat{a}_i^\dagger + \hat{a}_i \hat{a}_R) & +\frac{i}{4}(\hat{a}_R \hat{a}_R^\dagger - \hat{a}_R^\dagger \hat{a}_R) & \frac{1}{4}(\hat{a}_R^\dagger \hat{a}_R + \hat{a}_R \hat{a}_R^\dagger) \end{pmatrix} \quad (2.41)$$

$$V = \begin{pmatrix} \frac{1}{4}(2N_s + 1) & 0 & \frac{1}{2}\sqrt{\kappa N_s(N_s + 1)} & 0 \\ 0 & \frac{1}{4}(2N_s + 1) & 0 & -\frac{1}{2}\sqrt{\kappa N_s(N_s + 1)} \\ \frac{1}{2}\sqrt{\kappa N_s(N_s + 1)} & 0 & \frac{1}{4}(2\kappa N_s + 2N_B + 1) & 0 \\ 0 & -\frac{1}{2}\sqrt{\kappa N_s(N_s + 1)} & 0 & \frac{1}{4}(2\kappa N_s + 2N_B + 1) \end{pmatrix} \quad (2.42)$$

sections. The evaluated covariance matrix is shown in Equation (2.42). Note how the off-diagonal elements of the covariance matrix matches the off-diagonal elements of both of the previous covariance matrices up to a multiplicative constant. For the quadrature covariance, a $1/2$ factor account for the fact the the correlations are split between I and Q .

2.5 Analysis

As mentioned earlier, there is no commutation between the electric field operator and the number operator, this means that if it is possible to determine the electric field with certainty, there is no information known about the photon count and vice versa. The claim of this chapter is not a dual-measurement of the photon count and the electric field measurement, but to show the relationship between the covariance of these independent measurements in separate systems. To make the electric field able to be compared directly with the number operator and quadrature, the correlation coefficient must be found for

each. This correlation coefficient can be found using:

$$r_{xy} = \frac{\text{cov}(x, y)}{\sqrt{\sigma_x \sigma_y}} \quad (2.43)$$

where σ represents the standard deviation. The necessary terms have already been calculated for all three measurement schemes. Therefore, for the electric field:

$$r_{E_{si}} = \frac{\langle \hat{E}_s \hat{E}_i \rangle}{\sqrt{\langle \hat{E}_s^2 \rangle \langle \hat{E}_i^2 \rangle}} = \frac{2\sqrt{\kappa N_s}}{\sqrt{2\kappa N_s + 2N_B + 1}} \quad (2.44)$$

It is easily found that the correlation coefficient for the quadrature method is identical to that of the electric field. Although this implies identical performance, in practice, multiple quadratures are being measured and they can be combined in various ways to construct detector functions which yield differing performance [13, 16]. Therefore, one would expect better performance overall simply by the nature of collecting more information (multiple measurements). Here, we ignore these complexities and simply show them to be equal as any single correlation between two quadratures will result in identical performance. For photon counting, the correlation coefficient is found to be:

$$r_{N_{si}} = \frac{\langle \hat{N}_s \hat{N}_i \rangle}{\sqrt{\langle \hat{N}_s^2 \rangle \langle \hat{N}_i^2 \rangle}} = \frac{\kappa \sqrt{N_s(N_s + 1)}}{\sqrt{\kappa^2 N_s(1 + N_s) + N_B(1 - \kappa + N_B)}} \quad (2.45)$$

To compare these correlation coefficients, curves are generated for each one over a given range of N_s , κ , and the background noise photons per mode N_B . In addition, each of the three curves will have a small N_s and large N_s behavior that dictates its overall performance. Due to all of these variables, there exist many possible scenarios where one particular sensor out-performs the others in particular N_s regimes. We cannot possibly showcase all of these scenarios, so we restrict the presentation of results to the most important outcomes learned by our parametric sweeps and a small subset of plots which we believe best represents these lessons. An expanded analysis of these many scenarios will be done in future work. A summary of the most important results are given below.

1. For very low N_s , the electric field and quadrature measurements appear to always outperform photon counting.
2. Photon-counting appears to be dominant as long as there are enough photons returning to the radar. For low transmissivity (high noise), it performs the worst out of all of the methods.

3. If N_B is not too small, changing its value does not appear to affect the general behaviors of the curves, but rather, will simply change the N_s regimes with which these behaviors occur.

Quantum radar applications focus in the regime where $N_B \gg N_s$. For the following plots, we choose an N_B of 10 with the understanding that entangled photon powers are such that N_s is on the order of 1×10^{-3} [15]. Figure (2.2) shows the various correlation coefficients for a scenario in which $\kappa = 0.7$. Note how for very low N_s , the electric field amplitude and quadrature measurements outperforms the photon counting method. For larger values of N_s , the photon counting method becomes dominant. Again note that the E-field and E-field quadrature curves are identical. However, as mentioned earlier, in practice, using quadratures will improve the performance because there are simply more measurements taking place and one can combine I and Q in various ways to obtain differing performance [13,16]. Next, observe Figure 2.3 for a second scenario, one with

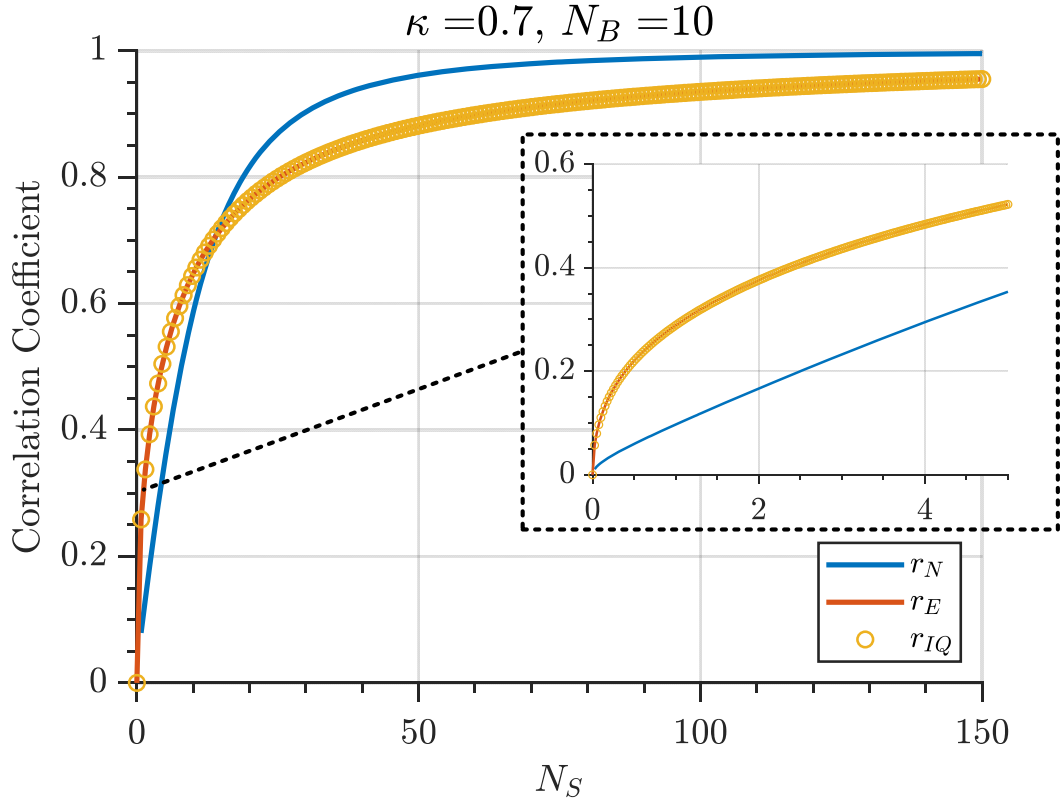


Figure 2.2. Correlation coefficient of the various methods for Scenario 1. ($\kappa=.7, N_B=10$)

the transmissivity much lower. In this case, there are not enough photons making it back to the radar for low N_s and consequently photon counting is the worst performer at this signal power. This is because at low signal powers and high background noise, it is easier for the background noise to dominate the correlation with accidentals. As N_s increases, more photons make it back to the receiver and photon counting becomes dominant again. Figure 2.4 shows a correlation over a range of N_s that is more typical

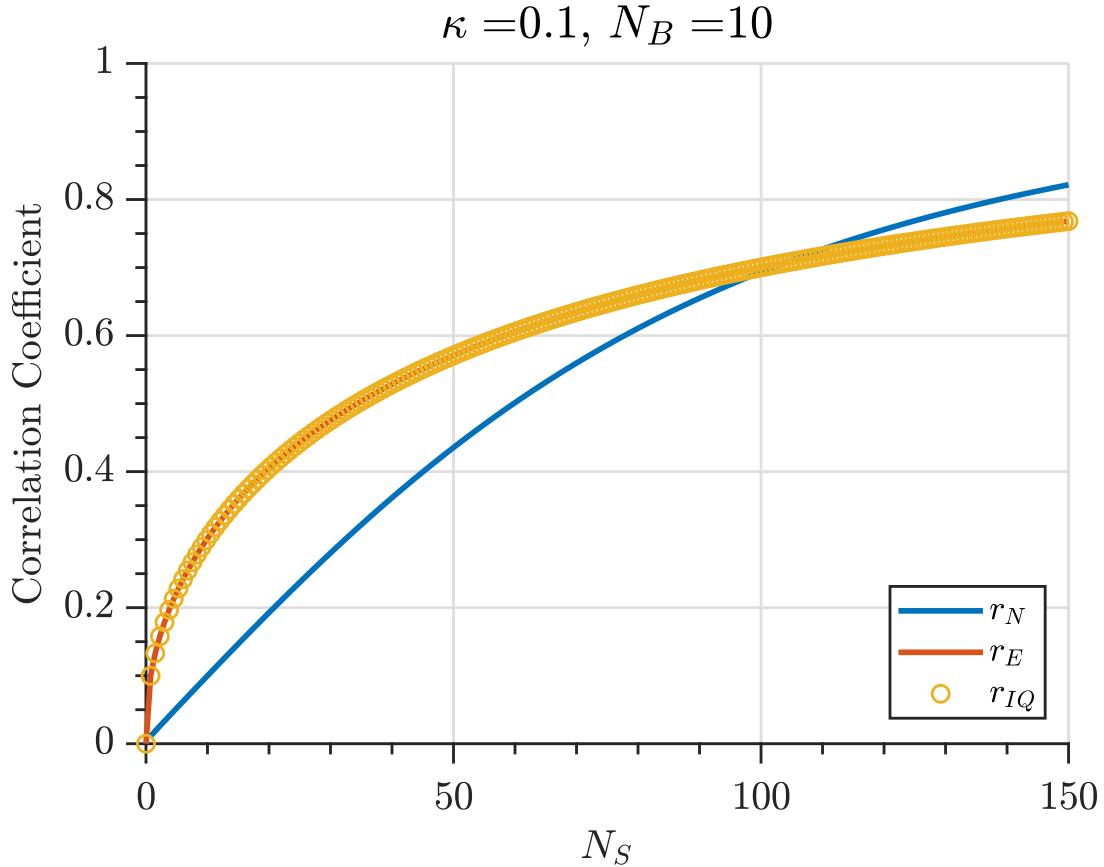


Figure 2.3. Correlation coefficient of the various methods for Scenario 2. ($\kappa=.1, N_B=10$)

of current SPDC power outputs to better illustrate the very low N_s regime performance. Clearly the electric field measurements perform better in this regime.

2.6 Conclusion

In this chapter, the immediate idler, many measurement correlation of the two-mode squeezed vacuum state has been evaluated, compared and contrasted for three different quantum radar measurement strategies, all of which are post-correlation techniques

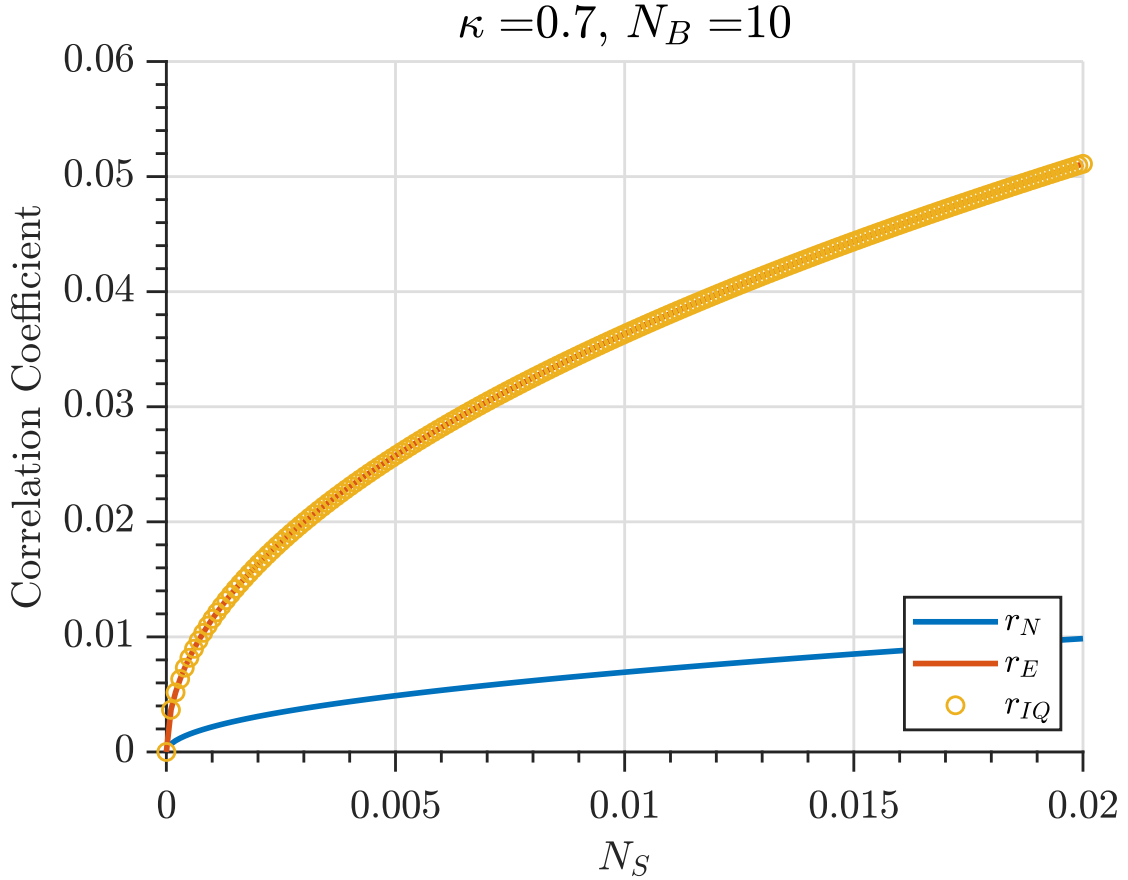


Figure 2.4. Correlation coefficient for low N_s for scenario 1

(photon counting, E-field measurement, and quadrature measurement). It was found that the most optimal measurement strategy is a function of the transmit power N_s , background noise N_B , and transmissivity κ , depending on the regime of interest. Two particularly interesting scenarios were presented to showcase the behavior of the curves. One can experiment with the above equations for different scenarios of interest for trade-off analysis of the approaches presented herein. The work presented here can help to guide future experiments and applications in obtaining the most optimal design and implementation strategy.

Chapter 3 | Analysis of Tripartite Electric Field Correlation

3.1 Introduction

The previous chapter discussed a bipartite quantum radar design that uses spontaneous parametric down conversion (SPDC) where one high energy photon is split into two photons of half the original energy. With this, one of the photons created is kept as an idler and the other is sent at the target as the signal. When the signal returns, a correlation method is used to determine if the returning photons are from the original signal. This bipartite quantum system has shown a 3-dB improvement in the error exponential which means that it has better detection in high noise environments [12, 20, 22, 29, 31, 32]. Similarly to the two-photon method, the three-photon method looks to obtain a quantum advantage through the use of signal and idler beams. However, with the tripartite state we are able to transmit two signals that are correlated with a single idler. We believe that this arrangement with a single idler could lead to benefits in correlation performance in lossy channels. We seek to explore whether having more photons per generation leads to correlation benefits of the returned beams. Conventional SPDC methods can only create equal photon number states on each branch of the photon generation, namely one photon each for the signal and idler, two photons each, three photons each, and so on [4]. These higher number states are increasingly less probable to generate and although they would possess more photons per generation, there would be less photons overall. A state specifically constructed to be tripartite (three-particles) can potentially alleviate this problem by using a different experimental setup entirely for the generation, keeping the same detection paradigm as bipartite systems, namely, storing or detecting the idler photon [3, 4, 10] and then later measuring the returned signal photons. However, in our

tripartite case, each idler can correlate with *two* returning signal photons. In the setup described here, this would be done with a single detector for the signals and another detector to immediately detect the idler.

A basic setup of this is seen in Figure (3.1).

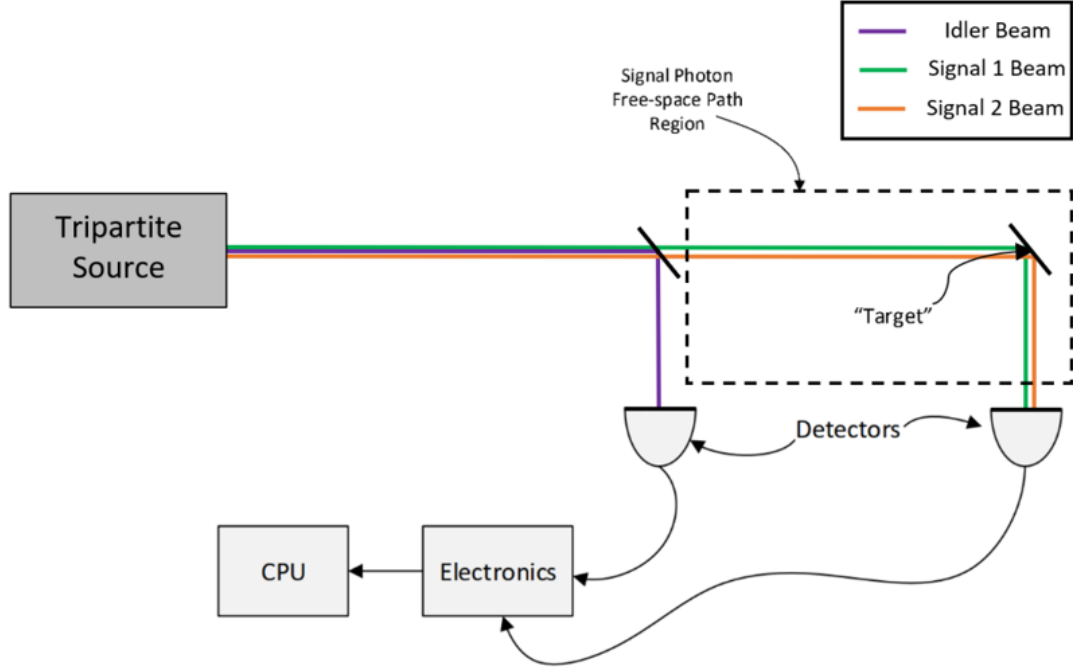


Figure 3.1. Basic setup for tripartite system with both signals staying together and the idler being immediately detected. This setup is valid for both the electric field measurement and the photon counting measurement.

Here, we mathematically evaluate a tripartite radar system using a coupled three mode squeezed state introduced by Zhang and Glaser [14] which is generated through the use of an Rb atomic vapor and a four-wave-mixing process. For this calculation, we assume that the target is ideal (perfectly reflective). In this scheme, two lasers are used with non-linear crystals and one path from each of the signal idler pairs are mixed to create three part entanglement. In our evaluation, we solve for all parts of the covariance matrix and determine the covariance between the signal and idler beams for the system. Additionally, we simulate the correlation coefficient to be able to directly compare to the current literature. After we have determined the correlation coefficients of each of the path, we then compare it to the current bipartite system. To do this, we define a detection scheme for the tripartite system that will allow for an apples-to-apples comparison.

Again, it must be stated that this is looking to obtain the maximum limit of this

technology and therefore perfect reflection and a perfect quantum detector is assumed.

3.2 Tripartite Derivation

The following tripartite derivation is made of two parts. First, we define the wave function in terms of the mean photon number per mode for each of the paths to allow for an easier comparison to transmit power. Secondly, the wave function in terms of the mean photon number per mode is used to derive the covariance matrix for the system.

3.2.1 Wave function derivation in terms of mean photon number per mode

We begin with a coupled three-mode squeezed vacuum state [14].

$$|\Psi\rangle = \frac{1}{\cosh(r)} \sum_{n,l}^{\infty} (-1)^{n+l} e^{i(n\theta_1+l\theta_2)} \left(\frac{r_1}{r} \tanh(r) \right)^n \left(\frac{r_2}{r} \tanh(r) \right)^l \sqrt{\frac{(n+l)!}{n!l!}} |n, n+l, l\rangle_{s_1, i, s_2} \quad (3.1)$$

where r_1 , and r_2 are the squeezing factors, $r = \sqrt{r_1^2 + r_2^2}$, and θ_1 and θ_2 are the phase terms.

The first task is to rewrite $\cosh(r)$ and $\tanh(r)$ in terms of the mean photon number per mode as is commonly done for the bipartite two mode squeezed light frequently used in quantum radar analysis [3, 4, 6, 12, 16]. In our case however, each branch will, in general, be a different mean photon number per mode, which we denote as N_{s_1} , N_{s_2} , and N_i for signal 1, signal 2, and the idler respectively. This allows for the covariance to be more directly comparable to the power level of each beam because these values directly relate to the amount of photons transmitted.

Since the tripartite implementation consists of three beams, there are multiple combinations of beams one can keep at the radar and send into free space. We propose the following system which uses two of the photon paths as signals and one of the photon paths as an idler. The reasoning behind this choice is to send as much energy into the free space path as possible to increase transmit power. We also choose to use the electric field which corresponds to the use of balanced homodyne detection.

First, the evaluation of the mean idler photon number, $N_i = \hat{a}_i^\dagger \hat{a}_i$:

$$\begin{aligned} \langle \Psi | \hat{a}_i \hat{a}_i^\dagger | \Psi \rangle &= \frac{1}{\cosh^2(r)} \sum_{m,k}^{\infty} \sum_{n,l}^{\infty} e^{i(n\theta_1 + l\theta_2)} e^{-i(m\theta_1 + k\theta_2)} \left(\frac{r_1^{n+m}}{r^2} \tanh^{(n+m)}(r) \right) \left(\frac{r_2^{l+k}}{r^2} \tanh^{(l+k)}(r) \right) \\ &\times \sqrt{\frac{(n+l)!}{n!l!}} \sqrt{\frac{m!+k!}{m!k!}} (n+l) \langle m, m+k, k | n, n+l, l \rangle \end{aligned} \quad (3.2)$$

Orthogonality causes $m = n$ and $k = l$ which yields:

$$\langle \Psi | \hat{a}_i \hat{a}_i^\dagger | \Psi \rangle = \frac{1}{\cosh^2(r)} \sum_{n,l=0}^{\infty} \tanh^{2(n+l)}(r) \frac{(n+l)!}{n!l!} \frac{r_1^{2n} r_2^{2l}}{r^{2(n+l)}} (n+l) \quad (3.3)$$

The above double summation can be evaluated by first applying different values of n to the formula, then evaluating the resulting sums over l . Doing this for the first few values of n gives (denoting each partial sum as F_n):

$$\begin{aligned} F_0 &= \frac{r^2 \operatorname{sech}^2(r) r_2^2 \tanh^2(r)}{(r^2 - r_2^2 \tanh^2(r))^2} \\ F_1 &= \frac{r^2 \operatorname{sech}^2(r) r_1^2 (r^2 \tanh^2(r) + r_2^2 \tanh^4(r))}{(r^2 - r_2^2 \tanh^2(r))^3} \\ F_2 &= \frac{r^2 \operatorname{sech}^2(r) r_1^4 (2r^2 \tanh^4(r) + r_2^2 \tanh^6(r))}{(r^2 - r_2^2 \tanh^2(r))^4} \\ F_3 &= \frac{r^2 \operatorname{sech}^2(r) r_1^6 (3r^2 \tanh^6(r) + r_2^2 \tanh^8(r))}{(r^2 - r_2^2 \tanh^2(r))^5} \end{aligned} \quad (3.4)$$

Given the above pattern of partial sums, the general formula is found to be:

$$\langle \Psi | \hat{a}_i \hat{a}_i^\dagger | \Psi \rangle = \frac{r^2}{\cosh^2(r)} \sum_{i=0}^{\infty} \frac{1}{(r^2 - r_2^2 \tanh^2(r))^{(i+2)}} r_1^{2i} \left(i r^2 \tanh^{2i}(r) + r_2^2 \tanh^{2(i+1)}(r) \right) \quad (3.5)$$

The above sum can be evaluated and yields:

$$\langle \Psi | \hat{a}_i \hat{a}_i^\dagger | \Psi \rangle = N_i = \sinh^2(r) \quad (3.6)$$

Next, the mean photon number per mode of one of the signal beams is evaluated in a similar manner as the previous case, which yields:

$$\langle \Psi | \hat{a}_{s_1} \hat{a}_{s_1}^\dagger | \Psi \rangle = N_{s_1} = \frac{\sinh^2(r) r_2^2}{r^2} \quad (3.7)$$

Furthermore, evaluating $\hat{a}_{s_2}\hat{a}_{s_2}^\dagger$ in a similar manner gives:

$$\langle \Psi | \hat{a}_{s_2}\hat{a}_{s_2}^\dagger | \Psi \rangle = N_{s_2} = \frac{\sinh^2(r)r_1^2}{r^2} \quad (3.8)$$

In order to write $\tanh(r)$ and $\cosh(r)$ in terms of N_i , N_{s_1} , and N_{s_2} , we start by solving Equation (3.6) for $\cosh(r)$:

$$N_i = \sinh^2(r) = \cosh^2(r) - 1 \rightarrow \cosh(r) = \sqrt{N_i + 1} \quad (3.9)$$

We then solve for $\tanh(r)$ by dividing Equation (3.6) by Equation (3.9) which yields:

$$\sqrt{\frac{N_i N_{s_1} r^2}{N_i^2 r_2^2 + N_{s_1} r^2}} = \tanh(r) \quad (3.10)$$

One can also obtain this result in reference to the other signal beam by dividing Equation (3.6) by Equation (3.8):

$$\sqrt{\frac{N_i N_{s_2} r^2}{N_i^2 r_1^2 + N_{s_2} r^2}} = \tanh(r) \quad (3.11)$$

Using the terms found for $\tanh(r)$ in (3.10) and for $\cosh(r)$ in (3.9), we can now write the wave function in terms of the mean photon number per modes for the paths:

$$\begin{aligned} |\Psi\rangle &= \frac{1}{\sqrt{N_i + 1}} \sum_{n,l} (-1)^{n+1} e^{i(n\theta_1 + l\theta_2)} \left(\frac{r_1}{r} \times \sqrt{\frac{N_i N_{s_1} r^2}{N_i^2 r_2^2 + N_{s_1} r^2}} \right)^n \left(\frac{r_2}{r} \sqrt{\frac{N_i N_{s_1} r^2}{N_i^2 r_2^2 + N_{s_1} r^2}} \right)^l \\ &\times \sqrt{\frac{(n+l)!}{n!l!}} |n, n+l, l\rangle_{s_1, i, s_2} \end{aligned} \quad (3.12)$$

where we will set $\alpha = \frac{1}{\sqrt{N_i + 1}}$ and $\beta(r) = \sqrt{\frac{N_i N_{s_1} r^2}{N_i^2 r_2^2 + N_{s_1} r^2}}$, making the wave function:

$$|\Psi\rangle = \alpha \sum_{n,l} (-1)^{n+1} e^{i(n\theta_1 + l\theta_2)} \left(\frac{r_1}{r} \beta(r) \right)^n \left(\frac{r_2}{r} \beta(r) \right)^l \sqrt{\frac{(n+l)!}{n!l!}} |n, n+l, l\rangle_{s_1, i, s_2} \quad (3.13)$$

3.2.2 Covariance Matrix

Now that we have obtained for the wave function in terms of the mean photon number per modes for the individual beams, we can now calculate the terms in the covariance

matrix, namely:

$$V = \begin{pmatrix} \langle E_i^2 \rangle & \langle E_i E_{R_1} \rangle & \langle E_i E_{R_2} \rangle \\ \langle E_{R_1} E_i \rangle & \langle E_{R_1}^2 \rangle & \langle E_{R_1} E_{R_2} \rangle \\ \langle E_{R_2} E_i \rangle & \langle E_{R_2} E_{R_1} \rangle & \langle E_{R_2}^2 \rangle \end{pmatrix} \quad (3.14)$$

where E_x is the electric field operator for the idler, first signal path, or second signal path ($x = i, s_1$, and s_2 respectively) defined by [25]:

$$E(r, t) = \sum_{\mathbf{k}} \hat{\epsilon}_{\mathbf{k}} \mathcal{E}_{\mathbf{k}} a_{\mathbf{k}} e^{-i\chi} + \hat{\epsilon}_{\mathbf{k}} \mathcal{E}_{\mathbf{k}} a_{\mathbf{k}}^\dagger e^{i\chi} \quad (3.15)$$

where $\hat{a}_{\mathbf{k}}$ is the frequency mode's creation operator, \mathbf{k} is the wave vector, and χ is the phase (which we can suppress by assuming that the signal and idler are aligned in time and space via shifting the data or using a delay line), $\hat{\epsilon}_{\mathbf{k}}$ is a unit polarization vector, given by

$$\mathcal{E}_{\mathbf{k}} = \left(\frac{\hbar \nu_{\mathbf{k}}}{2\epsilon_0 V} \right)^{\frac{1}{2}} \quad (3.16)$$

where \hbar is Planck's constant divided by 2π , $\nu_{\mathbf{k}}$ is the frequency associated with the momentum mode \mathbf{k} , ϵ_0 is the permittivity of free space, and V is the quantization volume. $\mathcal{E}_{\mathbf{k}}$ will be suppressed since it will be canceled in the final correlation calculations due to the fact these correlations are normalized. This will allow for greater calculation simplicity and easier to understand solutions. The integral formalism is also not required for the solution as we assume the field is approximately monochromatic (a single momentum mode) where future work will look at a full band signal. For an aligned signal and idler measurement with a linear polarization, Equation (4.4) reduces to:

$$\hat{E} = \hat{a} + \hat{a}^\dagger \quad (3.17)$$

It should be noted that the physically realizable version of these calculations is a tensor product between Equation (3.1) and the thermal noise state. Formally, this calculation is done with a density matrix approach [18, 26], where we first determine the density matrix for the coupled three-mode squeezed vacuum state:

$$\begin{aligned} \rho_{CTSV} &= \frac{1}{\cosh^2(r)} \sum_{n,l,m,k}^{\infty} (-1)^{n+m+2} e^{i(n\theta_1+l\theta_2)} e^{-i(m\theta_1+k\theta_2)} \\ &\times \left(\frac{r_1}{r} \beta(r) \right)^{m+n} \left(\frac{r_2}{r} \beta(r) \right)^{l+k} \sqrt{\frac{(n+l)!}{n!l!}} \sqrt{\frac{(m+k)!}{m!k!}} |n, n+l, l, j\rangle \langle m, m+k, k, j| \end{aligned} \quad (3.18)$$

and the density matrix for the thermal noise state [26, 27]:

$$\rho_T = \frac{1}{N_T + 1} \sum_i \left(\frac{N_T}{N_T + 1} \right)^i |i\rangle \langle i| \quad (3.19)$$

where N_T is the mean photon number of the thermal state. The return density matrix is defined as:

$$\begin{aligned} \rho_{return} = \rho_{CTSV} \otimes \rho_T &= \frac{1}{\cosh^2(r)} \frac{1}{N_T + 1} \sum_{n,l,m,k}^{\infty} (-1)^{n+m+2} e^{i(n\theta_1+l\theta_2)} e^{-i(m\theta_1+k\theta_2)} \\ &\times \left(\frac{r_1}{r} \tanh(r) \right)^{m+n} \left(\frac{r_2}{r} \tanh(r) \right)^{l+k} \sqrt{\frac{(n+l)!}{n!l!}} \sqrt{\frac{(m+k)!}{m!k!}} |n, n+l, l, i, j\rangle \langle m, m+k, k, i, j| \end{aligned} \quad (3.20)$$

which can be shown to be approximately valid in the high-noise regime.

The evaluation begins by looking at the on-diagonal terms for this matrix, which amounts to the variance of the respective beams. Beginning with the E_i^2 term:

$$E_i^2 = \hat{a}_i^2 + \hat{a}_i \hat{a}_i^\dagger + \hat{a}_i^\dagger \hat{a}_i + \hat{a}_i^{\dagger 2} \quad (3.21)$$

Using the Fock State basis we are able to determine terms that will become zero due to orthogonality. To maintain conciseness within the main body these calculations have been moved to Appendix (A). Now we begin evaluating the non-zero terms. To do this, we find the recursion formula for the two terms by setting values for n and finding the summations in terms of l . We then solve this recursion formula to obtain the value for the covariance. We start with the $\hat{a}_i \hat{a}_i^\dagger$ term:

$$F_n = \alpha^2 \sum_{l=0}^{\infty} \beta(r)^{2(n+l)} \frac{(n+l)!}{n!l!} \frac{r_1^{2n} r_2^{2l}}{r^{2(n+l)}} (n+l+1) \quad (3.22)$$

$$\begin{aligned} F_0 &= \frac{\alpha^2 r^4}{(r^2 - \beta(r)^2 r_2^2)^2} \\ F_1 &= \frac{2\alpha^2 \beta(r)^2 r^4 r_1^2}{(r^2 - \beta(r)^2 r_2^2)^3} \\ F_2 &= \frac{3\alpha^2 \beta(r)^4 r^4 r_1^4}{(r^2 - \beta(r)^2 r_2^2)^4} \\ F_3 &= \frac{4\alpha^2 \beta(r)^6 r^4 r_1^6}{(r^2 - \beta(r)^2 r_2^2)^5} \end{aligned} \quad (3.23)$$

Here we can see the recursion formula will be of the form:

$$\begin{aligned}\langle \Psi | \hat{a}_i \hat{a}_i^\dagger | \Psi \rangle &= \alpha^2 r^2 \sum_{i=0}^{\infty} \left(\frac{1}{r^2 - \beta(r)^2 r_2^2} \right)^{i+2} \beta(r)^{2i} r_1^{2i} (i+1) \\ &= \frac{\alpha^2}{(-1 + \beta(r)^2)^2}\end{aligned}\quad (3.24)$$

Now looking at the terms from $\hat{a}_i^\dagger \hat{a}_i$:

$$F_n = \alpha^2 \sum_{l=0}^{\infty} \beta(r)^{2(n+l)} \frac{(n+l)!}{n!l!} \frac{r_1^{2n} r_2^{2l}}{r^{2(n+l)}} (n+l) \quad (3.25)$$

$$\begin{aligned}F_0 &= \frac{\alpha^2 \beta(r)^2 r^2 r_2^2}{(r^2 - \beta(r)^2 r_2^2)^2} \\ F_1 &= \frac{\alpha^2 r^2 r_1^2 (\beta(r)^2 r^2 + \beta(r)^4 r_2^2)}{(r^2 - \beta(r)^2 r_2^2)^3} \\ F_2 &= \frac{\alpha^2 r^2 r_1^4 (2\beta(r)^4 r^2 + \beta(r)^6 r_2^2)}{(r^2 - \beta(r)^2 r_2^2)^4} \\ F_3 &= \frac{\alpha^2 r^2 r_1^6 (3\beta(r)^6 r^2 + \beta(r)^8 r_2^2)}{(r^2 - \beta(r)^2 r_2^2)^5}\end{aligned}\quad (3.26)$$

Here we can see the recursion formula will be of the form:

$$\begin{aligned}\langle \Psi | \hat{a}_i^\dagger \hat{a}_i | \Psi \rangle &= \alpha^2 r^2 \sum_{i=0}^{\infty} \left(\frac{1}{r^2 - \beta(r)^2 r_2^2} \right)^{i+2} r_1^{2i} (i\beta(r)^2 r^2 + \beta(r)^{2(i+1)} r_2^2) \\ &= \frac{\alpha^2 \beta(r)^2}{(-1 + \beta(r)^2)^2}\end{aligned}\quad (3.27)$$

We then combine Equations 4.73 and 3.27 to find:

$$E_i^2 = \frac{\alpha^2 (1 + \beta(r)^2)}{(-1 + \beta(r)^2)^2} \quad (3.28)$$

Now we will look at the two signal paths beginning with $E_{s_1}^2$. These terms differ from the idler path because the signal paths will have an added noise terms as these beams propagate in free space.

$$\begin{aligned}E_{R_1} &= \sqrt{\kappa} (\hat{a}_{s_1} + \hat{a}_{s_1}^\dagger) + \sqrt{1 - \kappa} (\hat{a}_{B_1} + \hat{a}_{B_1}^\dagger) \\ E_{R_1}^2 &= \kappa (\hat{a}_{s_1}^2 + \hat{a}_{s_1}^{2\dagger} + a_{s_1} a_{s_1}^\dagger + a_{s_1}^\dagger a_{s_1}) + (1 - \kappa) (a_{B_1}^2 + a_{B_1}^{\dagger 2} + a_{B_1} a_{B_1}^\dagger + a_{B_1}^\dagger a_{B_1})\end{aligned}$$

$$+ \sqrt{\kappa(1-\kappa)} \left(\hat{a}_{s_1} \hat{a}_{B_1} + \hat{a}_{s_1}^\dagger \hat{a}_{B_1}^\dagger + \hat{a}_{s_1} \hat{a}_{B_1}^\dagger + \hat{a}_{s_1}^\dagger \hat{a}_{B_1} + \hat{a}_{B_1} \hat{a}_{s_1} + \hat{a}_{B_1}^\dagger \hat{a}_{s_1}^\dagger + \hat{a}_{B_1} \hat{a}_{s_1}^\dagger + \hat{a}_{B_1}^\dagger \hat{a}_{s_1} \right) \quad (3.29)$$

where a_{s_1} , a_{s_2} , and a_B are the field mode operators for the signal 1, signal 2, and the noise state respectively. Using the orthogonality conditions we determine that the only non-zero terms are $\hat{a}_{s_1}^\dagger \hat{a}_{s_1}$, $\hat{a}_{s_1} \hat{a}_{s_1}^\dagger$, $\hat{a}_{B_1}^\dagger \hat{a}_{B_1}$, and $\hat{a}_{B_1} \hat{a}_{B_1}^\dagger$ where the coefficients generated from the evaluation of the expectation creation and annihilation operators are $n+1$, n , $N_{B_1}+1$, and N_B respectively. Therefore the expectation value to be evaluated composed of non-zero terms takes the form:

$$\langle \Psi | \hat{a}_{s_1}^\dagger \hat{a}_{s_1} + \hat{a}_{s_1} \hat{a}_{s_1}^\dagger + \hat{a}_{B_1}^\dagger \hat{a}_{B_1} + \hat{a}_{B_1} \hat{a}_{B_1}^\dagger | \Psi \rangle \quad (3.30)$$

Using the same process as Equations A.1-A.4 we determine that the only non-zero terms are $\hat{a}_{s_1}^\dagger \hat{a}_{s_1}$, $\hat{a}_{s_1} \hat{a}_{s_1}^\dagger$, $\hat{a}_{B_1}^\dagger \hat{a}_{B_1}$, and $\hat{a}_{B_1} \hat{a}_{B_1}^\dagger$ where the coefficients generated from the evaluation of the expectation creation and annihilation operators are $n+1$, n , $N_{B_1}+1$, and N_B respectively. Therefore the expectation value to be evaluated composed of non-zero terms takes the form:

$$\langle \Psi | \hat{a}_{s_1}^\dagger \hat{a}_{s_1} + \hat{a}_{B_1}^\dagger \hat{a}_{B_1} + \hat{a}_{B_1} \hat{a}_{B_1}^\dagger + \hat{a}_{B_1}^\dagger \hat{a}_{B_1} | \Psi \rangle \quad (3.31)$$

The evaluation of this expectation value is separated into its four terms where the first term evaluated is $\hat{a}_{s_1} \hat{a}_{s_1}^\dagger$:

$$F_n = \kappa \alpha^2 \sum_{l=0}^{\infty} \beta(r)^{2(n+l)} \frac{(n+l)!}{n!l!} \frac{r_1^{2n} r_2^{2l}}{r^{2(n+l)}} (n+1) \quad (3.32)$$

$$\begin{aligned} F_0 &= \kappa \frac{\alpha^2 r^2}{r^2 - \beta(r)^2 r_2^2} \\ F_1 &= \kappa \frac{2\alpha^2 r^2 \beta(r)^2 r_1^2}{(r^2 - \beta(r)^2 r_2^2)^2} \\ F_2 &= \kappa \frac{3\alpha^2 r^2 \beta(r)^4 r_1^4}{(r^2 - \beta(r)^2 r_2^2)^3} \\ F_3 &= \kappa \frac{4\alpha^2 r^2 \beta(r)^6 r_1^6}{(r^2 - \beta(r)^2 r_2^2)^4} \end{aligned} \quad (3.33)$$

Where the recursion formula will be of the form:

$$\langle \Psi | \hat{a}_{s_1} \hat{a}_{s_1}^\dagger | \Psi \rangle = \kappa \alpha^2 r^2 \sum_{i=0}^{\infty} \left(\frac{1}{r^2 - \beta(r)^2 r_2^2} \right)^{i+1} (i+1) \beta(r)^{2i} r_1^{2i} \quad (3.34)$$

which evaluates to:

$$\langle \Psi | \hat{a}_{s_1} \hat{a}_{s_1}^\dagger | \Psi \rangle = \kappa \frac{\alpha^2 (r^2 - \beta(r)^2 r_2^2)}{r^2 (-1 + \beta(r)^2)^2} \quad (3.35)$$

Next $\hat{a}_{s_1}^\dagger \hat{a}_{s_1}$ is evaluated:

$$F_n = \kappa \alpha^2 \sum_{l=0}^{\infty} \beta(r)^{2(n+l)} \frac{(n+l)!}{n!l!} \frac{r_1^{2n} r_2^{2l}}{r^{2(n+l)}} n \quad (3.36)$$

$$F_0 = 0$$

$$F_1 = \kappa \frac{\alpha^2 r^2 \beta(r)^2 r_1^2}{(r^2 - \beta(r)^2 r_2^2)^2}$$

$$F_2 = \kappa \frac{2\alpha^2 r^2 \beta(r)^4 r_1^4}{(r^2 - \beta(r)^2 r_2^2)^3}$$

$$F_3 = \kappa \frac{3\alpha^2 r^2 \beta(r)^6 r_1^6}{(r^2 - \beta(r)^2 r_2^2)^4} \quad (3.37)$$

Here the recursion formula is seen to be of the form:

$$\begin{aligned} \langle \Psi | \hat{a}_{s_1}^\dagger \hat{a}_{s_1} | \Psi \rangle &= \kappa \alpha^2 r^2 \sum_{i=0}^{\infty} \left(\frac{1}{r^2 - \beta(r)^2 r_2^2} \right)^{i+1} i \beta(r)^{2i} r_1^{2i} \\ &= \kappa \frac{\alpha^2 \beta(r)^2 r_1^2}{r^2 (-1 + \beta(r)^2)^2} \end{aligned} \quad (3.38)$$

Now we complete the noise terms together, $\hat{a}_B \hat{a}_B^\dagger + \hat{a}_B^\dagger \hat{a}_B$ term:

$$F_n = (1 - \kappa) \alpha^2 \sum_{l=0}^{\infty} \beta(r)^{2(n+l)} \frac{(n+l)!}{n!l!} \frac{r_1^{2n} r_2^{2l}}{r^{2(n+l)}} (2N_T + 1) \quad (3.39)$$

$$F_0 = (1 - \kappa) \frac{\alpha^2 r^2 (1 + 2N_T)}{r^2 - \beta(r)^2 r_2^2}$$

$$F_1 = (1 - \kappa) \frac{\alpha^2 r^2 \beta(r)^2 (1 + 2N_T) r_1^2}{(r^2 - \beta(r)^2 r_2^2)^2}$$

$$F_2 = (1 - \kappa) \frac{\alpha^2 r^2 \beta(r)^4 (1 + 2N_T) r_1^4}{(r^2 - \beta(r)^2 r_2^2)^3}$$

$$F_3 = (1 - \kappa) \frac{\alpha^2 r^2 \beta(r)^6 (1 + 2N_T) r_1^6}{(r^2 - \beta(r)^2 r_2^2)^4} \quad (3.40)$$

Here the recursion formula will be of the form:

$$\begin{aligned}\langle \Psi | \hat{a}_B \hat{a}_B^\dagger + \hat{a}_B^\dagger \hat{a}_B | \Psi \rangle &= (1 - \kappa) \alpha^2 r^2 \sum_{i=0}^{\infty} \left(\frac{1}{r^2 - \beta(r)^2 r_2^2} \right)^{i+1} (1 + 2N_T) \beta(r)^{2i} r_1^{2i} \\ &= -(1 - \kappa) \frac{\alpha^2 (1 + 2N_T)}{-1 + \beta(r)^2}\end{aligned}\quad (3.41)$$

To find the covariance term, Equations (3.34), (3.38), and (3.41) are combined:

$$\langle \Psi | E_{R_1}^2 | \Psi \rangle = \frac{\alpha^2 ((1 + \beta(r)^2 (-1 + \kappa - 2N_{B_2}) + 2N_{B_2}) r^2 + \beta(r)^2 \kappa (r_1^2 - r_2^2))}{(-1 + \beta(r)^2)^2 r^2} \quad (3.42)$$

Similarly, the variance term of the second signal path can be found: $\hat{a}_{s_2} \hat{a}_{s_2}^\dagger$ is the first term to be evaluated:

$$F_n = \kappa \alpha^2 \sum_{l=0}^{\infty} \beta(r)^{2(n+l)} \frac{(n+l)!}{n!l!} \frac{r_1^{2n} r_2^{2l}}{r^{2(n+l)}} (l+1) \quad (3.43)$$

$$\begin{aligned}F_0 &= \kappa \frac{\alpha^2 r^2}{(r^2 - \beta(r)^2 r_2^2)^2} \\ F_1 &= \kappa \frac{\alpha^2 r^2 r_1^2 (\beta(r)^2 r^2 + \beta(r)^4 r_2^2)}{(r^2 - \beta(r)^2 r_2^2)^3} \\ F_2 &= \kappa \frac{\alpha^2 r^2 r_1^4 (\beta(r)^4 r^2 + 2\beta(r)^6 r_2^2)}{(r^2 - \beta(r)^2 r_2^2)^4} \\ F_3 &= \kappa \frac{\alpha^2 r^2 r_1^6 (\beta(r)^6 r^2 + 3\beta(r)^8 r_2^2)}{(r^2 - \beta(r)^2 r_2^2)^5}\end{aligned}\quad (3.44)$$

Here we can see the recursion formula will be of the form:

$$\begin{aligned}\langle \Psi | \hat{a}_{s_2} \hat{a}_{s_2}^\dagger | \Psi \rangle &= \kappa \alpha^2 r^2 \sum_{i=0}^{\infty} \left(\frac{1}{r^2 - \beta(r)^2 r_2^2} \right)^{i+2} r_1^{2i} (\beta(r)^{2i} r^2 + i \beta(r)^{2(i+1)} r_2^2) \\ &= \kappa \frac{\alpha^2 (r^2 - \beta(r)^2 r_1^2)}{(-1 + \beta(r)^2)^2 r^2}\end{aligned}\quad (3.45)$$

Now solving the $\hat{a}_{s_2}^\dagger \hat{a}_{s_2}$ term:

$$\begin{aligned}F_n &= \kappa \alpha^2 \sum_{l=0}^{\infty} \beta(r)^{2(n+l)} \frac{(n+l)!}{n!l!} \frac{r_1^{2n} r_2^{2l}}{r^{2(n+l)}} l \\ F_0 &= \kappa \frac{\alpha^2 \beta(r)^2 r^2 r_2^2}{(r^2 - \beta(r)^2 r_2^2)^2} \\ F_1 &= \kappa \frac{2\alpha^2 \beta(r)^4 r^2 r_1^2 r_2^2}{(r^2 - \beta(r)^2 r_2^2)^3}\end{aligned}\quad (3.46)$$

$$\begin{aligned}
F_2 &= \kappa \frac{3\alpha^2 \beta(r)^6 r^2 r_1^4 r_2^2}{(r^2 - \beta(r)^2 r_2^2)^4} \\
F_3 &= \kappa \frac{4\alpha^2 \beta(r)^8 r^2 r_1^6 r_2^2}{(r^2 - \beta(r)^2 r_2^2)^5}
\end{aligned} \tag{3.47}$$

Where the recursion formula will be of the form:

$$\begin{aligned}
\langle \Psi | \hat{a}_{s_2}^\dagger \hat{a}_{s_2} | \Psi \rangle &= \kappa \alpha^2 r^2 r_2^2 \sum_{i=0}^{\infty} \left(\frac{1}{r^2 - \beta(r)^2 r_2^2} \right)^{i+2} r_1^{2i} \beta(r)^{2(i+1)} (i+1) \\
&= \kappa \frac{\alpha^2 \beta(r)^2 r_2^2}{(-1 + \beta(r)^2)^2 r^2}
\end{aligned} \tag{3.48}$$

Where the noise term, (3.41), is combined with Equations (3.45) and (3.48):

$$\langle \Psi | E_{R_2}^2 | \Psi \rangle = \frac{\alpha^2 ((1 + \beta(r)^2 (-1 + \kappa - 2N_{B_2}) + 2N_{B_2}) r^2 + \beta(r)^2 \kappa (-r_1^2 + r_2^2))}{(-1 + \beta(r)^2)^2 r^2} \tag{3.49}$$

Now we will look at the first cross-correlation term in our covariance matrix, but first it should be noted that the final covariance matrix is simplified because it can be shown that the electric fields between branches commute due to the differing mode operator commutators. This allows us to simply solve for only three cross-correlation terms instead of the six that are in the matrix, in other words, the covariance matrix is symmetric. We now determine $E_{R_1} E_{R_2}$, where we again use the orthonormality of the Fock state basis to find the non-zero terms. These terms are found to be $\hat{a}_{s_1}^\dagger \hat{a}_{s_2}$ and $\hat{a}_{s_1} \hat{a}_{s_2}^\dagger$ with coefficients $\kappa \sqrt{l(n+1)}$ and $\kappa \sqrt{n(l+1)}$ respectively. Where we first evaluate $\hat{a}_{s_1} \hat{a}_{s_2}^\dagger$:

$$\langle \Psi | \hat{a}_{s_1} \hat{a}_{s_2}^\dagger | \psi \rangle = \kappa \alpha^2 \sum_{l=0}^{\infty} \beta(r)^{2(n+l)} \frac{(n+l)!}{n!l!} \frac{r_1^{2n} r_2^{2l}}{r^{2(n+l)}} \sqrt{l(n+1)} \tag{3.50}$$

we also see that the function for $\hat{a}_{s_1}^\dagger \hat{a}_{s_2}$ is:

$$\langle \Psi | \hat{a}_{s_1}^\dagger \hat{a}_{s_2} | \psi \rangle = \kappa \alpha^2 \sum_{l=0}^{\infty} \beta(r)^{2(n+l)} \frac{(n+l)!}{n!l!} \frac{r_1^{2n} r_2^{2l}}{r^{2(n+l)}} \sqrt{n(l+1)} \tag{3.51}$$

These equations are not able to be solved trivially using the methods from Equations (3.2) to (3.4). To solve this, we must numerically calculate the resulting expressions because it does not have a closed form evaluation of the sums. We use the above results

together to write:

$$\langle \Psi | E_{s_1} E_{s_2} | \Psi \rangle = \kappa \alpha^2 \sum_{n,l=0}^{\infty} \Xi(n,l) \sqrt{n(l+1)} + \sqrt{l(n+1)} \quad (3.52)$$

where we have defined:

$$\Xi(n,l) = \beta(r)^{2(n+l)} \frac{(n+l)!}{n!l!} \frac{r_1^{2n} r_2^{2l}}{r^{2(n+l)}} \quad (3.53)$$

We now evaluate $E_{s_1} E_i$, where again the signal has an added noise term:

$$\begin{aligned} E_{R_1} &= \sqrt{\kappa}(\hat{a}_{s_1} + \hat{a}_{s_1}^\dagger) + \sqrt{1-\kappa}(\hat{a}_{B_1} + \hat{a}_{B_1}^\dagger) \\ E_i &= \hat{a}_i + \hat{a}_i^\dagger \\ E_{R_1} E_i &= \sqrt{\kappa} \hat{a}_{s_1} \hat{a}_i + \sqrt{\kappa} \hat{a}_{s_1}^\dagger \hat{a}_i + \sqrt{\kappa} \hat{a}_{s_1} \hat{a}_i^\dagger + \sqrt{\kappa} \hat{a}_{s_1}^\dagger \hat{a}_i^\dagger \\ &\quad + \sqrt{1-\kappa} \hat{a}_{B_1} \hat{a}_i + \sqrt{1-\kappa} \hat{a}_{B_1}^\dagger \hat{a}_i + \sqrt{1-\kappa} \hat{a}_{B_1} \hat{a}_i^\dagger + \sqrt{1-\kappa} \hat{a}_{B_1}^\dagger \hat{a}_i^\dagger \end{aligned} \quad (3.54)$$

We again use a general formula to solve this similar to Equation (3.4) and find the solution to be:

$$\langle \Psi | E_{s_1} E_i | \Psi \rangle = \kappa \alpha^2 \sum_{n,l=0}^{\infty} \Xi(n,l) \left(\sqrt{n(n+l)} + \sqrt{(n+1)(n+l+1)} \right)$$

Finally, we calculate $E_{s_2} E_i$ and determine it to be:

$$\langle \Psi | E_{s_2} E_i | \Psi \rangle = \kappa \alpha^2 \sum_{n,l=0}^{\infty} \Xi(n,l) \left(\sqrt{l(n+l)} + \sqrt{(l+1)(n+l+1)} \right) \quad (3.55)$$

Combining the solutions to these terms, and putting them into the covariance matrix discussed earlier, we obtain the matrix seen in Equation (3.56).

$$V = \begin{pmatrix} \langle E_i^2 \rangle & \langle E_i E_{s_1} \rangle & \langle E_i E_{s_2} \rangle \\ \langle E_{s_1} E_i \rangle & \langle E_{s_1}^2 \rangle & \langle E_{s_1} E_{s_2} \rangle \\ \langle E_{s_2} E_i \rangle & \langle E_{s_2} E_{s_1} \rangle & \langle E_{s_2}^2 \rangle \end{pmatrix} \quad (3.56)$$

where for ease of reading, the elements of the matrix are listed below in Equation (4.98):

$$E_i^2 = \frac{\alpha^2(1 + \beta(r)^2)}{(-1 + \beta(r)^2)^2}$$

$$\begin{aligned}
E_{s_1}^2 &= \frac{\alpha^2((1 + \beta(r)^2(-1 + \kappa - 2N_{B_1}) + 2N_{B_1})r^2 + \beta(r)^2\kappa(r_1^2 - r_2^2))}{(-1 + \beta(r)^2)^2 r^2} \\
E_{s_2}^2 &= \frac{\alpha^2((1 + \beta(r)^2(-1 + \kappa - 2N_{B_2}) + 2N_{B_2})r^2 + \beta(r)^2\kappa(-r_1^2 + r_2^2))}{(-1 + \beta(r)^2)^2 r^2} \\
E_{s_1}E_i &= \kappa\alpha^2 \sum_{n,l=0}^{\infty} \Xi(n,l) \left(\sqrt{n(n+l)} + \sqrt{(n+1)(n+l+1)} \right) \\
E_{s_1}E_{s_2} &= \kappa\alpha^2 \sum_{n,l=0}^{\infty} \Xi(n,l) \left(\sqrt{n(l+1)} + \sqrt{l(n+1)} \right) \\
E_{s_2}E_i &= \kappa\alpha^2 \sum_{n,l=0}^{\infty} \Xi(n,l) \left(\sqrt{l(n+l)} + \sqrt{(l+1)(n+l+1)} \right)
\end{aligned} \tag{3.57}$$

3.3 Analysis

Now, that the tripartite covariance matrices has been derived, we plot the correlations at various transmissivities in Figure 3.2. These correlations are solved using the covariances and variances, σ :

$$r_{xy} = \frac{\text{cov}(x, y)}{\sqrt{\sigma_x^2 \sigma_y^2}} \tag{3.58}$$

where the horizontal and vertical axes are r_1 and r_2 respectively. Here one can see that

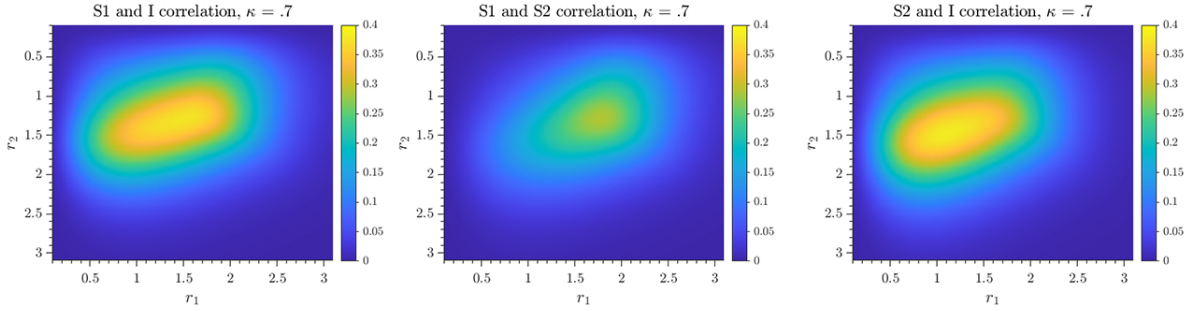


Figure 3.2. Correlations of the three path combinations in terms of r_1 and r_2 , $N_B = 10$.

the correlations between the idler and the individual signal paths are higher than just the signal paths. This may be due to the idler being created through a mixing of the signal paths and the signal paths being created through independent lasers.

Next, we define a detector function that will allow for the system to yield the best possible performance. This detector function is designed to keep the two signals together and correlate them both with the idler at the same time.

To define this system mathematically, we begin with the formula to determine the correlation shown in Equation (3.58) and applying the tripartite system we obtain the

detector function:

$$r_{df} = \frac{\langle (E_{s_1} + E_{s_2}) E_i \rangle}{\sqrt{\langle E_i^2 \rangle \langle E_{s_1}^2 + E_{s_2}^2 + E_{s_1} E_{s_2} \rangle}} \quad (3.59)$$

where each part of this function has been previously solved and is plotted in Figure 3.3 at $\kappa = .07$, $.4$, and $.7$. Where one can see that as the environment becomes more

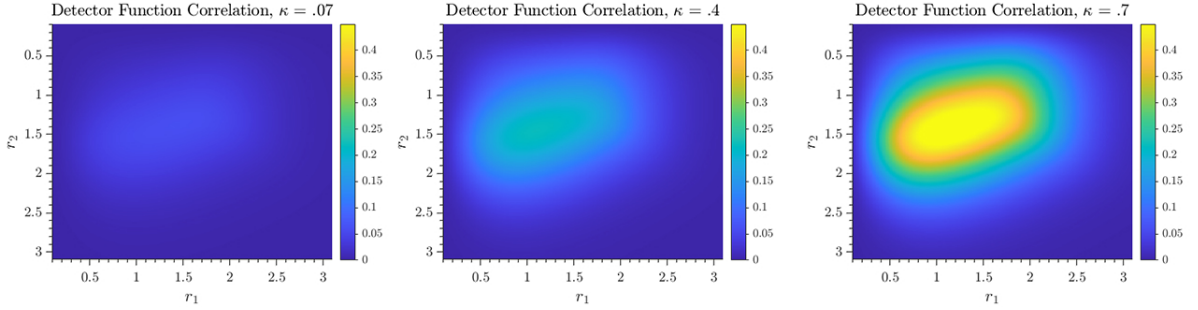


Figure 3.3. Correlations for for the tripartite system using the detector function at various transmissivities, $N_B = 10$.

transmissive (i.e., higher κ), the correlation increases. One can also see based on the correlations determined from the detector function, κ , changing r_1 independently does not have the same effect on the correlation as r_2 . Due to this and the relationship between the individual squeezing factors, one value of N_s can have multiple different correlations. For example, $r_1 = 1.5$ and $r_2 = 1$ has a different correlation than $r_1 = 1$ and $r_2 = 1.5$, but will have the same N_s . To alleviate these degeneracies in the plot, we show the case where $r_1 = r_2$ in Figure 3.4 where it is plotted in comparison to the known bipartite correlation coefficient [33]. One can see that much like current quantum radar systems, the system is more effective at lower signal powers; however, compared to the bipartite system, it does not obtain as high of a correlation. One can also see that the bipartite system continues at higher N_s to have the high correlation, while the tripartite system falls off at high N_s , which again may be due to how N_s is defined. This means that for the tripartite system there is a finite region of significant correlation and increasing the squeezing factor does not always increase the correlation, while the bipartite system continues increasing as the squeezing factor increases until the correlation becomes 1.

3.4 Conclusion

In this paper we derived the electric field covariance matrix for the tripartite quantum radar system. We then showed that with a combined electric field measurement we

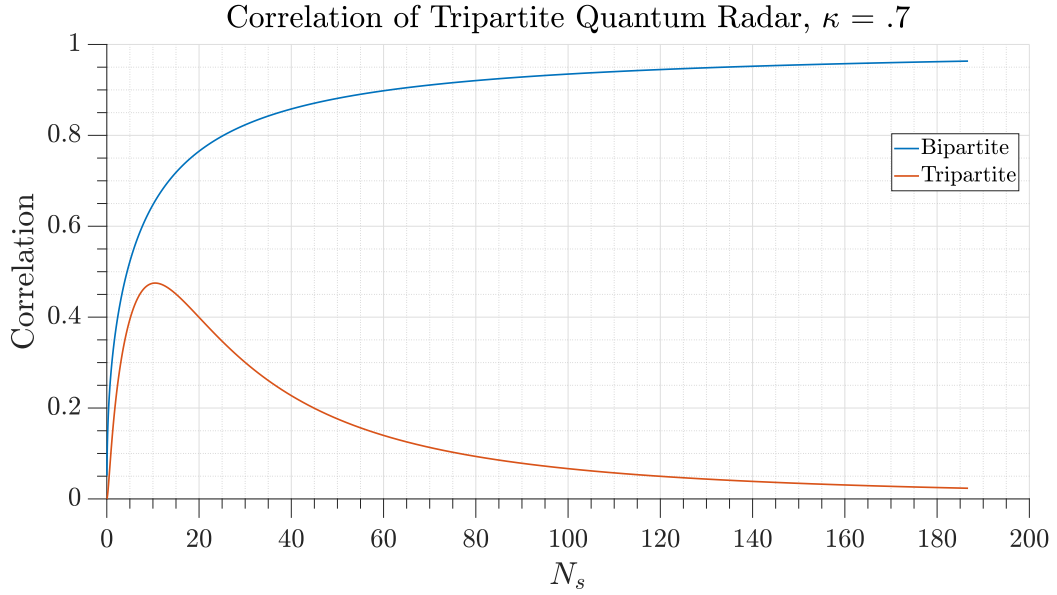


Figure 3.4. Correlations for the tripartite system when $r_1 = r_2$ versus the bipartite system, $N_B=10$

are able to obtain correlations between the different beam paths where, like bipartite quantum radar, the correlations are higher at lower power. However, at higher power levels, these correlations seem to fall off. While more research would have to be done to fully prove these theories, the reason for the fall off of these correlations may be do to how the state is created. The correlation for the bipartite state increases due to the simultaneous creation of the signal and idler photon, while the four-wave mixing that occurs to create the tripartite state could potentially affect the symmetrical nature of the photon waveforms.

From these correlations, it was found that all three paths have correlations with each other which could be useful in creating new detection functions that could be used within a radar or quantum communication system to prevent eavesdropping and increase security.

Overall it seems that the tripartite quantum system is viable for use in correlation based tasks, but lacks in comparison to the current two photon systems. Although, due to the addition of the third photon, a tripartite system may be able to obtain higher N_s , compared to the bipartite system.

Chapter 4 | Derivation of the Tripartite Number Operator Correlation

4.1 Introduction

Much like the previous chapter, this chapter looks to explore the correlation of the tripartite state. However, this section looks at the correlations of photon counting. Both of these methods are extremely common as the measurement systems in quantum radar experiments, so a comparison of their viability with the tripartite state is necessary to have the greatest understanding. Although, this chapter is purely a derivation and the simulation will be discussed as future work. Again, it must be stated that this is looking to obtain the maximum limit of this technology and therefore perfect reflection and a perfect quantum detector is assumed.

4.2 Derivation

We again begin with the coupled three-mode squeezed vacuum state [14]:

$$|\Psi\rangle = \frac{1}{\cosh(r)} \sum_{n,l} (-1)^{n+1} e^{i(n\theta_1+l\theta_2)} \left(\frac{r_1}{r} \tanh(r)\right)^n \left(\frac{r_2}{r} \tanh(r)\right)^l \sqrt{\frac{(n+l)!}{n!l!}} |n, n+l, l\rangle_{s_1, i, s_2} \quad (4.1)$$

where r_1 , and r_2 are the squeezing factors, $r = \sqrt{r_1^2 + r_2^2}$, and θ_1 and θ_2 are the phase terms.

Where we have redefined the wave function in terms of the mean photon number per

mode in Equation (3.13), again stated here:

$$|\Psi\rangle = \alpha \sum_{n,l}^{\infty} (-1)^{n+1} e^{i(n\theta_1 + l\theta_2)} \left(\frac{r_1}{r}\beta(r)\right)^n \left(\frac{r_2}{r}\beta(r)\right)^l \sqrt{\frac{(n+l)!}{n!l!}} |n, n+l, l\rangle_{s_1, i, s_2} \quad (4.2)$$

where $\alpha = \frac{1}{\sqrt{N_i+1}}$ and $\beta(r) = \sqrt{\frac{N_i N_{s_1} r^2}{N_i^2 r_2^2 + N_{s_1} r^2}}$

We can now calculate the terms for the number operator for the covariance matrix. Where unlike the electric field operator the number operator has a non-zero mean:

$$V = \begin{pmatrix} \langle \hat{N}_i^2 \rangle - \langle \hat{N}_i \rangle \langle \hat{N}_i \rangle & \langle \hat{N}_i \hat{N}_{R_1} \rangle - \langle \hat{N}_i \rangle \langle \hat{N}_{R_1} \rangle & \langle \hat{N}_i \hat{N}_{R_2} \rangle - \langle \hat{N}_i \rangle \langle \hat{N}_{R_2} \rangle \\ \langle \hat{N}_{R_1} \hat{N}_i \rangle - \langle \hat{N}_{R_1} \rangle \langle \hat{N}_i \rangle & \langle \hat{N}_{R_1}^2 \rangle - \langle \hat{N}_{R_1} \rangle \langle \hat{N}_{R_1} \rangle & \langle \hat{N}_{R_1} \hat{N}_{R_2} \rangle - \langle \hat{N}_{R_1} \rangle \langle \hat{N}_{R_2} \rangle \\ \langle \hat{N}_{R_2} \hat{N}_i \rangle - \langle \hat{N}_{R_2} \rangle \langle \hat{N}_i \rangle & \langle \hat{N}_{R_2} \hat{N}_{R_1} \rangle - \langle \hat{N}_{R_2} \rangle \langle \hat{N}_{R_1} \rangle & \langle \hat{N}_{R_2}^2 \rangle - \langle \hat{N}_{R_2} \rangle \langle \hat{N}_{R_2} \rangle \end{pmatrix} \quad (4.3)$$

where \hat{N}_x is the number operator for the idler, first signal path, or second signal path ($x = i, s_1,$ and s_2 respectively) defined by [25]:

$$\hat{N}(r, t) \stackrel{\text{def}}{=} \hat{a}^\dagger \hat{a} \quad (4.4)$$

where \hat{a}^\dagger is the creation operator and \hat{a} is the annihilation operator.

Again a tensor product is done to find the physically realizable version of these calculations, this tensor product is done between Equation (4.1) and the thermal noise state. Formally, this calculation is done with a density matrix approach [18, 26], where we first determine the density matrix for the coupled three-mode squeezed vacuum state:

$$\begin{aligned} \rho_{CTSV} &= \frac{1}{\cosh^2(r)} \sum_{n,l,m,k}^{\infty} (-1)^{n+m+2} e^{i(n\theta_1 + l\theta_2)} e^{-i(m\theta_1 + k\theta_2)} \\ &\times \left(\frac{r_1}{r}\beta(r)\right)^{m+n} \left(\frac{r_2}{r}\beta(r)\right)^{l+k} \sqrt{\frac{(n+l)!}{n!l!}} \sqrt{\frac{(m+k)!}{m!k!}} |n, n+l, l, j\rangle \langle m, m+k, k, j| \end{aligned} \quad (4.5)$$

and the density matrix for the thermal noise state [26, 27]:

$$\rho_T = \frac{1}{N_T + 1} \sum_i \left(\frac{N_T}{N_T + 1}\right)^i |i\rangle \langle i| \quad (4.6)$$

where N_T is the mean photon number of the thermal state. The return density matrix is

defined as:

$$\begin{aligned} \rho_{return} &= \rho_{CTSV} \otimes \rho_T = \frac{1}{\cosh^2(r)} \frac{1}{N_T + 1} \sum_{n,l,m,k}^{\infty} (-1)^{n+m+2} e^{i(n\theta_1+l\theta_2)} e^{-i(m\theta_1+k\theta_2)} \\ &\times \left(\frac{r_1}{r} \tanh(r)\right)^{m+n} \left(\frac{r_2}{r} \tanh(r)\right)^{l+k} \sqrt{\frac{(n+l)!}{n!l!}} \sqrt{\frac{(m+k)!}{m!k!}} |n, n+l, l, i, j\rangle \langle m, m+k, k, i, j| \end{aligned} \quad (4.7)$$

which can be shown to be approximately valid in the high-noise regime.

From the covariance matrix it can be seen there are 6 different expectation values that need to be solved: $\langle \hat{N}_i^2 \rangle$, $\langle \hat{N}_{R_1}^2 \rangle$, $\langle \hat{N}_{R_2}^2 \rangle$, $\langle \hat{N}_i \rangle$, $\langle \hat{N}_{R_1} \rangle$, and $\langle \hat{N}_{R_2} \rangle$. We begin evaluating the non-zero terms of $\langle \hat{N}_i^2 \rangle$ first:

$$N_i^2 = \hat{a}_i^\dagger \hat{a}_i \hat{a}_i^\dagger \hat{a}_i \quad (4.8)$$

Where applying this as an operator on the wave function gives us the coefficient:

$$\langle m, m+k, k | \hat{a}_i^\dagger \hat{a}_i \hat{a}_i^\dagger \hat{a}_i | n, n+l, l \rangle = (n+l)^2 \quad (4.9)$$

which gives us the function:

$$\langle \Psi | \hat{a}_i^\dagger \hat{a}_i \hat{a}_i^\dagger \hat{a}_i | \Psi \rangle = \alpha^2 \sum_{n,l=0}^{\infty} \beta^{2(n+l)} \frac{(n+l)!}{n!l!} \frac{r_1^{2n} r_2^{2l}}{r^{2(n+l)}} (n+l)^2 \quad (4.10)$$

which does not have a trivial solution, therefore we solve it with a recursion relation:

$$F_n = \alpha^2 \sum_{l=0}^{\infty} \beta(r)^{2(n+l)} \frac{(n+l)!}{n!l!} \frac{r_1^{2n} r_2^{2l}}{r^{2(n+l)}} (n+l)^2 \quad (4.11)$$

$$F_0 = \frac{\alpha^2 \beta^2 r^2 r_2^2 (r^2 + \beta^2 r_2^2)}{(r^2 - \beta(r)^2 r_2^2)^3}$$

$$F_1 = \frac{\alpha^2 r^2 r_1^2 (\beta^2 r^4 + 4\beta^4 r^2 r_2^2 + \beta^6 r_2^4)}{(r^2 - \beta(r)^2 r_2^2)^4}$$

$$F_2 = \frac{\alpha^2 r^2 r_1^4 (4\beta^4 r^4 + 7\beta^6 r^2 r_2^2 + \beta^8 r_2^4)}{(r^2 - \beta(r)^2 r_2^2)^5}$$

$$F_3 = \frac{\alpha^2 r^2 r_1^6 (9\beta^6 r^2 + 10\beta^8 r^2 r_2^2 + \beta^{10} r_2^4)}{(r^2 - \beta(r)^2 r_2^2)^6} \quad (4.12)$$

Here we can see the recursion formula will be of the form:

$$\begin{aligned}\langle \Psi | \hat{a}_i^\dagger \hat{a}_i \hat{a}_i^\dagger \hat{a}_i | \Psi \rangle &= \alpha^2 r^2 \sum_{i=0}^{\infty} \left(\frac{1}{r^2 - \beta(r)^2 r_2^2} \right)^{i+3} r_1^{2i} \left(i^2 \beta^{2i} r^4 + (3i+1) \beta^{2(i+1)} r^2 r_2^2 + \beta^{2(i+2)} r_2^4 \right) \\ &= \frac{\alpha^2 \beta^2 (1 + \beta^2)}{(\beta^2 - 1)^3}\end{aligned}\quad (4.13)$$

Now we look at solving $\langle N_i \rangle$:

$$\langle \Psi | \hat{a}_i^\dagger \hat{a}_i | \Psi \rangle = \alpha^2 \sum_{n,l=0}^{\infty} \beta^{2(n+1)} \frac{(n+l)!}{n!l!} \frac{r_1^{2n} r_2^{2l}}{r^{2(n+1)}} (n+l) \quad (4.14)$$

which again is not trivially solvable:

$$F_n = \alpha^2 \sum_{l=0}^{\infty} \beta(r)^{2(n+l)} \frac{(n+l)!}{n!l!} \frac{r_1^{2n} r_2^{2l}}{r^{2(n+l)}} (n+l) \quad (4.15)$$

$$\begin{aligned}F_0 &= \frac{\alpha^2 \beta^2 r^2 r_2^2}{(r^2 - \beta(r)^2 r_2^2)^2} \\ F_1 &= \frac{\alpha^2 r^2 r_1^2 (\beta^2 r^2 + 4\beta^4 r_2^2)}{(r^2 - \beta(r)^2 r_2^2)^3} \\ F_2 &= \frac{\alpha^2 r^2 r_1^4 (2\beta^4 r^2 + \beta^6 r_2^2)}{(r^2 - \beta(r)^2 r_2^2)^4} \\ F_3 &= \frac{\alpha^2 r^2 r_1^6 (3\beta^6 r^2 + \beta^8 r_2^2)}{(r^2 - \beta(r)^2 r_2^2)^5}\end{aligned}\quad (4.16)$$

and gives the form:

$$\begin{aligned}\langle \Psi | \hat{a}_i^\dagger \hat{a}_i | \Psi \rangle &= \alpha^2 r^2 \sum_{i=0}^{\infty} \left(\frac{1}{r^2 - \beta(r)^2 r_2^2} \right)^{i+2} r_1^{2i} \left(i \beta^{2i} r^2 + \beta^{2(i+1)} r_2^2 \right) \\ &= -\frac{\alpha^2 \beta^2}{(\beta^2 - 1)^2}\end{aligned}\quad (4.17)$$

To solve two signal paths we again have to include the thermal noise:

$$\hat{a}_R = \sqrt{\kappa} \hat{a}_s + \sqrt{1 - \kappa} \hat{a}_B \quad (4.18)$$

Now looking at the number operator of the form $\hat{a}_R^\dagger \hat{a}_R$, we find:

$$\begin{aligned}\hat{N}_R &= \left(\sqrt{\kappa} \hat{a}_s^\dagger + \sqrt{1 - \kappa} \hat{a}_B^\dagger \right) \left(\sqrt{\kappa} \hat{a}_s + \sqrt{1 - \kappa} \hat{a}_B \right) \\ &= \kappa \hat{a}_s^\dagger \hat{a}_s + \sqrt{\kappa(1 - \kappa)} (\hat{a}_s^\dagger \hat{a}_B + \hat{a}_B^\dagger \hat{a}_s) + (1 - \kappa) \hat{a}_B^\dagger \hat{a}_B\end{aligned}\quad (4.19)$$

where due to the orthogonality of the Fock State basis, the middle term is zero, and therefore begin with solving $\langle N_{R_1} \rangle$:

$$\langle \Psi | \hat{a}_{s_1}^\dagger \hat{a}_{s_1} | \Psi \rangle = \alpha^2 \sum_{n,l=0}^{\infty} \beta^{2(n+l)} \frac{(n+l)!}{n!l!} \frac{r_1^{2n} r_2^{2l}}{r^{2(n+l)}} n \quad (4.20)$$

where we use the recursion relationship:

$$F_n = \alpha^2 \sum_{l=0}^{\infty} \beta(r)^{2(n+l)} \frac{(n+l)!}{n!l!} \frac{r_1^{2n} r_2^{2l}}{r^{2(n+l)}} n \quad (4.21)$$

$$F_0 = 0$$

$$F_1 = \frac{\alpha^2 \beta^2 r^2 r_1^2}{(r^2 - \beta(r)^2 r_2^2)^2}$$

$$F_2 = \frac{2\alpha^2 \beta^4 r^2 r_1^4}{(r^2 - \beta(r)^2 r_2^2)^3}$$

$$F_3 = \frac{3\alpha^2 \beta^6 r^2 r_1^6}{(r^2 - \beta(r)^2 r_2^2)^4} \quad (4.22)$$

finding the form to be:

$$\begin{aligned} \langle \Psi | \hat{a}_{s_1}^\dagger \hat{a}_{s_1} | \Psi \rangle &= \alpha^2 r^2 \sum_{i=0}^{\infty} \left(\frac{1}{r^2 - \beta(r)^2 r_2^2} \right)^{i+1} i \beta^{2i} r_1^{2i} \\ &= \frac{\alpha^2 \beta^2 r_1^2}{(\beta^2 - 1)^2 r^2} \end{aligned} \quad (4.23)$$

Now we solve the noise portion, $\hat{a}_B^\dagger \hat{a}_B$:

$$\langle \Psi | \hat{a}_B^\dagger \hat{a}_B | \Psi \rangle = \alpha^2 \frac{1}{N_T + 1} \sum_{n,l=0}^{\infty} \beta^{2(n+l)} \frac{(n+l)!}{n!l!} \frac{r_1^{2n} r_2^{2l}}{r^{2(n+l)}} N_T \quad (4.24)$$

where using recursion:

$$F_n = \alpha^2 \sum_{l=0}^{\infty} \beta(r)^{2(n+l)} \frac{(n+l)!}{n!l!} \frac{r_1^{2n} r_2^{2l}}{r^{2(n+l)}} N_T \quad (4.25)$$

$$F_0 = \frac{\alpha^2 N_T r^2}{r^2 - \beta^2 r_2^2}$$

$$F_1 = \frac{\alpha^2 \beta^2 N_T r^2 r_1^2}{(r^2 - \beta^2 r_2^2)^2}$$

$$F_2 = \frac{\alpha^2 \beta^4 N_T r^2 r_1^4}{(r^2 - \beta^2 r_2^2)^3}$$

$$F_3 = \frac{\alpha^2 \beta^6 N_T r^2 r_1^6}{(r^2 - \beta^2 r_2^2)^4} \quad (4.26)$$

we find:

$$\begin{aligned} \langle \Psi | \hat{a}_B^\dagger \hat{a}_B | \Psi \rangle &= \alpha^2 r^2 N_T \sum_{i=0}^{\infty} \left(\frac{1}{r^2 - \beta(r)^2 r_2^2} \right)^{i+1} \beta^{2i} r_1^{2i} \\ &= \frac{\alpha^2 N_T}{1 - \beta^2} \end{aligned} \quad (4.27)$$

therefore:

$$\langle N_{R_1} \rangle = \kappa \frac{\alpha^2 \beta^2 r_1^2}{(\beta^2 - 1)^2 r^2} + (1 - \kappa) \frac{\alpha^2 N_T}{1 - \beta^2} \quad (4.28)$$

where $N_T = \frac{1}{1-\kappa} N_B$ and N_B is the mean noise number per mode. Therefore we find:

$$\langle N_{R_1} \rangle = \alpha^2 \left(\frac{N_B}{1 - \beta^2} + \frac{\beta^2 \kappa r_1^2}{(-1 + \beta^2) r^2} \right) \quad (4.29)$$

Now we do the same steps with $\langle N_{s_2} \rangle$:

$$\langle \Psi | \hat{a}_{s_2}^\dagger \hat{a}_{s_2} | \Psi \rangle = \alpha^2 \sum_{n,l=0}^{\infty} \beta^{2(n+l)} \frac{(n+l)!}{n!l!} \frac{r_1^{2n} r_2^{2l}}{r^{2(n+l)}} l \quad (4.30)$$

using recursion:

$$F_n = \alpha^2 \sum_{l=0}^{\infty} \beta(r)^{2(n+l)} \frac{(n+l)!}{n!l!} \frac{r_1^{2n} r_2^{2l}}{r^{2(n+l)}} l \quad (4.31)$$

$$\begin{aligned} F_0 &= \frac{\alpha^2 \beta^2 r^2 r_2^2}{(r^2 - \beta(r)^2 r_2^2)^2} \\ F_1 &= \frac{2\alpha^2 \beta^4 r^2 r_1^2 r_2^2}{(r^2 - \beta(r)^2 r_2^2)^3} \\ F_2 &= \frac{3\alpha^2 \beta^6 r^2 r_1^4 r_2^2}{(r^2 - \beta(r)^2 r_2^2)^4} \\ F_3 &= \frac{4\alpha^2 \beta^8 r^2 r_1^6 r_2^2}{(r^2 - \beta(r)^2 r_2^2)^5} \end{aligned} \quad (4.32)$$

finding:

$$\langle \Psi | \hat{a}_{s_2}^\dagger \hat{a}_{s_2} | \Psi \rangle = \alpha^2 r^2 \sum_{i=0}^{\infty} \left(\frac{1}{r^2 - \beta(r)^2 r_2^2} \right)^{i+2} (i+1) \beta^{2(i+1)} r_1^{2i}$$

$$= \frac{\alpha^2 \beta^2 r_2^2}{(\beta^2 - 1)^2 r^2} \quad (4.33)$$

Now while the noise experience by the signal paths will be different, the atmosphere in which the signals travel will be the same. Due to this we make a simplifying assumption that $N_{B_1} = N_{B_2}$. Therefore we find:

$$\begin{aligned} \langle N_{R_2} \rangle &= \kappa \frac{\alpha^2 \beta^2 r_2^2}{(\beta^2 - 1)^2 r^2} + (1 - \kappa) \frac{\alpha^2 N_T}{1 - \beta^2} \\ &= \langle N_{R_2} \rangle = \alpha^2 \left(\frac{N_B}{1 - \beta^2} + \frac{\beta^2 \kappa r_2^2}{(-1 + \beta^2) r^2} \right) \end{aligned} \quad (4.34)$$

It should be noted that $\langle N_{s_1} \rangle$ and $\langle N_{s_2} \rangle$ are remarkably similar differing only by which squeezing factor is used within the equation in the signal portion. Therefore if r_1 is equal to r_2 the variance of these two terms is identical.

Similarly to the previous noisy terms, the squared terms, $\langle N_{s_1} \rangle^2$ and $\langle N_{s_2} \rangle^2$, have non-zero terms due to the orthogonality of the Fock States Basis. To find these terms we expand the form $\hat{a}_R^\dagger \hat{a}_R \hat{a}_R^\dagger \hat{a}_R$:

$$\begin{aligned} \hat{N}_R^2 &= \left(\sqrt{\kappa} \hat{a}_s^\dagger + \sqrt{1 - \kappa} \hat{a}_B^\dagger \right) \left(\sqrt{\kappa} \hat{a}_s + \sqrt{1 - \kappa} \hat{a}_B \right) \left(\sqrt{\kappa} \hat{a}_s^\dagger + \sqrt{1 - \kappa} \hat{a}_B^\dagger \right) \left(\sqrt{\kappa} \hat{a}_s + \sqrt{1 - \kappa} \hat{a}_B \right) \\ &= \left(\kappa \hat{a}_s^\dagger \hat{a}_s + \sqrt{\kappa(1 - \kappa)} (\hat{a}_s^\dagger \hat{a}_B + \hat{a}_B^\dagger \hat{a}_s) + (1 - \kappa) \hat{a}_B^\dagger \hat{a}_B \right) \\ &\quad * \left(\kappa \hat{a}_s^\dagger \hat{a}_s + \sqrt{\kappa(1 - \kappa)} (\hat{a}_s^\dagger \hat{a}_B + \hat{a}_B^\dagger \hat{a}_s) + (1 - \kappa) \hat{a}_B^\dagger \hat{a}_B \right) \end{aligned} \quad (4.35)$$

where we eliminate the non-zero terms to simplify factoring:

$$\langle \hat{N}_R^2 \rangle = \kappa^2 \hat{a}_s^\dagger \hat{a}_s \hat{a}_s^\dagger \hat{a}_s + 2\kappa(1 - \kappa) \hat{a}_s^\dagger \hat{a}_s + (1 - \kappa) \hat{a}_B^\dagger \hat{a}_B + \kappa(1 - \kappa) (\hat{a}_s^\dagger \hat{a}_B \hat{a}_B^\dagger \hat{a}_s + \hat{a}_B^\dagger \hat{a}_s \hat{a}_s^\dagger \hat{a}_B) \quad (4.36)$$

Now beginning to solve $\langle N_{s_1} \rangle^2$ with the pure signal term:

$$\langle \Psi | \hat{a}_{s_1}^\dagger \hat{a}_{s_1} \hat{a}_{s_1}^\dagger \hat{a}_{s_1} | \Psi \rangle = \alpha^2 \sum_{n,l=0}^{\infty} \beta^{2(n+l)} \frac{(n+l)!}{n!l!} \frac{r_1^{2n} r_2^{2l}}{r^{2(n+l)}} n^2 \quad (4.37)$$

where we again use a recursion relation:

$$\begin{aligned} F_n &= \alpha^2 \sum_{l=0}^{\infty} \beta(r)^{2(n+l)} \frac{(n+l)!}{n!l!} \frac{r_1^{2n} r_2^{2l}}{r^{2(n+l)}} n^2 \\ F_0 &= 0 \end{aligned} \quad (4.38)$$

$$\begin{aligned}
F_1 &= \frac{\alpha^2 \beta^2 r^2 r_1^2}{(r^2 - \beta(r)^2 r_2^2)^2} \\
F_2 &= \frac{4\alpha^2 \beta^4 r^2 r_1^4}{(r^2 - \beta(r)^2 r_2^2)^3} \\
F_3 &= \frac{9\alpha^2 \beta^6 r^2 r_1^6}{(r^2 - \beta(r)^2 r_2^2)^4}
\end{aligned} \tag{4.39}$$

which when evaluated finds:

$$\begin{aligned}
\langle \Psi | \hat{a}_{s_1}^\dagger \hat{a}_{s_1} \hat{a}_{s_1}^\dagger \hat{a}_{s_1} | \Psi \rangle &= \alpha^2 r^2 \sum_{i=0}^{\infty} \left(\frac{1}{r^2 - \beta(r)^2 r_2^2} \right)^{i+1} i^2 \beta^{2i} r_1^{2i} \\
&= -\frac{\alpha^2 \beta^2 r_1^2 (r^2 + \beta^2 (r_1^2 - r_2^2))}{(\beta^2 - 1)^3 r^4}
\end{aligned} \tag{4.40}$$

Now solving the mixed term:

$$\langle \Psi | \hat{a}_B^\dagger \hat{a}_B \hat{a}_{s_1}^\dagger \hat{a}_{s_1} | \Psi \rangle = \alpha^2 \frac{1}{N_T + 1} \sum_{n,l=0}^{\infty} \beta^{2(n+1)} \frac{(n+l)!}{n!l!} \frac{r_1^{2n} r_2^{2l}}{r^{2(n+1)}} N_T n \tag{4.41}$$

which does not have a trivial solution, therefore we solve it with a recursion relation:

$$\begin{aligned}
F_n &= \alpha^2 \sum_{l=0}^{\infty} \beta(r)^{2(n+l)} \frac{(n+l)!}{n!l!} \frac{r_1^{2n} r_2^{2l}}{r^{2(n+l)}} N_T n \\
F_0 &= 0 \\
F_1 &= \frac{\alpha^2 \beta^2 N_T r^2 r_1^2}{(r^2 - \beta^2 r_2^2)^2} \\
F_2 &= \frac{2\alpha^2 \beta^4 N_T r^2 r_1^4}{(r^2 - \beta^2 r_2^2)^3} \\
F_3 &= \frac{3\alpha^2 \beta^6 N_T r^2 r_1^6}{(r^2 - \beta^2 r_2^2)^4}
\end{aligned} \tag{4.42}$$

$$\begin{aligned}
F_1 &= \frac{\alpha^2 \beta^2 N_T r^2 r_1^2}{(r^2 - \beta^2 r_2^2)^2} \\
F_2 &= \frac{2\alpha^2 \beta^4 N_T r^2 r_1^4}{(r^2 - \beta^2 r_2^2)^3} \\
F_3 &= \frac{3\alpha^2 \beta^6 N_T r^2 r_1^6}{(r^2 - \beta^2 r_2^2)^4}
\end{aligned} \tag{4.43}$$

Here we can see the recursion formula will be of the form:

$$\begin{aligned}
\langle \Psi | \hat{a}_B^\dagger \hat{a}_B \hat{a}_{s_1}^\dagger \hat{a}_{s_1} | \Psi \rangle &= \alpha^2 r^2 N_T \sum_{i=0}^{\infty} \left(\frac{1}{r^2 - \beta(r)^2 r_2^2} \right)^{i+1} i \beta^{2i} r_1^{2i} \\
&= \frac{\alpha^2 \beta^2 N_T r_1^2}{(-1 + \beta^2)^2}
\end{aligned} \tag{4.44}$$

another mixed term:

$$\langle \Psi | \hat{a}_{s_1}^\dagger \hat{a}_B \hat{a}_B^\dagger \hat{a}_{s_1} | \Psi \rangle = \alpha^2 \frac{1}{N_T + 1} \sum_{n,l=0}^{\infty} \beta^{2(n+l)} \frac{(n+l)!}{n!l!} \frac{r_1^{2n} r_2^{2l}}{r^{2(n+l)}} (N_T(n+1)) \quad (4.45)$$

which does not have a trivial solution, therefore we solve it with a recursion relation:

$$F_n = \alpha^2 \sum_{l=0}^{\infty} \beta(r)^{2(n+l)} \frac{(n+l)!}{n!l!} \frac{r_1^{2n} r_2^{2l}}{r^{2(n+l)}} (N_T(n+1)) \quad (4.46)$$

$$\begin{aligned} F_0 &= \frac{\alpha^2 N_T r^2}{(r^2 - \beta^2 r_2^2)} \\ F_1 &= \frac{2\alpha^2 \beta^2 N_T r^2 r_1^2}{(r^2 - \beta^2 r_2^2)^2} \\ F_2 &= \frac{3\alpha^2 \beta^4 N_T r^2 r_1^4}{(r^2 - \beta^2 r_2^2)^3} \\ F_3 &= \frac{4\alpha^2 \beta^6 N_T r^2 r_1^6}{(r^2 - \beta^2 r_2^2)^4} \end{aligned} \quad (4.47)$$

Here we can see the recursion formula will be of the form:

$$\begin{aligned} \langle \Psi | \hat{a}_{s_1}^\dagger \hat{a}_B \hat{a}_B^\dagger \hat{a}_{s_1} | \Psi \rangle &= \alpha^2 r^2 N_T \sum_{i=0}^{\infty} \left(\frac{1}{r^2 - \beta(r)^2 r_2^2} \right)^{i+1} (i+1) \beta^{2i} r_1^{2i} \\ &= \frac{\alpha^2 N_T (r^2 - \beta^2 r_2^2)}{(-1 + \beta^2)^2 r^2} \end{aligned} \quad (4.48)$$

the final mixed term:

$$\langle \Psi | \hat{a}_B^\dagger \hat{a}_{s_1} \hat{a}_{s_1}^\dagger \hat{a}_B | \Psi \rangle = \alpha^2 \frac{1}{N_T + 1} \sum_{n,l=0}^{\infty} \beta^{2(n+l)} \frac{(n+l)!}{n!l!} \frac{r_1^{2n} r_2^{2l}}{r^{2(n+l)}} (n(N_T + 1)) \quad (4.49)$$

which does not have a trivial solution, therefore we solve it with a recursion relation:

$$F_n = \alpha^2 \sum_{l=0}^{\infty} \beta(r)^{2(n+l)} \frac{(n+l)!}{n!l!} \frac{r_1^{2n} r_2^{2l}}{r^{2(n+l)}} (n(N_T + 1)) \quad (4.50)$$

$$\begin{aligned} F_0 &= 0 \\ F_1 &= \frac{\alpha^2 (\beta^2 r^2 r_1^2 + \beta^2 N_T r^2 r_1^2)}{(r^2 - \beta^2 r_2^2)^2} \\ F_2 &= \frac{2\alpha^2 (\beta^4 r^2 r_1^4 + \beta^4 N_T r^2 r_1^4)}{(r^2 - \beta^2 r_2^2)^3} \\ F_3 &= \frac{3\alpha^2 (\beta^6 r^2 r_1^6 + \beta^6 N_T r^2 r_1^6)}{(r^2 - \beta^2 r_2^2)^4} \end{aligned} \quad (4.51)$$

Here we can see the recursion formula will be of the form:

$$\begin{aligned}\langle \Psi | \hat{a}_B^\dagger \hat{a}_{s_1} \hat{a}_{s_1}^\dagger \hat{a}_B | \Psi \rangle &= \alpha^2 r^2 \sum_{i=0}^{\infty} \left(\frac{1}{r^2 - \beta(r)^2 r_2^2} \right)^{i+1} i(N_T + 1) \beta^{2i} r_1^{2i} \\ &= \frac{\alpha^2 \beta^2 (1 + N_T) r_1^2}{(-1 + \beta^2)^2 r^2}\end{aligned}\quad (4.52)$$

Finally solving the pure noise term:

$$\langle \Psi | \hat{a}_B^\dagger \hat{a}_B \hat{a}_B^\dagger \hat{a}_B | \Psi \rangle = \alpha^2 \frac{1}{N_T + 1} \sum_{n,l=0}^{\infty} \beta^{2(n+l)} \frac{(n+l)!}{n!l!} \frac{r_1^{2n} r_2^{2l}}{r^{2(n+l)}} N_T \quad (4.53)$$

which has a recursion relation:

$$F_n = \alpha^2 \sum_{l=0}^{\infty} \beta(r)^{2(n+l)} \frac{(n+l)!}{n!l!} \frac{r_1^{2n} r_2^{2l}}{r^{2(n+l)}} N_T \quad (4.54)$$

$$\begin{aligned}F_0 &= \frac{\alpha^2 N_T^2 r^2}{r^2 - \beta^2 r_2^2} \\ F_1 &= \frac{\alpha^2 \beta^2 N_T^2 r^2 r_1^2}{(r^2 - \beta^2 r_2^2)^2} \\ F_2 &= \frac{\alpha^2 \beta^4 N_T^2 r^2 r_1^4}{(r^2 - \beta^2 r_2^2)^3} \\ F_3 &= \frac{\alpha^2 \beta^6 N_T^2 r^2 r_1^6}{(r^2 - \beta^2 r_2^2)^4}\end{aligned}\quad (4.55)$$

which is solvable:

$$\begin{aligned}\langle \Psi | \hat{a}_B^\dagger \hat{a}_B \hat{a}_B^\dagger \hat{a}_B | \Psi \rangle &= \alpha^2 r^2 N_T^2 \sum_{i=0}^{\infty} \left(\frac{1}{r^2 - \beta(r)^2 r_2^2} \right)^{i+1} \beta^{2i} r_1^{2i} \\ &= \frac{\alpha^2 N_T^2}{1 - \beta^2}\end{aligned}\quad (4.56)$$

Now combining these five terms:

$$\begin{aligned}\langle N_{s_1} \rangle^2 &= \frac{\alpha^2 N_B^2}{1 - \beta^2} + \frac{2\alpha^2 \beta^2 \kappa N_B r_1^2}{(-1 + \beta^2)^2 r^2} + \frac{\alpha^4 \beta^2 \kappa (-1 + \kappa - N_B) N_B^2 r_1^2 (-r^2 + \beta^2 r_2^2)}{(-1 + \beta^2)^2 (-1 + \kappa)^2 r^2} \\ &\quad - \frac{\alpha^2 \beta^2 \kappa^2 r_1^2 (r^2 + \beta^2 (r_1^2 - r_2^2))}{(-1 + \beta^2)^3 r^4}\end{aligned}\quad (4.57)$$

Now solving $\langle N_{s_2}^2 \rangle$ beginning with the only signal term:

$$\langle \Psi | \hat{a}_{s_2}^\dagger \hat{a}_{s_2} \hat{a}_{s_2}^\dagger \hat{a}_{s_2} | \Psi \rangle = \alpha^2 \sum_{n,l=0}^{\infty} \beta^{2(n+l)} \frac{(n+l)!}{n!l!} \frac{r_1^{2n} r_2^{2l}}{r^{2(n+l)}} l^2 \quad (4.58)$$

we solve it with a recursion relation:

$$F_n = \alpha^2 \sum_{l=0}^{\infty} \beta(r)^{2(n+l)} \frac{(n+l)!}{n!l!} \frac{r_1^{2n} r_2^{2l}}{r^{2(n+l)}} l^2 \quad (4.59)$$

$$\begin{aligned} F_0 &= \frac{\alpha^2 \beta^2 r^2 r_2^2 (r^2 + \beta^2 r_2^2)}{(r^2 - \beta(r)^2 r_2^2)^3} \\ F_1 &= \frac{2\alpha^2 \beta^4 r^2 r_1^2 r_2^2 (r^2 + 2\beta^2 r_2^2)}{(r^2 - \beta(r)^2 r_2^2)^4} \\ F_2 &= \frac{3\alpha^2 \beta^6 r^2 r_1^4 r_2^2 (r^2 + 3\beta^2 r_2^2)}{(r^2 - \beta(r)^2 r_2^2)^5} \\ F_3 &= \frac{4\alpha^2 \beta^6 r^2 r_1^6 r_2^2 (r^2 + 4\beta^2 r_2^2)}{(r^2 - \beta(r)^2 r_2^2)^6} \end{aligned} \quad (4.60)$$

finding the form:

$$\begin{aligned} \langle \Psi | \hat{a}_{s_2}^\dagger \hat{a}_{s_2} \hat{a}_{s_2}^\dagger \hat{a}_{s_2} | \Psi \rangle &= \alpha^2 r^2 \sum_{i=0}^{\infty} \left(\frac{1}{r^2 - \beta(r)^2 r_2^2} \right)^{i+3} (i+1) r_1^{2i} \beta^{2(i+1)} (r^2 + (i+1)\beta^2 r_2^2) \\ &= -\frac{\alpha^2 \beta^2 r_1^2 (r^2 + \beta^2 (-r_1^2 + r_2^2))}{(\beta^2 - 1)^3 r^4} \end{aligned} \quad (4.61)$$

Now we calculate the mixed term:

$$\langle \Psi | \hat{a}_B^\dagger \hat{a}_B \hat{a}_{s_1}^\dagger \hat{a}_{s_1} | \Psi \rangle = \alpha^2 \frac{1}{N_T + 1} \sum_{n,l=0}^{\infty} \beta^{2(n+l)} \frac{(n+l)!}{n!l!} \frac{r_1^{2n} r_2^{2l}}{r^{2(n+l)}} N_T l \quad (4.62)$$

which is not trivial, therefore:

$$\begin{aligned} F_n &= \alpha^2 \sum_{l=0}^{\infty} \beta(r)^{2(n+l)} \frac{(n+l)!}{n!l!} \frac{r_1^{2n} r_2^{2l}}{r^{2(n+l)}} N_T l \\ F_0 &= \frac{\alpha^2 \beta^2 N_T r^2 r_2^2}{(r^2 - \beta^2 r_2^2)^2} \\ F_1 &= \frac{2\alpha^2 \beta^2 N_T r^2 r_1^2 r_2^2}{(r^2 - \beta^2 r_2^2)^3} \\ F_2 &= \frac{3\alpha^2 \beta^4 N_T r^2 r_1^4 r_2^2}{(r^2 - \beta^2 r_2^2)^4} \end{aligned} \quad (4.63)$$

$$F_3 = \frac{4\alpha^2\beta^6 N_T r^2 r_1^6 r_2^2}{(r^2 - \beta^2 r_2^2)^5} \quad (4.64)$$

finding:

$$\begin{aligned} \langle \Psi | \hat{a}_B^\dagger \hat{a}_B \hat{a}_{s_1}^\dagger \hat{a}_{s_1} | \Psi \rangle &= \alpha^2 r^2 r_2^2 N_T \sum_{i=0}^{\infty} \left(\frac{1}{r^2 - \beta(r)^2 r_2^2} \right)^{i+2} (i+1) \beta^{2(i+1)} r_1^{2i} \\ &= \frac{\alpha^2 \beta^2 N_T r_2^2}{(-1 + \beta^2)^2} \end{aligned} \quad (4.65)$$

another mixed term:

$$\langle \Psi | \hat{a}_{s_2}^\dagger \hat{a}_B \hat{a}_B^\dagger \hat{a}_{s_2} | \Psi \rangle = \alpha^2 \frac{1}{N_T + 1} \sum_{n,l=0}^{\infty} \beta^{2(n+l)} \frac{(n+l)!}{n!l!} \frac{r_1^{2n} r_2^{2l}}{r^{2(n+l)}} (N_T(l+1)) \quad (4.66)$$

which does not have a trivial solution, therefore we solve it with a recursion relation:

$$F_n = \alpha^2 \sum_{l=0}^{\infty} \beta(r)^{2(n+l)} \frac{(n+l)!}{n!l!} \frac{r_1^{2n} r_2^{2l}}{r^{2(n+l)}} (N_T(l+1)) \quad (4.67)$$

$$\begin{aligned} F_0 &= \frac{\alpha^2 N_T r^4}{(r^2 - \beta^2 r_2^2)} \\ F_1 &= \frac{\alpha^2 N_T r^2 r_1^2 (\beta^2 r^2 + \beta^4 r_2^2)}{(r^2 - \beta^2 r_2^2)^3} \\ F_2 &= \frac{\alpha^2 N_T r^2 r_1^4 (\beta^4 r^2 + \beta^6 r_2^2)}{(r^2 - \beta^2 r_2^2)^4} \\ F_3 &= \frac{\alpha^2 N_T r^2 r_1^6 (\beta^6 r^2 + \beta^8 r_2^2)}{(r^2 - \beta^2 r_2^2)^5} \end{aligned} \quad (4.68)$$

Here we can see the recursion formula will be of the form:

$$\begin{aligned} \langle \Psi | \hat{a}_{s_1}^\dagger \hat{a}_B \hat{a}_B^\dagger \hat{a}_{s_1} | \Psi \rangle &= \alpha^2 r^2 N_T \sum_{i=0}^{\infty} \left(\frac{1}{r^2 - \beta(r)^2 r_2^2} \right)^{i+2} r_1^{2i} (\beta^{2i} r^2 + i \beta^{2(i+1)} r_2^2) \\ &= \frac{\alpha^2 N_T (r^2 - \beta^2 r_2^2)}{(-1 + \beta^2)^2 r^2} \end{aligned} \quad (4.69)$$

the final mixed term:

$$\langle \Psi | \hat{a}_B^\dagger \hat{a}_{s_2} \hat{a}_{s_2}^\dagger \hat{a}_B | \Psi \rangle = \alpha^2 \frac{1}{N_T + 1} \sum_{n,l=0}^{\infty} \beta^{2(n+l)} \frac{(n+l)!}{n!l!} \frac{r_1^{2n} r_2^{2l}}{r^{2(n+l)}} (l(N_T + 1)) \quad (4.70)$$

which does not have a trivial solution, therefore we solve it with a recursion relation:

$$F_n = \alpha^2 \sum_{l=0}^{\infty} \beta(r)^{2(n+l)} \frac{(n+l)!}{n!l!} \frac{r_1^{2n} r_2^{2l}}{r^{2(n+l)}} (l(N_T + 1)) \quad (4.71)$$

$$\begin{aligned} F_0 &= \frac{\alpha^2(\beta^2 r^2 r_2^2 + \beta^2 N_T r^2 r_2^2)}{(r^2 - \beta^2 r_2^2)^2} \\ F_1 &= \frac{2\alpha^2(\beta^4 r^2 r_2^4 + \beta^4 N_T r^2 r_2^4)}{(r^2 - \beta^2 r_2^2)^3} \\ F_2 &= \frac{3\alpha^2(\beta^6 r^2 r_2^6 + \beta^6 N_T r^2 r_2^6)}{(r^2 - \beta^2 r_2^2)^4} \\ F_4 &= \frac{4\alpha^2(\beta^8 r^2 r_2^8 + \beta^8 N_T r^2 r_2^8)}{(r^2 - \beta^2 r_2^2)^5} \end{aligned} \quad (4.72)$$

Here we can see the recursion formula will be of the form:

$$\begin{aligned} \langle \Psi | \hat{a}_B^\dagger \hat{a}_{s_1} \hat{a}_{s_1}^\dagger \hat{a}_B | \Psi \rangle &= \alpha^2 r^2 \sum_{i=0}^{\infty} \left(\frac{1}{r^2 - \beta(r)^2 r_2^2} \right)^{i+2} (i+1)(N_T + 1) \beta^{2(i+1)} r_1^{2i} r_2^2 \\ &= \frac{\alpha^2 \beta^2 (1 + N_T) r_2^2}{(-1 + \beta^2)^2 r^2} \end{aligned} \quad (4.73)$$

Combining these terms and the earlier noise term we find the solution to be:

$$\begin{aligned} \langle N_{s_2} \rangle^2 &= \frac{\alpha^2 N_B^2}{1 - \beta^2} + \frac{2\alpha^2 \beta^2 \kappa N_B r_2^2}{(-1 + \beta^2)^2 r^2} + \frac{\alpha^4 \beta^2 \kappa (-1 + \kappa - N_B) N_B^2 r_2^2 (-r^2 + \beta^2 r_1^2)}{(-1 + \beta^2)^2 (-1 + \kappa)^2 r^2} \\ &\quad - \frac{\alpha^2 \beta^2 \kappa^2 r_2^2 (r^2 + \beta^2 (-r_1^2 + r_2^2))}{(-1 + \beta^2)^3 r^4} \end{aligned} \quad (4.74)$$

Where when compared with the equation for $\langle N_{s_1} \rangle$ there are only a few differences, namely some switching of the squeezing factors. Now to calculate $\langle \hat{N}_{R_1} \hat{N}_i \rangle$ we first define the terms:

$$\begin{aligned} \langle \hat{N}_{R_1} \hat{N}_i \rangle &= \hat{a}_{R_1}^\dagger \hat{a}_{R_1} \hat{a}_i^\dagger \hat{a}_i \\ &= (\kappa \hat{a}_s^\dagger \hat{a}_s + \sqrt{\kappa(1 - \kappa)} (\hat{a}_s^\dagger \hat{a}_B + \hat{a}_B^\dagger \hat{a}_s) + (1 - \kappa) \hat{a}_B^\dagger \hat{a}_B) (\hat{a}_i^\dagger \hat{a}_i) \\ &= \kappa \hat{a}_s^\dagger \hat{a}_s \hat{a}_i^\dagger \hat{a}_i + (1 - \kappa) \hat{a}_B^\dagger \hat{a}_B \hat{a}_i^\dagger \hat{a}_i \end{aligned} \quad (4.75)$$

First we solve the noiseless term:

$$\langle \Psi | \hat{a}_{s_1}^\dagger \hat{a}_{s_1} \hat{a}_i^\dagger \hat{a}_i | \Psi \rangle = \alpha^2 \frac{1}{N_T + 1} \sum_{n,l=0}^{\infty} \beta^{2(n+l)} \frac{(n+l)!}{n!l!} \frac{r_1^{2n} r_2^{2l}}{r^{2(n+l)}} (n+l)n \quad (4.76)$$

which is solved with recursion:

$$F_n = \alpha^2 \sum_{l=0}^{\infty} \beta(r)^{2(n+l)} \frac{(n+l)!}{n!!} \frac{r_1^{2n} r_2^{2l}}{r^{2(n+l)}} (n+l)n \quad (4.77)$$

$$F_0 = 0$$

$$F_1 = \frac{\alpha^2 r^2 r_1^2 (\beta^2 r^2 + \beta^4 r_2^2)}{(r^2 - \beta^2 r_2^2)^3}$$

$$F_2 = \frac{2\alpha^2 r^2 r_1^4 (2\beta^4 r^2 + \beta^6 r_2^2)}{(r^2 - \beta^2 r_2^2)^4}$$

$$F_3 = \frac{3\alpha^2 r^2 r_1^6 (3\beta^6 r^2 + \beta^8 r_2^2)}{(r^2 - \beta^2 r_2^2)^5} \quad (4.78)$$

finding:

$$\begin{aligned} \langle \Psi | \hat{a}_{s_1}^\dagger \hat{a}_{s_1} \hat{a}_i^\dagger \hat{a}_i | \Psi \rangle &= \alpha^2 r^2 \sum_{i=0}^{\infty} \left(\frac{1}{r^2 - \beta(r)^2 r_2^2} \right)^{i+2} r_1^{2i} (i\beta^{2i} r^2 + \beta^{2(i+1)} r_2^2) \\ &= \frac{\alpha^2 \beta^2 (1 + \beta^2) r_1^2}{(-1 + \beta^2)^3 r^2} \end{aligned} \quad (4.79)$$

Now the final term:

$$\langle \Psi | \hat{a}_B^\dagger \hat{a}_B \hat{a}_i^\dagger \hat{a}_i | \Psi \rangle = \alpha^2 \frac{1}{N_T + 1} \sum_{n,l=0}^{\infty} \beta^{2(n+l)} \frac{(n+l)!}{n!!} \frac{r_1^{2n} r_2^{2l}}{r^{2(n+l)}} (n+l)n \quad (4.80)$$

recursively:

$$F_n = \alpha^2 \sum_{l=0}^{\infty} \beta(r)^{2(n+l)} \frac{(n+l)!}{n!!} \frac{r_1^{2n} r_2^{2l}}{r^{2(n+l)}} (n+l) N_T \quad (4.81)$$

$$F_0 = \frac{\alpha^2 \beta^2 N_T r^2 r_2^2}{(r^2 - \beta^2 r_2^2)^2}$$

$$F_1 = \frac{\alpha^2 N_T r^2 r_1^2 (\beta^2 r^2 + \beta^4 r_2^2)}{(r^2 - \beta^2 r_2^2)^3}$$

$$F_2 = \frac{\alpha^2 N_T r^2 r_1^4 (2\beta^4 r^2 + \beta^6 r_2^2)}{(r^2 - \beta^2 r_2^2)^4}$$

$$F_3 = \frac{\alpha^2 N_T r^2 r_1^6 (3\beta^6 r^2 + \beta^8 r_2^2)}{(r^2 - \beta^2 r_2^2)^5} \quad (4.82)$$

which takes the form:

$$\langle \Psi | \hat{a}_B^\dagger \hat{a}_B \hat{a}_i^\dagger \hat{a}_i | \Psi \rangle = \alpha^2 r^2 N_T \sum_{i=0}^{\infty} \left(\frac{1}{r^2 - \beta(r)^2 r_2^2} \right)^{i+2} r_1^{2i} (i\beta^{2i} r^2 + \beta^{2(i+1)} r_2^2)$$

$$= \frac{\alpha^2 \beta^2 N_T}{(-1 + \beta^2)^2} \quad (4.83)$$

Combining these terms and substituting for N_T :

$$\langle \hat{N}_{R_1} \hat{N}_i \rangle = \frac{\alpha^2 \beta^2 \left(\frac{(-1+\beta^2)N_B}{\sqrt{1-\kappa}} - \frac{(1+\beta^2)\sqrt{\kappa}r_1^2}{r^2} \right)}{(-1 + \beta^2)^3} \quad (4.84)$$

Now to calculate $\langle \hat{N}_{R_2} \hat{N}_i \rangle$ we first define the terms:

$$\begin{aligned} \langle \hat{N}_{R_2} \hat{N}_i \rangle &= \hat{a}_{R_2}^\dagger \hat{a}_{R_2} \hat{a}_i^\dagger \hat{a}_i \\ &= (\kappa \hat{a}_{s_2}^\dagger \hat{a}_{s_2} + \sqrt{\kappa(1-\kappa)}(\hat{a}_{s_2}^\dagger \hat{a}_B + \hat{a}_B^\dagger \hat{a}_{s_2}) + (1-\kappa)\hat{a}_B^\dagger \hat{a}_B)(\hat{a}_i^\dagger \hat{a}_i) \\ &= \kappa \hat{a}_{s_2}^\dagger \hat{a}_{s_2} \hat{a}_i^\dagger \hat{a}_i + (1-\kappa)\hat{a}_B^\dagger \hat{a}_B \hat{a}_i^\dagger \hat{a}_i \end{aligned} \quad (4.85)$$

First we solve the noiseless term:

$$\langle \Psi | \hat{a}_{s_2}^\dagger \hat{a}_{s_2} \hat{a}_i^\dagger \hat{a}_i | \Psi \rangle = \alpha^2 \frac{1}{N_T + 1} \sum_{n,l=0}^{\infty} \beta^{2(n+l)} \frac{(n+l)!}{n!l!} \frac{r_1^{2n} r_2^{2l}}{r^{2(n+l)}} (n+l)l \quad (4.86)$$

which is solved with recursion:

$$\begin{aligned} F_n &= \alpha^2 \sum_{l=0}^{\infty} \beta(r)^{2(n+l)} \frac{(n+l)!}{n!l!} \frac{r_1^{2n} r_2^{2l}}{r^{2(n+l)}} (n+l)l \quad (4.87) \\ F_0 &= \frac{\alpha^2 \beta^2 r^2 r_2^2 (r^2 + \beta^2 r_2^2)}{(r^2 - \beta^2 r_2^2)^3} \\ F_1 &= \frac{2\alpha^2 \beta^4 r^2 r_1^2 r_2^2 (2r^2 + \beta^2 r_2^2)}{(r^2 - \beta^2 r_2^2)^4} \\ F_2 &= \frac{3\alpha^2 \beta^6 r^2 r_1^4 r_2^2 (3r^2 + \beta^2 r_2^2)}{(r^2 - \beta^2 r_2^2)^5} \\ F_3 &= \frac{4\alpha^2 \beta^8 r^2 r_1^6 r_2^2 (4r^2 + \beta^2 r_2^2)}{(r^2 - \beta^2 r_2^2)^6} \end{aligned} \quad (4.88)$$

finding:

$$\begin{aligned} \langle \Psi | \hat{a}_{s_1}^\dagger \hat{a}_{s_1} \hat{a}_i^\dagger \hat{a}_i | \Psi \rangle &= \alpha^2 r^2 r_2^2 \sum_{i=0}^{\infty} \left(\frac{1}{r^2 - \beta(r)^2 r_2^2} \right)^{i+3} r_1^{2i} \beta^{2(i+1)} (i+1) \left((i+1)r^2 + \beta^2 r_2^2 \right) \\ &= \frac{\alpha^2 \beta^2 (1 + \beta^2) r_2^2}{(-1 + \beta^2)^3 r^2} \end{aligned} \quad (4.89)$$

Combining this term with the previously calculated noise cross term in Equation

(4.83) and substituting for N_T :

$$\langle \hat{N}_{R_2} \hat{N}_i \rangle = \frac{\alpha^2 \beta^2 \left(\frac{(-1+\beta^2)N_B}{\sqrt{1-\kappa}} - \frac{(1+\beta^2)\sqrt{\kappa}r_2^2}{r^2} \right)}{(-1+\beta^2)^3} \quad (4.90)$$

Now to calculate $\langle \hat{N}_{R_1} \hat{N}_{R_2} \rangle$ we first define the terms:

$$\begin{aligned} \langle \hat{N}_{R_1} \hat{N}_{R_2} \rangle &= \hat{a}_{R_1}^\dagger \hat{a}_{R_1} \hat{a}_{R_2}^\dagger \hat{a}_{R_2} \\ &= (\kappa \hat{a}_{s_1}^\dagger \hat{a}_{s_1} + \sqrt{\kappa(1-\kappa)}(\hat{a}_{s_1}^\dagger \hat{a}_B + \hat{a}_B^\dagger \hat{a}_{s_1}) + (1-\kappa)\hat{a}_B^\dagger \hat{a}_B) \\ &\quad (\kappa \hat{a}_{s_2}^\dagger \hat{a}_{s_2} + \sqrt{\kappa(1-\kappa)}(\hat{a}_{s_2}^\dagger \hat{a}_B + \hat{a}_B^\dagger \hat{a}_{s_2}) + (1-\kappa)\hat{a}_B^\dagger \hat{a}_B) \\ &= \kappa^2 \hat{a}_{s_1}^\dagger \hat{a}_{s_1} \hat{a}_{s_2}^\dagger \hat{a}_{s_2} + \kappa(1-\kappa)\hat{a}_{s_1}^\dagger \hat{a}_{s_1} \hat{a}_B^\dagger \hat{a}_B + \kappa(1-\kappa)\hat{a}_{s_2}^\dagger \hat{a}_{s_2} \hat{a}_B^\dagger \hat{a}_B + (1-\kappa)^2 \hat{a}_B^\dagger \hat{a}_B \hat{a}_B^\dagger \hat{a}_B \end{aligned} \quad (4.91)$$

Most of these terms have already been calculated previously, however $\langle \hat{a}_{s_1}^\dagger \hat{a}_{s_1} \hat{a}_{s_2}^\dagger \hat{a}_{s_2} \rangle$ has not been calculated.

$$\langle \Psi | \hat{a}_{s_2}^\dagger \hat{a}_{s_2} \hat{a}_i^\dagger \hat{a}_i | \Psi \rangle = \alpha^2 \frac{1}{N_T + 1} \sum_{n,l=0}^{\infty} \beta^{2(n+l)} \frac{(n+l)!}{n!l!} \frac{r_1^{2n} r_2^{2l}}{r^{2(n+l)}} nl \quad (4.92)$$

which is solved with recursion:

$$F_n = \alpha^2 \sum_{l=0}^{\infty} \beta(r)^{2(n+l)} \frac{(n+l)!}{n!l!} \frac{r_1^{2n} r_2^{2l}}{r^{2(n+l)}} nl \quad (4.93)$$

$$F_0 = 0$$

$$F_1 = \frac{2\alpha^2 \beta^4 r^2 r_1^2 r_2^2}{(r^2 - \beta^2 r_2^2)^3}$$

$$F_2 = \frac{6\alpha^2 \beta^6 r^2 r_1^4 r_2^2}{(r^2 - \beta^2 r_2^2)^4}$$

$$F_3 = \frac{12\alpha^2 \beta^8 r^2 r_1^6 r_2^2}{(r^2 - \beta^2 r_2^2)^5} \quad (4.94)$$

finding:

$$\begin{aligned} \langle \Psi | \hat{a}_{s_1}^\dagger \hat{a}_{s_1} \hat{a}_i^\dagger \hat{a}_i | \Psi \rangle &= \alpha^2 r^2 r_2^2 \sum_{i=0}^{\infty} \left(\frac{1}{r^2 - \beta(r)^2 r_2^2} \right)^{i+2} r_1^{2i} \beta^{2(i+1)} i(i+1) \\ &= -\frac{2\alpha^2 \beta^4 r_1^2 r_2^2}{(-1+\beta^2)^3 r^4} \end{aligned} \quad (4.95)$$

Combining all the terms:

$$\begin{aligned}
\langle \hat{N}_{R_1} \hat{N}_{R_2} \rangle &= -\kappa^2 \frac{2\alpha^2 \beta^4 r_1^2 r_2^2}{(-1 + \beta^2)^3 r^4} + \kappa(1 - \kappa) \left(\frac{\alpha^2 \beta^2 N_T r_2^2}{(-1 + \beta^2)^2} + \frac{\alpha^2 \beta^2 N_T r_1^2}{(-1 + \beta^2)^2} \right) + (1 - \kappa)^2 \frac{\alpha^2 N_T^2}{1 - \beta^2} \\
&= \frac{\alpha^2 (\beta^2 \kappa r_1^2 ((-1 + \beta^2) N_B r^2 - 2\beta^2 \kappa r_2^2) + (-1 + \beta^2) N_B r^2 ((1 - \beta^2) N_B r^2 + \beta^2 \kappa r_2^2))}{(-1 + \beta^2)^3 r^4}
\end{aligned} \tag{4.96}$$

Now we combine the solutions to these terms, and put them into the covariance matrix, we obtain the matrix seen in Equation (4.97).

$$V = \begin{pmatrix} \langle \hat{N}_i^2 \rangle - \langle \hat{N}_i \rangle \langle \hat{N}_i \rangle & \langle \hat{N}_i \hat{N}_{R_1} \rangle - \langle \hat{N}_i \rangle \langle \hat{N}_{R_1} \rangle & \langle \hat{N}_i \hat{N}_{R_2} \rangle - \langle \hat{N}_i \rangle \langle \hat{N}_{R_2} \rangle \\ \langle \hat{N}_{R_1} \hat{N}_i \rangle - \langle \hat{N}_{R_1} \rangle \langle \hat{N}_i \rangle & \langle \hat{N}_{R_1}^2 \rangle - \langle \hat{N}_{R_1} \rangle \langle \hat{N}_{R_1} \rangle & \langle \hat{N}_{R_1} \hat{N}_{R_2} \rangle - \langle \hat{N}_{R_1} \rangle \langle \hat{N}_{R_2} \rangle \\ \langle \hat{N}_{R_2} \hat{N}_i \rangle - \langle \hat{N}_{R_2} \rangle \langle \hat{N}_i \rangle & \langle \hat{N}_{R_2} \hat{N}_{R_1} \rangle - \langle \hat{N}_{R_2} \rangle \langle \hat{N}_{R_1} \rangle & \langle \hat{N}_{R_2}^2 \rangle - \langle \hat{N}_{R_2} \rangle \langle \hat{N}_{R_2} \rangle \end{pmatrix} \tag{4.97}$$

where for ease of reading, the elements of the matrix are listed below in Equation (4.98):

$$\begin{aligned}
\langle \hat{N}_i^2 \rangle &= -\frac{\alpha^2 \beta^2 (1 + \beta^2)}{(\beta^2 - 1)^3} \\
\langle N_{s_1} \rangle^2 &= \frac{\alpha^2 N_B^2}{1 - \beta^2} + \frac{2\alpha^2 \beta^2 \kappa N_B r_1^2}{(-1 + \beta^2)^2 r^2} + \frac{\alpha^4 \beta^2 \kappa (-1 + \kappa - N_B) N_B^2 r_1^2 (-r^2 + \beta^2 r_2^2)}{(-1 + \beta^2)^2 (-1 + \kappa)^2 r^2} \\
&\quad - \frac{\alpha^2 \beta^2 \kappa^2 r_1^2 (r^2 + \beta^2 (r_1^2 - r_2^2))}{(-1 + \beta^2)^3 r^4} \\
\langle N_{s_1} \rangle^2 &= \frac{\alpha^2 N_B^2}{1 - \beta^2} + \frac{2\alpha^2 \beta^2 \kappa N_B r_1^2}{(-1 + \beta^2)^2 r^2} + \frac{\alpha^4 \beta^2 \kappa (-1 + \kappa - N_B) N_B^2 r_1^2 (-r^2 + \beta^2 r_2^2)}{(-1 + \beta^2)^2 (-1 + \kappa)^2 r^2} \\
&\quad - \frac{\alpha^2 \beta^2 \kappa^2 r_1^2 (r^2 + \beta^2 (r_1^2 - r_2^2))}{(-1 + \beta^2)^3 r^4} \\
\langle \hat{N}_i \rangle &= \frac{\alpha^2 \beta^2}{(\beta^2 - 1)^2} \\
\langle \hat{N}_{R_1} \rangle &= \alpha^2 \left(\frac{N_B}{1 - \beta^2} + \frac{\beta^2 \kappa r_1^2}{(-1 + \beta^2)^2 r^2} \right) \\
\langle \hat{N}_{R_2} \rangle &= \alpha^2 \left(\frac{N_B}{1 - \beta^2} + \frac{\beta^2 \kappa r_2^2}{(-1 + \beta^2)^2 r^2} \right) \\
\langle \hat{N}_{R_1} \hat{N}_{R_2} \rangle &= \frac{\alpha^2 (\beta^2 \kappa r_1^2 ((-1 + \beta^2) N_B r^2 - 2\beta^2 \kappa r_2^2) + (-1 + \beta^2) N_B r^2 ((1 - \beta^2) N_B r^2 + \beta^2 \kappa r_2^2))}{(-1 + \beta^2)^3 r^4} \\
\langle \hat{N}_{R_1} \hat{N}_i \rangle &= \frac{\alpha^2 \beta^2 \left(\frac{(-1 + \beta^2) N_B}{\sqrt{1 - \kappa}} - \frac{(1 + \beta^2) \sqrt{\kappa} r_1^2}{r^2} \right)}{(-1 + \beta^2)^3}
\end{aligned} \tag{4.98}$$

$$\langle \hat{N}_{R_2} \hat{N}_i \rangle = \frac{\alpha^2 \beta^2 \left(\frac{(-1+\beta^2)N_B}{\sqrt{1-\kappa}} - \frac{(1+\beta^2)\sqrt{\kappa}r_2^2}{r^2} \right)}{(-1 + \beta^2)^3} \quad (4.98)$$

4.3 Conclusion

In this chapter we derived the photon counting covariance matrix for the tripartite quantum radar system. A simulation similar to the electric field measurement for the tripartite system was done, but only imaginary results were obtained. After a thorough evaluation of the mathematics of the system, it is believed that the four-wave mixing augments the spatial coherence of the idler waveform in such a way that the waveform is no longer equivalent to a mixture of the two signal waveforms. This would cause the sign changes to not lineup in the correlation coefficients and give imaginary values, which are physically realizable. More tests and alternate ways to correlate this signals should be explored.

Chapter 5 |

Conclusions and Future Work

This dissertation evaluated and analyzed the correlation coefficients for a number of measurement styles for both bipartite and tripartite radar systems. As quantum radar continues to grow and evolve, so will our understanding of the underlying principles of the technology. With the newfound focus on quantum materials in the search for quantum supremacy, quantum radar has the chance to quickly surpass classical technologies. With this analysis of the measurement and creation schemes of quantum radar systems, hopefully a greater understanding on what carries the greatest viability is already understood and able to quickly acted upon. Although all of these schemes have advantages, the following should be known:

- The coupled-three mode state does not seem to be a viable option at increasing the power over the bipartite state without increasing our understanding of current technologies. Bipartite quantum radar seems to be vastly superior in every way, including ease of use, and should be the focus of research until another way to easily generate tripartite states is posited.
- In a low power bipartite quantum radar system, electric field measurements and quadrature measurements appear to always outperform the photon counting measurements. Although photon counting measurements seem to reach higher correlations when a greater number of photons is achieved. With the current focus on using quantum radar as a low-power substitute for classical systems, these measurement schemes will be more effective.
- Within these bipartite system, changing N_B does not seem to have an effect on the overall correlations of the system. This seems to back the idea that the increase in resolution in the low signal-to-noise ration regime is caused by the ability to correlate the binary waveforms instead of just the macro waveforms.

5.1 Future Work

Due to the ideal nature of the calculations done in this dissertation, future work is proposed that evaluates the correlation loss of these systems without ideal assumptions. The main assumption that should be addressed is the effect of scattering on photon waveform correlations that are used in quantum radar systems. While scattering was included within these calculations via the use of transmissivity, a simple percentage may not realistically convey the system. If scattering has a great effect on the systems that were derived in this paper than the long-term viability of quantum radar as a long-distance, discrete sensing system may be called into question.

Appendix A | Evaluating the Fock State Basis of the Tripartite State

A.1 Electric Field Operator

This section shows the Fock state analysis of each term in the tripartite electric field analysis. We begin with \hat{a}_i^2 :

$$\begin{aligned} \langle m, m+k, k | \hat{a}_i^2 | n, n+l, l \rangle &= \sqrt{(n+l)(n+l-1)} \langle m, m+k, k | n, n+l-2, l \rangle \\ m &= n \\ m+k &= n+l-2 \\ k &= l \end{aligned} \tag{A.1}$$

We see that these equations do not have a possible solution that would satisfy a nonzero inner product, therefore $\langle \Psi | \hat{a}_i^2 | \Psi \rangle = 0$. Next we evaluate $\hat{a}_i^{\dagger 2}$:

$$\begin{aligned} \langle m, m+k, k | \hat{a}_i^{\dagger 2} | n, n+l, l \rangle &= \sqrt{(n+l+1)(n+l+2)} \langle m, m+k, k | n, n+l+2, l \rangle \\ m &= n \\ m+k &= n+l+2 \\ k &= l \end{aligned} \tag{A.2}$$

It is again found that there is no solution to satisfy the inner product, which gives, $\langle \Psi | \hat{a}_i^{\dagger 2} | \Psi \rangle = 0$. Now, $\langle \Psi | \hat{a}_i \hat{a}_i^\dagger | \Psi \rangle$. Now we evaluate $\hat{a}_i \hat{a}_i^\dagger$:

$$\langle m, m+k, k | \hat{a}_i \hat{a}_i^\dagger | n, n+l, l \rangle = (n+l+1) \langle m, m+k, k | n, n+l, l \rangle$$

$$\begin{aligned}
m &= n \\
m + k &= n + l \\
k &= l
\end{aligned} \tag{A.3}$$

These equations do indeed yield a non-zero inner product, the details of which will be given shortly. Finally, we look at $\langle \Psi | \hat{a}_i^\dagger \hat{a}_i | \Psi \rangle$:

$$\begin{aligned}
\langle m, m + k, k | \hat{a}_i^\dagger \hat{a}_i | n, n + l, l \rangle &= (n + l) \langle m, m + k, k | n, n + l, l \rangle \\
m &= n \\
m + k &= n + l \\
k &= l
\end{aligned} \tag{A.4}$$

This term also is non-zero.

$E_{R_1}^2$ terms, $\hat{a}_{1_2}^2$:

$$\begin{aligned}
\langle m, m + k, k | \hat{a}_{s_1}^2 | n, n + l, l \rangle &= \sqrt{n(n-1)} \langle m, m + k, k | n - 2, n + l, l \rangle \\
m &= n - 2 \\
m + k &= n + l \\
k &= l
\end{aligned} \tag{A.5}$$

which is zero, $\hat{a}_{s_1}^{2\dagger}$:

$$\begin{aligned}
\langle m, m + k, k | \hat{a}_{s_1}^2 \hat{a}_{s_1}^{2\dagger} | n, n + l, l \rangle &= \sqrt{(n+2)(n+1)} \langle m, m + k, k | n + 2, n + l, l \rangle \\
m &= n + 2 \\
m + k &= n + l \\
k &= l
\end{aligned} \tag{A.6}$$

which is zero, $\hat{a}_{s_1} \hat{a}_{s_1}^\dagger$:

$$\begin{aligned}
\langle m, m + k, k | \hat{a}_{s_1} \hat{a}_{s_1}^\dagger | n, n + l, l \rangle &= (n + 1) \langle m, m + k, k | n, n + l, l \rangle \\
m &= n \\
m + k &= n + l \\
k &= l
\end{aligned} \tag{A.7}$$

which is nonzero, $\hat{a}_{s_1}^\dagger \hat{a}_{s_1}$:

$$\begin{aligned} \langle m, m+k, k | \hat{a}_{s_1}^\dagger \hat{a}_{s_1} | n, n+l, l \rangle &= n \langle m, m+k, k | n, n+l, l \rangle \\ m &= n \\ m+k &= n+l \\ k &= l \end{aligned} \tag{A.8}$$

which is nonzero, \hat{a}_B^2 :

$$\begin{aligned} \langle m, m+k, k, N_P | \hat{a}_B^2 | n, n+l, l, N_T \rangle &= \sqrt{N_T(N_T+1)} \langle m, m+k, k, N_P | n+2, n+l, l, N_T-2 \rangle \\ m &= n+2 \\ m+k &= n+l \\ k &= l \\ N_P &= N_T-2 \end{aligned} \tag{A.9}$$

which is zero, $\hat{a}_B^{2\dagger}$:

$$\begin{aligned} \langle m, m+k, k, N_P | \hat{a}_B^{2\dagger} | n, n+l, l, N_T \rangle &= \sqrt{(N_T+2)(M+T+1)} \langle m, m+k, k, N_P | n+1, n+l, l, N_T+2 \rangle \\ m &= n+2 \\ m+k &= n+l \\ k &= l \\ N_P &= N_T+2 \end{aligned} \tag{A.10}$$

which is zero, $\hat{a}_B \hat{a}_B^\dagger$:

$$\begin{aligned} \langle m, m+k, k, N_P | \hat{a}_B \hat{a}_B^\dagger | n, n+l, l, N_T \rangle &= (N_T+1) \langle m, m+k, k, N_P | n, n+l, l, N_T \rangle \\ m &= n \\ m+k &= n+l \\ k &= l \\ N_P &= N_T \end{aligned} \tag{A.11}$$

which is nonzero, $\hat{a}_B^\dagger \hat{a}_B$:

$$\langle m, m+k, k, N_P | \hat{a}_B^\dagger \hat{a}_B | n, n+l, l, N_T \rangle = N_T \langle m, m+k, k, N_P | n, n+l, l, N_T \rangle$$

$$\begin{aligned}
m &= n \\
m + k &= n + l \\
k &= l \\
N_P &= N_T
\end{aligned} \tag{A.12}$$

which is nonzero, $\hat{a}_B \hat{a}_{s_1}^\dagger$:

$$\begin{aligned}
\langle m, m + k, k, N_P | \hat{a}_B \hat{a}_{s_1}^\dagger | n, n + l, l, N_T \rangle &= \sqrt{N_T(n + 1)} \langle m, m + k, k, N_P | n + 1, n + l, l, N_T - 1 \rangle \\
m &= n + 1 \\
m + k &= n + l \\
k &= l \\
N_P &= N_T - 1
\end{aligned} \tag{A.13}$$

which is zero, $\hat{a}_B^\dagger \hat{a}_s$:

$$\begin{aligned}
\langle m, m + k, k, N_P | \hat{a}_B^\dagger \hat{a}_s | n, n + l, l, N_T \rangle &= \sqrt{n(N_T + 1)} \langle m, m + k, k, N_P | n - 1, n + l, l, N_T + 1 \rangle \\
m &= n - 1 \\
m + k &= n + l \\
k &= l \\
N_P &= N_T + 1
\end{aligned} \tag{A.14}$$

which is zero, $\hat{a}_B^\dagger \hat{a}_s^\dagger$:

$$\begin{aligned}
\langle m, m + k, k, N_P | \hat{a}_B^\dagger \hat{a}_s^\dagger | n, n + l, l, N_T \rangle &= \sqrt{(n + 1)(N_T + 1)} \langle m, m + k, k, N_P | n + 1, n + l, l, N_T + 1 \rangle \\
m &= n + 1 \\
m + k &= n + l \\
k &= l \\
N_P &= N_T + 1
\end{aligned} \tag{A.15}$$

which is zero, $\hat{a}_B \hat{a}_s$:

$$\begin{aligned}
\langle m, m + k, k, N_P | \hat{a}_B \hat{a}_s | n, n + l, l, N_T \rangle &= \sqrt{n N_T} \langle m, m + k, k, N_P | n - 1, n + l, l, N_T - 1 \rangle \\
m &= n - 1 \\
m + k &= n + l
\end{aligned}$$

$$\begin{aligned}
k &= l \\
N_P &= N_T - 1
\end{aligned} \tag{A.16}$$

Which is zero.

Now we look at the $E_{R_2}^2$ terms, $\hat{a}_{s_2}^2$:

$$\begin{aligned}
\langle m, m+k, k | \hat{a}_{s_2}^2 | n, n+l, l \rangle &= \sqrt{l(l-1)} \langle m, m+k, k | n, n+l, l-2 \rangle \\
m &= n \\
m+k &= n+l \\
k &= l-2
\end{aligned} \tag{A.17}$$

which is zero, $\hat{a}_{s_2}^{2\dagger}$:

$$\begin{aligned}
\langle m, m+k, k | \hat{a}_{s_2}^2 \hat{a}_{s_2}^{2\dagger} | n, n+l, l \rangle &= \sqrt{(l+2)(l+1)} \langle m, m+k, k | n, n+l, l+2 \rangle \\
m &= n \\
m+k &= n+l \\
k &= l+2
\end{aligned} \tag{A.18}$$

which is zero, $\hat{a}_{s_2} \hat{a}_{s_2}^\dagger$:

$$\begin{aligned}
\langle m, m+k, k | \hat{a}_{s_2} \hat{a}_{s_2}^\dagger | n, n+l, l \rangle &= (l+1) \langle m, m+k, k | n, n+l, l \rangle \\
m &= n \\
m+k &= n+l \\
k &= l
\end{aligned} \tag{A.19}$$

which is nonzero, $\hat{a}_{s_2}^\dagger \hat{a}_{s_2}$:

$$\begin{aligned}
\langle m, m+k, k | \hat{a}_{s_2}^\dagger \hat{a}_{s_2} | n, n+l, l \rangle &= l \langle m, m+k, k | n, n+l, l \rangle \\
m &= n \\
m+k &= n+l \\
k &= l
\end{aligned} \tag{A.20}$$

which is nonzero, \hat{a}_B^2 :

$$\langle m, m+k, k, N_P | \hat{a}_B^2 | n, n+l, l, N_T \rangle = \sqrt{N_T(N_T+1)} \langle m, m+k, k, N_P | n, n+l, l, N_T-2 \rangle$$

$$\begin{aligned}
m &= n \\
m + k &= n + l \\
k &= l \\
N_P &= N_T - 2
\end{aligned} \tag{A.21}$$

which is zero, $\hat{a}_B^{2\dagger}$:

$$\begin{aligned}
\langle m, m + k, k, N_P | \hat{a}_B^{2\dagger} | n, n + l, l, N_T \rangle &= \sqrt{(N_T + 2)(M + T + 1)} \langle m, m + k, k, N_P | n, n + l, l, N_T + 2 \rangle \\
m &= n \\
m + k &= n + l \\
k &= l \\
N_P &= N_T + 2
\end{aligned} \tag{A.22}$$

which is zero, $\hat{a}_B \hat{a}_B^\dagger$:

$$\begin{aligned}
\langle m, m + k, k, N_P | \hat{a}_B \hat{a}_B^\dagger | n, n + l, l, N_T \rangle &= (N_T + 1) \langle m, m + k, k, N_P | n, n + l, l, N_T \rangle \\
m &= n \\
m + k &= n + l \\
k &= l \\
N_P &= N_T
\end{aligned} \tag{A.23}$$

which is nonzero, $\hat{a}_B^\dagger \hat{a}_B$:

$$\begin{aligned}
\langle m, m + k, k, N_P | \hat{a}_B^\dagger \hat{a}_B | n, n + l, l, N_T \rangle &= N_T \langle m, m + k, k, N_P | n, n + l, l, N_T \rangle \\
m &= n \\
m + k &= n + l \\
k &= l \\
N_P &= N_T
\end{aligned} \tag{A.24}$$

which is nonzero, $\hat{a}_B \hat{a}_{s_2}^\dagger$:

$$\begin{aligned}
\langle m, m + k, k, N_P | \hat{a}_B \hat{a}_{s_2}^\dagger | n, n + l, l, N_T \rangle &= \sqrt{N_T(n + 1)} \langle m, m + k, k, N_P | n, n + l, l + 1, N_T - 1 \rangle \\
m &= n \\
m + k &= n + l
\end{aligned}$$

$$\begin{aligned}
k &= l + 1 \\
N_P &= N_T - 1
\end{aligned} \tag{A.25}$$

which is zero, $\hat{a}_B^\dagger \hat{a}_s$:

$$\begin{aligned}
\langle m, m + k, k, N_P | \hat{a}_B^\dagger \hat{a}_{s_2} | n, n + l, l, N_T \rangle &= \sqrt{l(N_T + 1)} \langle m, m + k, k, N_P | n, n + l, l - 1, N_T + 1 \rangle \\
m &= n \\
m + k &= n + l \\
k &= l - 1 \\
N_P &= N_T + 1
\end{aligned} \tag{A.26}$$

which is zero, $\hat{a}_B^\dagger \hat{a}_s^\dagger$:

$$\begin{aligned}
\langle m, m + k, k, N_P | \hat{a}_B^\dagger \hat{a}_{s_2}^\dagger | n, n + l, l, N_T \rangle &= \sqrt{(l + 1)(N_T + 1)} \langle m, m + k, k, N_P | n, n + l, l + 1, N_T + 1 \rangle \\
m &= n \\
m + k &= n + l \\
k &= l + 1 \\
N_P &= N_T + 1
\end{aligned} \tag{A.27}$$

which is zero, $\hat{a}_B \hat{a}_s$:

$$\begin{aligned}
\langle m, m + k, k, N_P | \hat{a}_B \hat{a}_{s_2} | n, n + l, l, N_T \rangle &= \sqrt{n N_T} \langle m, m + k, k, N_P | n, n + l, l - 1, N_T - 1 \rangle \\
m &= n \\
m + k &= n + l \\
k &= l - 1 \\
N_P &= N_T - 1
\end{aligned} \tag{A.28}$$

Which is zero.

Now we look at the $E_i E_{R_1}, \hat{a}_{s_1} \hat{a}_i$:

$$\begin{aligned}
\langle m, m + k, k, N_P | \hat{a}_{s_1} \hat{a}_i | n, n + l, l, N_T \rangle &= \sqrt{n(n + l)} \langle m, m + k, k, N_P | n - 1, n + l - 1, l, N_T \rangle \\
m &= n - 1 \\
m + k &= n + l - 1 \\
k &= l
\end{aligned}$$

$$N_P = N_T \quad (\text{A.29})$$

which is nonzero, $\hat{a}_{s_1}^\dagger \hat{a}_i^\dagger$:

$$\begin{aligned} \langle m, m+k, k, N_P | \hat{a}_{s_1}^\dagger \hat{a}_i^\dagger | n, n+l, l, N_T \rangle &= \sqrt{n+1(n+l+1)} \langle m, m+k, k, N_P | n+1, n+l+1, l, N_T \rangle \\ m &= n+1 \\ m+k &= n+l+1 \\ k &= l \\ N_P &= N_T \end{aligned} \quad (\text{A.30})$$

which is nonzero, $\hat{a}_{s_1}^\dagger \hat{a}_i$:

$$\begin{aligned} \langle m, m+k, k, N_P | \hat{a}_{s_1}^\dagger \hat{a}_i | n, n+l, l, N_T \rangle &= \sqrt{n+1(n+l)} \langle m, m+k, k, N_P | n+1, n+l-1, l, N_T \rangle \\ m &= n+1 \\ m+k &= n+l-1 \\ k &= l \\ N_P &= N_T \end{aligned} \quad (\text{A.31})$$

which is zero, $\hat{a}_{s_1} \hat{a}_i^\dagger$:

$$\begin{aligned} \langle m, m+k, k, N_P | \hat{a}_{s_1} \hat{a}_i^\dagger | n, n+l, l, N_T \rangle &= \sqrt{n(n+l+1)} \langle m, m+k, k, N_P | n-1, n+l+1, l, N_T \rangle \\ m &= n-1 \\ m+k &= n+l+1 \\ k &= l \\ N_P &= N_T \end{aligned} \quad (\text{A.32})$$

which is zero, $\hat{a}_B \hat{a}_i$:

$$\begin{aligned} \langle m, m+k, k, N_P | \hat{a}_B \hat{a}_i | n, n+l, l, N_T \rangle &= \sqrt{(n+l)N_T} \langle m, m+k, k, N_P | n, n+l-1, l, N_T-1 \rangle \\ m &= n \\ m+k &= n+l-1 \\ k &= l \\ N_P &= N_T-1 \end{aligned} \quad (\text{A.33})$$

which is zero, $\hat{a}_B^\dagger \hat{a}_i^\dagger$:

$$\begin{aligned}
\langle m, m+k, k, N_P | \hat{a}_B^\dagger \hat{a}_i^\dagger | n, n+l, l, N_T \rangle &= \sqrt{(n+l+1)(N_T+1)} \langle m, m+k, k, N_P | n, n+l+1, l, N_T+1 \rangle \\
m &= n \\
m+k &= n+l+1 \\
k &= l \\
N_P &= N_T+1
\end{aligned} \tag{A.34}$$

which is zero, $\hat{a}_B^\dagger \hat{a}_i$:

$$\begin{aligned}
\langle m, m+k, k, N_P | \hat{a}_B^\dagger \hat{a}_i | n, n+l, l, N_T \rangle &= \sqrt{n(N_T+1)} \langle m, m+k, k, N_P | n, n+l-1, l, N_T+1 \rangle \\
m &= n \\
m+k &= n+l-1 \\
k &= l \\
N_P &= N_T+1
\end{aligned} \tag{A.35}$$

which is zero, $\hat{a}_B \hat{a}_i^\dagger$:

$$\begin{aligned}
\langle m, m+k, k, N_P | \hat{a}_B \hat{a}_i^\dagger | n, n+l, l, N_T \rangle &= \sqrt{N_T(n+1)} \langle m, m+k, k, N_P | n, n+l+1, l, N_T-1 \rangle \\
m &= n \\
m+k &= n+l+1 \\
k &= l \\
N_P &= N_T-1
\end{aligned} \tag{A.36}$$

Now we look at the $E_i E_{R_2}, \hat{a}_{s_2} \hat{a}_i$:

$$\begin{aligned}
\langle m, m+k, k, N_P | \hat{a}_{s_2} \hat{a}_i | n, n+l, l, N_T \rangle &= \sqrt{l(n+l)} \langle m, m+k, k, N_P | n, n+l-1, l-1, N_T \rangle \\
m &= n \\
m+k &= n+l-1 \\
k &= l-1 \\
N_P &= N_T
\end{aligned} \tag{A.37}$$

which is nonzero, $\hat{a}_{s_2}^\dagger \hat{a}_i^\dagger$:

$$\begin{aligned}
\langle m, m+k, k, N_P | \hat{a}_{s_2}^\dagger \hat{a}_i^\dagger | n, n+l, l, N_T \rangle &= \sqrt{nl+1(n+l+1)} \langle m, m+k, k, N_P | n, n+l+1, l+1, N_T \rangle \\
m &= n \\
m+k &= n+l+1 \\
k &= l+1 \\
N_P &= N_T
\end{aligned} \tag{A.38}$$

which is nonzero, $\hat{a}_{s_2}^\dagger \hat{a}_i$:

$$\begin{aligned}
\langle m, m+k, k, N_P | \hat{a}_{s_2}^\dagger \hat{a}_i | n, n+l, l, N_T \rangle &= \sqrt{l+1(n+l)} \langle m, m+k, k, N_P | n, n+l-1, l+1, N_T \rangle \\
m &= n \\
m+k &= n+l-1 \\
k &= l+1 \\
N_P &= N_T
\end{aligned} \tag{A.39}$$

which is zero, $\hat{a}_{s_2} \hat{a}_i^\dagger$:

$$\begin{aligned}
\langle m, m+k, k, N_P | \hat{a}_{s_2} \hat{a}_i^\dagger | n, n+l, l, N_T \rangle &= \sqrt{l(n+l+1)} \langle m, m+k, k, N_P | n, n+l+1, l-1, N_T \rangle \\
m &= n \\
m+k &= n+l+1 \\
k &= l-1 \\
N_P &= N_T
\end{aligned} \tag{A.40}$$

which is zero, $\hat{a}_B \hat{a}_i$:

$$\begin{aligned}
\langle m, m+k, k, N_P | \hat{a}_B \hat{a}_i | n, n+l, l, N_T \rangle &= \sqrt{(n+l)N_T} \langle m, m+k, k, N_P | n, n+l-1, l, N_T-1 \rangle \\
m &= n \\
m+k &= n+l-1 \\
k &= l \\
N_P &= N_T-1
\end{aligned} \tag{A.41}$$

which is zero, $\hat{a}_B^\dagger \hat{a}_i^\dagger$:

$$\begin{aligned}
\langle m, m+k, k, N_P | \hat{a}_B^\dagger \hat{a}_i^\dagger | n, n+l, l, N_T \rangle &= \sqrt{(n+l+1)(N_T+1)} \langle m, m+k, k, N_P | n, n+l+1, l, N_T+1 \rangle \\
m &= n \\
m+k &= n+l+1 \\
k &= l \\
N_P &= N_T+1
\end{aligned} \tag{A.42}$$

which is zero, $\hat{a}_B^\dagger \hat{a}_i$:

$$\begin{aligned}
\langle m, m+k, k, N_P | \hat{a}_B^\dagger \hat{a}_i | n, n+l, l, N_T \rangle &= \sqrt{n(N_T+1)} \langle m, m+k, k, N_P | n, n+l-1, l, N_T+1 \rangle \\
m &= n \\
m+k &= n+l-1 \\
k &= l \\
N_P &= N_T+1
\end{aligned} \tag{A.43}$$

which is zero, $\hat{a}_B \hat{a}_i^\dagger$:

$$\begin{aligned}
\langle m, m+k, k, N_P | \hat{a}_B \hat{a}_i^\dagger | n, n+l, l, N_T \rangle &= \sqrt{N_T(n+1)} \langle m, m+k, k, N_P | n, n+l+1, l, N_T-1 \rangle \\
m &= n \\
m+k &= n+l+1 \\
k &= l \\
N_P &= N_T-1
\end{aligned} \tag{A.44}$$

Now we look at the $E_{R_1} E_{R_2}, \hat{a}_{s_1} \hat{a}_{s_2}$:

$$\begin{aligned}
\langle m, m+k, k, N_P | \hat{a}_{s_1} \hat{a}_{s_2} | n, n+l, l, N_T \rangle &= \sqrt{nl} \langle m, m+k, k, N_P | n-1, n+l, l-1, N_T \rangle \\
m &= n-1 \\
m+k &= n+l \\
k &= l-1 \\
N_P &= N_T
\end{aligned} \tag{A.45}$$

which is zero, $\hat{a}_{s_1}^\dagger \hat{a}_{s_2}^\dagger$:

$$\begin{aligned}
\langle m, m+k, k, N_P | \hat{a}_{s_1}^\dagger \hat{a}_{s_2}^\dagger | n, n+l, l, N_T \rangle &= \sqrt{(n+1)(l+1)} \langle m, m+k, k, N_P | n+1, n+l, l+0, N_T \rangle \\
m &= n+1 \\
m+k &= n+l \\
k &= l+1 \\
N_P &= N_T
\end{aligned} \tag{A.46}$$

which is zero, $\hat{a}_{s_1} \hat{a}_{s_2}^\dagger$:

$$\begin{aligned}
\langle m, m+k, k, N_P | \hat{a}_{s_1} \hat{a}_{s_2}^\dagger | n, n+l, l, N_T \rangle &= \sqrt{n(l+1)} \langle m, m+k, k, N_P | n-1, n+l, l+1, N_T \rangle \\
m &= n-1 \\
m+k &= n+l \\
k &= l+1 \\
N_P &= N_T
\end{aligned} \tag{A.47}$$

which is nonzero, $\hat{a}_{s_1}^\dagger \hat{a}_{s_2}$:

$$\begin{aligned}
\langle m, m+k, k, N_P | \hat{a}_{s_1}^\dagger \hat{a}_{s_2} | n, n+l, l, N_T \rangle &= \sqrt{l(n+1)} \langle m, m+k, k, N_P | n+1, n+l, l-1, N_T \rangle \\
m &= n+1 \\
m+k &= n+l \\
k &= l-1 \\
N_P &= N_T
\end{aligned} \tag{A.48}$$

which is nonzero, $\hat{a}_{B_1} \hat{a}_{B_2}$:

$$\begin{aligned}
&\langle m, m+k, k, N_{P_1}, N_{P_2} | \hat{a}_{B_1} \hat{a}_{B_2} | n, n+l, l, N_{T_1}, N_{T_2} \rangle \\
&= \sqrt{N_{T_1} N_{T_2}} \langle m, m+k, k, N_{P_1}, N_{P_2} | n, n+l, l, N_{T_1}-1, N_{T_2}-1 \rangle \\
&\quad m = n \\
&\quad m+k = n+l \\
&\quad k = l \\
&\quad N_{P_1} = N_{T_1} - 1 N_{P_2} \qquad = N_{T_2} - 1 \tag{A.49}
\end{aligned}$$

$$\begin{aligned}
m &= n - 1 \\
m + k &= n + l \\
k &= l \\
N_{P_1} &= N_{T_1} \\
N_{P_2} &= N_{T_2} - 1
\end{aligned} \tag{A.53}$$

which is zero, $\hat{a}_{s_1}^\dagger \hat{a}_{B_2}^\dagger$:

$$\begin{aligned}
&\langle m, m + k, k, N_{P_1}, N_{P_2} | \hat{a}_{s_1}^\dagger \hat{a}_{B_2}^\dagger | n, n + l, l, N_{T_1}, N_{T_2} \rangle \\
&= \sqrt{(n + 1)(N_{T_2} + 1)} \langle m, m + k, k, N_{P_1}, N_{P_2} | n + 1, n + l, l, N_{T_1}, N_{T_2} + 1 \rangle \\
&\quad m = n + 1 \\
&\quad m + k = n + l \\
&\quad k = l \\
&\quad N_{P_1} = N_{T_1} \\
&\quad N_{P_2} = N_{T_2} + 1
\end{aligned} \tag{A.54}$$

which is zero, $\hat{a}_{s_1} \hat{a}_{B_2}^\dagger$:

$$\begin{aligned}
&\langle m, m + k, k, N_{P_1}, N_{P_2} | \hat{a}_{s_1} \hat{a}_{B_2}^\dagger | n, n + l, l, N_{T_1}, N_{T_2} \rangle \\
&= \sqrt{n(N_{T_2} + 1)} \langle m, m + k, k, N_{P_1}, N_{P_2} | n + 1, n + l, l, N_{T_1}, N_{T_2} + 1 \rangle \\
&\quad m = n - 1 \\
&\quad m + k = n + l \\
&\quad k = l \\
&\quad N_{P_1} = N_{T_1} \\
&\quad N_{P_2} = N_{T_2} + 1
\end{aligned} \tag{A.55}$$

which is zero, $\hat{a}_{s_1}^\dagger \hat{a}_{B_2}$:

$$\begin{aligned}
&\langle m, m + k, k, N_{P_1}, N_{P_2} | \hat{a}_{s_1}^\dagger \hat{a}_{B_2} | n, n + l, l, N_{T_1}, N_{T_2} \rangle \\
&= \sqrt{N_{T_2}(n + 1)} \langle m, m + k, k, N_{P_1}, N_{P_2} | n + 1, n + l, l, N_{T_1}, N_{T_2} - 1 \rangle \\
&\quad m = n + 1 \\
&\quad m + k = n + l
\end{aligned}$$

$$\begin{aligned}
k &= l \\
N_{P_1} &= N_{T_1} \\
N_{P_2} &= N_{T_2} - 1
\end{aligned} \tag{A.56}$$

which is zero, $\hat{a}_{B_1} \hat{a}_{s_2}$:

$$\begin{aligned}
&\langle m, m+k, k, N_{P_1}, N_{P_2} | \hat{a}_{B_1} \hat{a}_{s_2} | n, n+l, l, N_{T_1}, N_{T_2} \rangle \\
&= \sqrt{N_{T_1} l} \langle m, m+k, k, N_{P_1}, N_{P_2} | n-1, n+l, l, N_{T_1}-1, N_{T_2} \rangle \\
&\quad m = n-1 \\
&\quad m+k = n+l \\
&\quad k = l-1 \\
&\quad N_{P_1} = N_{T_1} - 1 \\
&\quad N_{P_2} = N_{T_2}
\end{aligned} \tag{A.57}$$

which is zero, $\hat{a}_{B_1}^\dagger \hat{a}_{s_2}^\dagger$:

$$\begin{aligned}
&\langle m, m+k, k, N_{P_1}, N_{P_2} | \hat{a}_{B_1}^\dagger \hat{a}_{s_2}^\dagger | n, n+l, l, N_{T_1}, N_{T_2} \rangle \\
&= \sqrt{(N_{T_1}+1)(l+1)} \langle m, m+k, k, N_{P_1}, N_{P_2} | n+1, n+l, l, N_{T_1}+1, N_{T_2} \rangle \\
&\quad m = n+1 \\
&\quad m+k = n+l \\
&\quad k = l+1 \\
&\quad N_{P_1} = N_{T_1} + 1 \\
&\quad N_{P_2} = N_{T_2}
\end{aligned} \tag{A.58}$$

which is zero, $\hat{a}_{B_1} \hat{a}_{s_2}^\dagger$:

$$\begin{aligned}
&\langle m, m+k, k, N_{P_1}, N_{P_2} | \hat{a}_{B_1} \hat{a}_{s_2}^\dagger | n, n+l, l, N_{T_1}, N_{T_2} \rangle \\
&= \sqrt{N_{T_1}(l+1)} \langle m, m+k, k, N_{P_1}, N_{P_2} | n-1, n+l, l, N_{T_1}-1, N_{T_2} \rangle \\
&\quad m = n-1 \\
&\quad m+k = n+l \\
&\quad k = l+1 \\
&\quad N_{P_1} = N_{T_1} - 1 \\
&\quad N_{P_2} = N_{T_2}
\end{aligned} \tag{A.59}$$

which is zero, $\hat{a}_{B_1}^\dagger \hat{a}_{s_2}$:

$$\begin{aligned}
& \langle m, m+k, k, N_{P_1}, N_{P_2} | \hat{a}_{B_1}^\dagger \hat{a}_{s_2} | n, n+l, l, N_{T_1}, N_{T_2} \rangle \\
&= \sqrt{l(N_{T_1} + 1)} \langle m, m+k, k, N_{P_1}, N_{P_2} | n, n+l, l-1, N_{T_1} + 1, N_{T_2} \rangle \\
&\quad m = n \\
&\quad m+k = n+l \\
&\quad k = l-1 \\
&\quad N_{P_1} = N_{T_1} + 1 \\
&\quad N_{P_2} = N_{T_2}
\end{aligned} \tag{A.60}$$

A.2 Number Operator

This section shows the Fock state analysis of each term in the tripartite number operator analysis. We begin with $\hat{N}_{R_1}, \hat{a}_{s_1}^\dagger \hat{a}_{s_1}$:

$$\begin{aligned}
& \langle m, m+k, k | \hat{a}_{s_1}^\dagger \hat{a}_{s_1} | n, n+l, l \rangle = n \langle m, m+k, k | n, n+l, l \rangle \\
&\quad m = n \\
&\quad m+k = n+l \\
&\quad k = l
\end{aligned} \tag{A.61}$$

which is nonzero, $\hat{a}_{s_1}^\dagger \hat{a}_B$:

$$\begin{aligned}
& \langle m, m+k, k, N_P | \hat{a}_{s_1}^\dagger \hat{a}_B | n, n+l, l, N_T \rangle = \sqrt{N_T(n+1)} \langle m, m+k, k, N_P | n+1, n+l, l, N_T-1 \rangle \\
&\quad m = n+1 \\
&\quad m+k = n+l \\
&\quad k = l \\
&\quad N_P = N_T - 1
\end{aligned} \tag{A.62}$$

which is zero, $\hat{a}_B^\dagger \hat{a}_{s_1}$:

$$\begin{aligned}
& \langle m, m+k, k, N_P | \hat{a}_B^\dagger \hat{a}_{s_1} | n, n+l, l, N_T \rangle = \sqrt{n(N_T+1)} \langle m, m+k, k | n-1, n+l, l, N_T+1 \rangle \\
&\quad m = n-1 \\
&\quad m+k = n+l
\end{aligned}$$

$$\begin{aligned}
k &= l \\
N_P &= N_T + 1
\end{aligned} \tag{A.63}$$

which is zero, $\hat{a}_B^\dagger \hat{a}_B$:

$$\begin{aligned}
\langle m, m+k, k, N_P | \hat{a}_B^\dagger \hat{a}_B | n, n+l, l, N_T \rangle &= N_T \langle m, m+k, k, N_P | n, n+l, l, N_T \rangle \\
m &= n \\
m+k &= n+l \\
k &= l \\
N_P &= N_T
\end{aligned} \tag{A.64}$$

which is nonzero.

Now looking at \hat{N}_{R_2} , $\hat{a}_{s_2}^\dagger \hat{a}_{s_2}$:

$$\begin{aligned}
\langle m, m+k, k | \hat{a}_{s_2}^\dagger \hat{a}_{s_2} | n, n+l, l \rangle &= l \langle m, m+k, k | n, n+l, l \rangle \\
m &= n \\
m+k &= n+l \\
k &= l
\end{aligned} \tag{A.65}$$

which is nonzero, $\hat{a}_{s_2}^\dagger \hat{a}_B$:

$$\begin{aligned}
\langle m, m+k, k, N_P | \hat{a}_{s_2}^\dagger \hat{a}_B | n, n+l, l, N_B \rangle &= \sqrt{N_T(l+1)} \langle m, m+k, k, N_P | n, n+l, l+1, N_T-1 \rangle \\
m &= n \\
m+k &= n+l \\
k &= l+1 \\
N_P &= N_T-1
\end{aligned} \tag{A.66}$$

which is zero, $\hat{a}_B^\dagger \hat{a}_{s_2}$:

$$\begin{aligned}
\langle m, m+k, k, N_P | \hat{a}_B^\dagger \hat{a}_{s_2} | n, n+l, l, N_T \rangle &= \sqrt{l(N_T+1)} \langle m, m+k, k, N_P | n, n+l, l-1, N_T+1 \rangle \\
m &= n \\
m+k &= n+l \\
k &= l-1 \\
N_P &= N_T+1
\end{aligned} \tag{A.67}$$

which is zero, $\hat{a}_B^\dagger \hat{a}_B$:

$$\begin{aligned}
\langle m, m+k, k, N_P | \hat{a}_B^\dagger \hat{a}_B | n, n+l, l, N_T \rangle &= N_T \langle m, m+k, k, N_P | n, n+l, l, N_T \rangle \\
m &= n \\
m+k &= n+l \\
k &= l \\
N_P &= N_T
\end{aligned} \tag{A.68}$$

Now $\hat{N}_{R_1}^2$, $\hat{a}_{s_1}^\dagger \hat{a}_{s_1} \hat{a}_{s_1}^\dagger \hat{a}_{s_1}$:

$$\begin{aligned}
\langle m, m+k, k | \hat{a}_{s_1}^\dagger \hat{a}_{s_1} \hat{a}_{s_1}^\dagger \hat{a}_{s_1} | n, n+l, l \rangle &= n^2 \langle m, m+k, k | n, n+l, l \rangle \\
m &= n \\
m+k &= n+l \\
k &= l
\end{aligned} \tag{A.69}$$

which is nonzero, $\hat{a}_{s_1}^\dagger \hat{a}_{s_1} \hat{a}_{s_1}^\dagger \hat{a}_B$:

$$\begin{aligned}
\langle m, m+k, k | \hat{a}_{s_1}^\dagger \hat{a}_{s_1} \hat{a}_{s_1}^\dagger \hat{a}_B | n, n+l, l \rangle &= n \sqrt{N_T(n+1)} \langle m, m+k, k | n+1, n+l, l, N_T-1 \rangle \\
m &= n+1 \\
m+k &= n+l \\
k &= l \\
N_P &= N_T-1
\end{aligned} \tag{A.70}$$

which is zero, $\hat{a}_{s_1}^\dagger \hat{a}_{s_1} \hat{a}_B^\dagger \hat{a}_{s_1}$:

$$\begin{aligned}
&\langle m, m+k, k, N_P | \hat{a}_{s_1}^\dagger \hat{a}_{s_1} \hat{a}_B^\dagger \hat{a}_{s_1} | n, n+l, l, N_T \rangle \\
&= n \sqrt{n(N_T+1)} \langle m, m+k, k, N_P | n-1, n+l, l, N_T+1 \rangle \\
m &= n-1 \\
m+k &= n+l \\
k &= l \\
N_P &= N_T+1
\end{aligned} \tag{A.71}$$

which is zero, $\hat{a}_{s_1}^\dagger \hat{a}_{s_1} \hat{a}_B^\dagger \hat{a}_B$:

$$\begin{aligned}
& \langle m, m+k, k, N_P | \hat{a}_{s_1}^\dagger \hat{a}_{s_1} \hat{a}_B^\dagger \hat{a}_{s_1} | n, n+l, l, N_T \rangle \\
&= n N_T \langle m, m+k, k, N_P | n, n+l, l, N_T \rangle \\
& \quad m = n \\
& \quad m+k = n+l \\
& \quad k = l \\
& \quad N_P = N_T
\end{aligned} \tag{A.72}$$

which is nonzero, $\hat{a}_{s_1}^\dagger \hat{a}_B \hat{a}_{s_1}^\dagger \hat{a}_B$:

$$\begin{aligned}
& \langle m, m+k, k, N_P | \hat{a}_{s_1}^\dagger \hat{a}_B \hat{a}_{s_1}^\dagger \hat{a}_B | n, n+l, l, N_T \rangle \\
&= \sqrt{(n+1)(n+2)N_T(N_T-1)} \langle m, m+k, k, N_P | n+2, n+l, l, N_T-2 \rangle \\
& \quad m = n+2 \\
& \quad m+k = n+l \\
& \quad k = l \\
& \quad N_P = N_T-2
\end{aligned} \tag{A.73}$$

which is zero, $\hat{a}_{s_1}^\dagger \hat{a}_B \hat{a}_B^\dagger \hat{a}_B$:

$$\begin{aligned}
& \langle m, m+k, k, N_P | \hat{a}_{s_1}^\dagger \hat{a}_B \hat{a}_{s_1}^\dagger \hat{a}_B | n, n+l, l, N_T \rangle \\
&= N_T \sqrt{N_T(n+1)} \langle m, m+k, k, N_P | n+1, n+l, l, N_T-1 \rangle \\
& \quad m = n+1 \\
& \quad m+k = n+l \\
& \quad k = l \\
& \quad N_P = N_T-1
\end{aligned} \tag{A.74}$$

which is nonzero, $\hat{a}_B^\dagger \hat{a}_{s_1} \hat{a}_B^\dagger \hat{a}_B$:

$$\begin{aligned}
& \langle m, m+k, k, N_P | \hat{a}_B^\dagger \hat{a}_{s_1} \hat{a}_B^\dagger \hat{a}_B | n, n+l, l, N_T \rangle \\
&= N_T \sqrt{n(N_T+1)} \langle m, m+k, k, N_P | n-1, n+l, l, N_T+1 \rangle \\
& \quad m = n-1 \\
& \quad m+k = n+l
\end{aligned}$$

$$\begin{aligned}
k &= l \\
N_P &= N_T + 1
\end{aligned} \tag{A.75}$$

which is nonzero, $\hat{a}_{s_1}^\dagger \hat{a}_B \hat{a}_B^\dagger \hat{a}_{s_1}$:

$$\begin{aligned}
&\langle m, m+k, k, N_P | \hat{a}_{s_1}^\dagger \hat{a}_B \hat{a}_B^\dagger \hat{a}_{s_1} | n, n+l, l, N_T \rangle \\
&= n(N_T + 1) \langle m, m+k, k, N_P | n, n+l, l, N_T \rangle \\
&\quad m = n \\
&\quad m+k = n+l \\
&\quad k = l \\
&\quad N_P = N_T
\end{aligned} \tag{A.76}$$

which is nonzero, $\hat{a}_B^\dagger \hat{a}_{s_1} \hat{a}_{s_1}^\dagger \hat{a}_B$:

$$\begin{aligned}
&\langle m, m+k, k, N_P | \hat{a}_B^\dagger \hat{a}_{s_1} \hat{a}_{s_1}^\dagger \hat{a}_B | n, n+l, l, N_T \rangle \\
&= N_T(n+1) \langle m, m+k, k, N_P | n, n+l, l, N_T \rangle \\
&\quad m = n \\
&\quad m+k = n+l \\
&\quad k = l \\
&\quad N_P = N_T
\end{aligned} \tag{A.77}$$

which is nonzero, $\hat{a}_B^\dagger \hat{a}_{s_1} \hat{a}_B^\dagger \hat{a}_{s_1}$:

$$\begin{aligned}
&\langle m, m+k, k, N_P | \hat{a}_B^\dagger \hat{a}_{s_1} \hat{a}_B^\dagger \hat{a}_{s_1} | n, n+l, l, N_T \rangle \\
&= \sqrt{n(n+1)(N_T+1)(N_T+2)} \langle m, m+k, k, N_P | n-2, n+l, l, N_T+2 \rangle \\
&\quad m = n-2 \\
&\quad m+k = n+l \\
&\quad k = l \\
&\quad N_P = N_T + 2
\end{aligned} \tag{A.78}$$

which is zero, $\hat{a}_B^\dagger \hat{a}_{s_1} \hat{a}_B^\dagger \hat{a}_{s_1}$:

$$\begin{aligned}
&\langle m, m+k, k, N_P | \hat{a}_B^\dagger \hat{a}_B \hat{a}_B^\dagger \hat{a}_B | n, n+l, l, N_T \rangle \\
&= N_T^2 \langle m, m+k, k, N_P | n, n, l, N_T \rangle
\end{aligned}$$

$$\begin{aligned}
m &= n - 2 \\
m + k &= n + l \\
k &= l \\
N_P &= N_T
\end{aligned} \tag{A.79}$$

which is nonzero.

Now $\hat{N}_{R_2}^2, \hat{a}_{s_2}^\dagger \hat{a}_{s_2} \hat{a}_{s_2}^\dagger \hat{a}_{s_2}$:

$$\begin{aligned}
\langle m, m + k, k | \hat{a}_{s_2}^\dagger \hat{a}_{s_2} \hat{a}_{s_2}^\dagger \hat{a}_{s_2} | n, n + l, l \rangle &= n^2 \langle m, m + k, k | n, n + l, l \rangle \\
m &= n \\
m + k &= n + l \\
k &= l
\end{aligned} \tag{A.80}$$

which is nonzero, $\hat{a}_{s_2}^\dagger \hat{a}_{s_2} \hat{a}_{s_2}^\dagger \hat{a}_B$:

$$\begin{aligned}
\langle m, m + k, k | \hat{a}_{s_2}^\dagger \hat{a}_{s_2} \hat{a}_{s_2}^\dagger \hat{a}_B | n, n + l, l \rangle &= n \sqrt{N_T(n + 1)} \langle m, m + k, k | n, n + l, l + 1, N_T - 1 \rangle \\
m &= n \\
m + k &= n + l \\
k &= l + 1 \\
N_P &= N_T - 1
\end{aligned} \tag{A.81}$$

which is zero, $\hat{a}_{s_2}^\dagger \hat{a}_{s_2} \hat{a}_B^\dagger \hat{a}_{s_2}$:

$$\begin{aligned}
&\langle m, m + k, k, N_P | \hat{a}_{s_2}^\dagger \hat{a}_{s_2} \hat{a}_B^\dagger \hat{a}_{s_2} | n, n + l, l, N_T \rangle \\
&= n \sqrt{n(N_T + 1)} \langle m, m + k, k, N_P | n, n + l, l - 1, N_T + 1 \rangle \\
m &= n \\
m + k &= n + l \\
k &= l - 1 \\
N_P &= N_T + 1
\end{aligned} \tag{A.82}$$

which is zero, $\hat{a}_{s_2}^\dagger \hat{a}_{s_2} \hat{a}_B^\dagger \hat{a}_B$:

$$\begin{aligned}
&\langle m, m + k, k, N_P | \hat{a}_{s_2}^\dagger \hat{a}_{s_2} \hat{a}_B^\dagger \hat{a}_{s_2} | n, n + l, l, N_T \rangle \\
&= n N_T \langle m, m + k, k, N_P | n, n + l, l, N_T \rangle
\end{aligned}$$

$$\begin{aligned}
m &= n \\
m + k &= n + l \\
k &= l \\
N_P &= N_T
\end{aligned} \tag{A.83}$$

which is nonzero, $\hat{a}_{s_2}^\dagger \hat{a}_B \hat{a}_{s_2}^\dagger \hat{a}_B$:

$$\begin{aligned}
& \langle m, m + k, k, N_P | \hat{a}_{s_2}^\dagger \hat{a}_B \hat{a}_{s_2}^\dagger \hat{a}_B | n, n + l, l, N_T \rangle \\
&= \sqrt{(n + 1)(n + 2)N_T(N_T - 1)} \langle m, m + k, k, N_P | n, n + l, l + 2, N_T - 2 \rangle \\
& \quad m = n \\
& \quad m + k = n + l \\
& \quad k = l + 2 \\
& \quad N_P = N_T - 2
\end{aligned} \tag{A.84}$$

which is zero, $\hat{a}_{s_2}^\dagger \hat{a}_B \hat{a}_B^\dagger \hat{a}_B$:

$$\begin{aligned}
& \langle m, m + k, k, N_P | \hat{a}_{s_2}^\dagger \hat{a}_B \hat{a}_B^\dagger \hat{a}_B | n, n + l, l, N_T \rangle \\
&= N_T \sqrt{N_T(n + 1)} \langle m, m + k, k, N_P | n, n + l, l + 1, N_T - 1 \rangle \\
& \quad m = n \\
& \quad m + k = n + l \\
& \quad k = l + 1 \\
& \quad N_P = N_T - 1
\end{aligned} \tag{A.85}$$

which is nonzero, $\hat{a}_B^\dagger \hat{a}_{s_2} \hat{a}_B^\dagger \hat{a}_B$:

$$\begin{aligned}
& \langle m, m + k, k, N_P | \hat{a}_B^\dagger \hat{a}_{s_2} \hat{a}_B^\dagger \hat{a}_B | n, n + l, l, N_T \rangle \\
&= N_T \sqrt{n(N_T + 1)} \langle m, m + k, k, N_P | n, n + l, l - 1, N_T + 1 \rangle \\
& \quad m = n \\
& \quad m + k = n + l \\
& \quad k = l - 1 \\
& \quad N_P = N_T + 1
\end{aligned} \tag{A.86}$$

which is nonzero, $\hat{a}_{s_2}^\dagger \hat{a}_B \hat{a}_B^\dagger \hat{a}_{s_2}$:

$$\begin{aligned}
& \langle m, m+k, k, N_P | \hat{a}_{s_2}^\dagger \hat{a}_B \hat{a}_B^\dagger \hat{a}_{s_2} | n, n+l, l, N_T \rangle \\
&= n(N_T + 1) \langle m, m+k, k, N_P | n, n+l, l, N_T \rangle \\
& \quad m = n \\
& \quad m+k = n+l \\
& \quad k = l \\
& \quad N_P = N_T
\end{aligned} \tag{A.87}$$

which is nonzero, $\hat{a}_B^\dagger \hat{a}_{s_2} \hat{a}_{s_2}^\dagger \hat{a}_B$:

$$\begin{aligned}
& \langle m, m+k, k, N_P | \hat{a}_B^\dagger \hat{a}_{s_2} \hat{a}_{s_2}^\dagger \hat{a}_B | n, n+l, l, N_T \rangle \\
&= N_T(n+1) \langle m, m+k, k, N_P | n, n+l, l, N_T \rangle \\
& \quad m = n \\
& \quad m+k = n+l \\
& \quad k = l \\
& \quad N_P = N_T
\end{aligned} \tag{A.88}$$

which is nonzero, $\hat{a}_B^\dagger \hat{a}_{s_2} \hat{a}_B^\dagger \hat{a}_{s_2}$:

$$\begin{aligned}
& \langle m, m+k, k, N_P | \hat{a}_B^\dagger \hat{a}_{s_2} \hat{a}_B^\dagger \hat{a}_{s_2} | n, n+l, l, N_T \rangle \\
&= \sqrt{n(n+1)(N_T+1)(N_T+2)} \langle m, m+k, k, N_P | n, n+l, l-2, N_T+2 \rangle \\
& \quad m = n \\
& \quad m+k = n+l \\
& \quad k = l-2 \\
& \quad N_P = N_T+2
\end{aligned} \tag{A.89}$$

which is zero, $\hat{a}_B^\dagger \hat{a}_{s_2} \hat{a}_B^\dagger \hat{a}_{s_2}$:

$$\begin{aligned}
& \langle m, m+k, k, N_P | \hat{a}_B^\dagger \hat{a}_{s_2} \hat{a}_B^\dagger \hat{a}_{s_2} | n, n+l, l, N_T \rangle \\
&= N_T^2 \langle m, m+k, k, N_P | n, n, l, N_T \rangle \\
& \quad m = n \\
& \quad m+k = n+l
\end{aligned}$$

$$\begin{aligned}
k &= l \\
N_P &= N_T
\end{aligned} \tag{A.90}$$

which is nonzero.

Now $\hat{N}_i \hat{N}_{R_1}, \hat{a}_i^\dagger \hat{a}_i \hat{a}_{s_1}^\dagger \hat{a}_{s_1}$:

$$\begin{aligned}
\langle m, m+k, k | \hat{a}_i^\dagger \hat{a}_i \hat{a}_{s_1}^\dagger \hat{a}_{s_1} | n, n+l, l \rangle &= l(n+l) \langle m, m+k, k | n, n+l, l \rangle \\
m &= n \\
m+k &= n+l \\
k &= l
\end{aligned} \tag{A.91}$$

which is nonzero, $\hat{a}_i^\dagger \hat{a}_i \hat{a}_{s_1}^\dagger \hat{a}_B$:

$$\begin{aligned}
\langle m, m+k, k, N_P | \hat{a}_i^\dagger \hat{a}_i \hat{a}_{s_1}^\dagger \hat{a}_{s_1} | n, n+l, l, N_T \rangle &= (n+l) \sqrt{N_T((l+1))} \langle m, m+k, k, N_P | n, n+l, l+1, N_T \rangle \\
m &= n \\
m+k &= n+l \\
k &= l+1 \\
N_P &= N_T - 1
\end{aligned} \tag{A.92}$$

which is zero, $\hat{a}_i^\dagger \hat{a}_i \hat{a}_B^\dagger \hat{a}_{s_1}$:

$$\begin{aligned}
\langle m, m+k, k, N_P | \hat{a}_i^\dagger \hat{a}_i \hat{a}_B^\dagger \hat{a}_{s_1} | n, n+l, l, N_T \rangle &= (n+l) \sqrt{l((N_T+l))} \langle m, m+k, k, N_P | n, n+l, l-1, N_T \rangle \\
m &= n \\
m+k &= n+l \\
k &= l-1 \\
N_P &= N_T + 1
\end{aligned} \tag{A.93}$$

which is zero, $\hat{a}_i^\dagger \hat{a}_i \hat{a}_B^\dagger \hat{a}_B$:

$$\begin{aligned}
\langle m, m+k, k, N_P | \hat{a}_i^\dagger \hat{a}_i \hat{a}_B^\dagger \hat{a}_B | n, n+l, l, N_T \rangle &= (n+l) N_T \langle m, m+k, k, N_P | n, n+l, l, N_T \rangle \\
m &= n \\
m+k &= n+l \\
k &= l \\
N_P &= N_T
\end{aligned} \tag{A.94}$$

which is nonzero.

Now $\hat{N}_i \hat{N}_{R_2}$, $\hat{a}_i^\dagger \hat{a}_i \hat{a}_{s_2}^\dagger \hat{a}_{s_2}$:

$$\begin{aligned} \langle m, m+k, k | \hat{a}_i^\dagger \hat{a}_i \hat{a}_{s_2}^\dagger \hat{a}_{s_2} | n, n+l, l \rangle &= n(n+l) \langle m, m+k, k | n, n+l, l \rangle \\ m &= n \\ m+k &= n+l \\ k &= l \end{aligned} \tag{A.95}$$

which is nonzero, $\hat{a}_i^\dagger \hat{a}_i \hat{a}_{s_2}^\dagger \hat{a}_B$:

$$\begin{aligned} \langle m, m+k, k, N_P | \hat{a}_i^\dagger \hat{a}_i \hat{a}_{s_2}^\dagger \hat{a}_{s_2} | n, n+l, l, N_T \rangle &= (n+l) \sqrt{N_T((n+l))} \langle m, m+k, k, N_P | n+1, n+l, l, N_T \rangle \\ m &= n+1 \\ m+k &= n+l \\ k &= l \\ N_P &= N_T - 1 \end{aligned} \tag{A.96}$$

which is zero, $\hat{a}_i^\dagger \hat{a}_i \hat{a}_B^\dagger \hat{a}_{s_2}$:

$$\begin{aligned} \langle m, m+k, k, N_P | \hat{a}_i^\dagger \hat{a}_i \hat{a}_B^\dagger \hat{a}_{s_2} | n, n+l, l, N_T \rangle &= (n+l) \sqrt{n((N_T+l))} \langle m, m+k, k, N_P | n-1, n+l, l, N_T \rangle \\ m &= n-1 \\ m+k &= n+l \\ k &= l \\ N_P &= N_T + 1 \end{aligned} \tag{A.97}$$

which is zero, $\hat{a}_i^\dagger \hat{a}_i \hat{a}_B^\dagger \hat{a}_B$:

$$\begin{aligned} \langle m, m+k, k, N_P | \hat{a}_i^\dagger \hat{a}_i \hat{a}_B^\dagger \hat{a}_B | n, n+l, l, N_T \rangle &= (n+l) N_T \langle m, m+k, k, N_P | n, n+l, l, N_T \rangle \\ m &= n \\ m+k &= n+l \\ k &= l \\ N_P &= N_T \end{aligned} \tag{A.98}$$

which is nonzero.

Now $\hat{N}_{R_1} \hat{N}_{R_2}, \hat{a}_{s_1}^\dagger \hat{a}_{s_1} \hat{a}_{s_2}^\dagger \hat{a}_{s_2}$:

$$\begin{aligned} \langle m, m+k, k | \hat{a}_{s_1}^\dagger \hat{a}_{s_1} \hat{a}_{s_2}^\dagger \hat{a}_{s_2} | n, n+l, l \rangle &= nl \langle m, m+k, k | n, n+l, l \rangle \\ m &= n \\ m+k &= n+l \\ k &= l \end{aligned} \tag{A.99}$$

which is nonzero, $\hat{a}_{s_1}^\dagger \hat{a}_{s_1} \hat{a}_{s_2}^\dagger \hat{a}_B$:

$$\begin{aligned} \langle m, m+k, k, N_P | \hat{a}_{s_1}^\dagger \hat{a}_{s_1} \hat{a}_{s_2}^\dagger \hat{a}_{B_2} | n, n+l, l, N_T \rangle &= n\sqrt{N_T((l+l))} \langle m, m+k, k, N_P | n, n+l, l+1, N_T - 1 \rangle \\ m &= n \\ m+k &= n+l \\ k &= l+1 \\ N_P &= N_T - 1 \end{aligned} \tag{A.100}$$

which is zero, $\hat{a}_{s_1}^\dagger \hat{a}_{s_1} \hat{a}_B^\dagger \hat{a}_{s_2}$:

$$\begin{aligned} \langle m, m+k, k, N_P | \hat{a}_{s_1}^\dagger \hat{a}_{s_1} \hat{a}_B^\dagger \hat{a}_{s_2} | n, n+l, l, N_T \rangle &= n\sqrt{l((N_T+l))} \langle m, m+k, k, N_P | n, n+l, l-1, N_T + 1 \rangle \\ m &= n \\ m+k &= n+l \\ k &= l-1 \\ N_P &= N_T + 1 \end{aligned} \tag{A.101}$$

which is zero, $\hat{a}_{s_1}^\dagger \hat{a}_{s_1} \hat{a}_B^\dagger \hat{a}_B$:

$$\begin{aligned} \langle m, m+k, k, N_P | \hat{a}_{s_1}^\dagger \hat{a}_{s_1} \hat{a}_B^\dagger \hat{a}_B | n, n+l, l, N_T \rangle &= nN_T \langle m, m+k, k, N_P | n, n+l, l, N_T \rangle \\ m &= n \\ m+k &= n+l \\ k &= l \\ N_P &= N_T \end{aligned} \tag{A.102}$$

which is nonzero, $\hat{a}_{s_1}^\dagger \hat{a}_B \hat{a}_{s_2}^\dagger \hat{a}_{s_2}$:

$$\langle m, m+k, k | \hat{a}_{s_1}^\dagger \hat{a}_B \hat{a}_{s_2}^\dagger \hat{a}_{s_2} | n, n+l, lN_{T_1}, N_{T_2} \rangle$$

$$\begin{aligned}
&= l\sqrt{N_{T_1}(n+1)} \langle m, m+k, k | n+1, n+l, l-1, N_{T_1}-1, N_{T_2} \rangle \\
&\quad m = n+1 \\
&\quad m+k = n+l \\
&\quad k = l \\
&\quad N_{P_1} = N_{T_1} - 1 \\
&\quad N_{P_2} = N_{T_2}
\end{aligned} \tag{A.103}$$

which is zero, $\hat{a}_{s_1}^\dagger \hat{a}_B \hat{a}_{s_2}^\dagger \hat{a}_B$:

$$\begin{aligned}
&\langle m, m+k, k, N_P | \hat{a}_{s_1}^\dagger \hat{a}_B \hat{a}_{s_2}^\dagger \hat{a}_{B_2} | n, n+l, l, N_{T_1}, N_{T_2} \rangle \\
&= \sqrt{N_{T_1} N_{T_2} (l+l)(n+1)} \langle m, m+k, k, N_P | n+1, n+l, l+1, N_{T_1}-1, N_{T_2}-1 \rangle \\
&\quad m = n+1 \\
&\quad m+k = n+l \\
&\quad k = l+1 \\
&\quad N_{P_1} = N_{T_1} - 1 \\
&\quad N_{P_2} = N_{T_2}
\end{aligned} \tag{A.104}$$

which is zero, $\hat{a}_{s_1}^\dagger \hat{a}_B \hat{a}_B^\dagger \hat{a}_{s_2}$:

$$\begin{aligned}
&\langle m, m+k, k, N_P | \hat{a}_{s_1}^\dagger \hat{a}_B \hat{a}_B^\dagger \hat{a}_{s_2} | n, n+l, l, N_{T_1}, N_{T_2} \rangle \\
&= \sqrt{n N_{T_1} ((N_{T_2}+l)(n+1))} \langle m, m+k, k, N_P | n+1, n+l, l-1, N_{T_1}-1, N_{T_2}+1 \rangle \\
&\quad m = n+1 \\
&\quad m+k = n+l \\
&\quad k = l-1 \\
&\quad N_{P_1} = N_{T_1} - 1 \\
&\quad N_{P_2} = N_{T_2} + 1
\end{aligned} \tag{A.105}$$

which is zero, $\hat{a}_{s_1}^\dagger \hat{a}_B \hat{a}_B^\dagger \hat{a}_B$:

$$\begin{aligned}
&\langle m, m+k, k, N_P | \hat{a}_{s_1}^\dagger \hat{a}_B \hat{a}_B^\dagger \hat{a}_B | n, n+l, l, N_{T_1}, N_{T_2} \rangle \\
&= N_{T_2} \sqrt{N_{T_1}(n+1)} \langle m, m+k, k, N_P | n+1, n+l, l, N_{T_1}-1, N_{T_2} \rangle \\
&\quad m = n+1
\end{aligned}$$

$$\begin{aligned}
m + k &= n + l \\
k &= l \\
N_{P_1} &= N_{T_1} - 1 \\
N_{P_2} &= N_{T_2}
\end{aligned} \tag{A.106}$$

which is zero, $\hat{a}_B^\dagger \hat{a}_{s_1} \hat{a}_{s_2}^\dagger \hat{a}_{s_2}$:

$$\begin{aligned}
&\langle m, m + k, k | \hat{a}_B^\dagger \hat{a}_{s_1} \hat{a}_{s_2}^\dagger \hat{a}_{s_2} | n, n + l, l, N_{T_1}, N_{T_2} \rangle \\
&= l \sqrt{n(N_{T_1} + 1)} \langle m, m + k, k | n - 1, n + l, l - 1, N_{T_1} + 1, N_{T_2} \rangle \\
&\quad m = n - 1 \\
&\quad m + k = n + l \\
&\quad k = l \\
&\quad N_{P_1} = N_{T_1} + 1 \\
&\quad N_{P_2} = N_{T_2}
\end{aligned} \tag{A.107}$$

which is zero, $\hat{a}_B^\dagger \hat{a}_{s_1} \hat{a}_{s_2}^\dagger \hat{a}_B$:

$$\begin{aligned}
&\langle m, m + k, k, N_P | \hat{a}_B^\dagger \hat{a}_{s_1} \hat{a}_{s_2}^\dagger \hat{a}_B | n, n + l, l, N_{T_1}, N_{T_2} \rangle \\
&= \sqrt{n N_{T_2} (N_{T_1} + 1) (l + 1)} \langle m, m + k, k, N_P | n - 1, n + l, l + 1, N_{T_1} + 1, N_{T_2} - 1 \rangle \\
&\quad m = n + 1 \\
&\quad m + k = n + l \\
&\quad k = l + 1 \\
&\quad N_{P_1} = N_{T_1} + 1 \\
&\quad N_{P_2} = N_{T_2} - 1
\end{aligned} \tag{A.108}$$

which is zero, $\hat{a}_B^\dagger \hat{a}_{s_1} \hat{a}_B^\dagger \hat{a}_{s_2}$:

$$\begin{aligned}
&\langle m, m + k, k, N_P | \hat{a}_B^\dagger \hat{a}_{s_1} \hat{a}_B^\dagger \hat{a}_{s_2} | n, n + l, l, N_{T_1}, N_{T_2} \rangle \\
&= \sqrt{nl(N_{T_1} + 1)(N_{T_2} + 1)} \langle m, m + k, k, N_P | n - 1, n + l, l - 1, N_{T_1} + 1, N_{T_2} + 1 \rangle \\
&\quad m = n + 1 \\
&\quad m + k = n + l \\
&\quad k = l - 1
\end{aligned}$$

$$\begin{aligned}
N_{P_1} &= N_{T_1} - 1 \\
N_{P_2} &= N_{T_2} + 1
\end{aligned} \tag{A.109}$$

which is zero, $\hat{a}_B^\dagger \hat{a}_{s_1} \hat{a}_B^\dagger \hat{a}_B$:

$$\begin{aligned}
&\langle m, m+k, k, N_P | \hat{a}_B^\dagger \hat{a}_{s_1} \hat{a}_B^\dagger \hat{a}_B | n, n+l, l, N_{T_1}, N_{T_2} \rangle \\
&= N_{T_2} \sqrt{n(N_{T_1} + 1)} \langle m, m+k, k, N_P | n-1, n+l, l, N_{T_1} + 1, N_{T_2} \rangle \\
&\quad m = n - 1 \\
&\quad m + k = n + l \\
&\quad k = l \\
&\quad N_{P_1} = N_{T_1} + 1 \\
&\quad N_{P_2} = N_{T_2}
\end{aligned} \tag{A.110}$$

which is zero. which is zero, $\hat{a}_B^\dagger \hat{a}_B \hat{a}_{s_2}^\dagger \hat{a}_{s_2}$:

$$\begin{aligned}
&\langle m, m+k, k | \hat{a}_B^\dagger \hat{a}_B \hat{a}_{s_2}^\dagger \hat{a}_{s_2} | n, n+l, l, N_{T_1}, N_{T_2} \rangle \\
&= l N_{T_1} \langle m, m+k, k | n, n+l, l, N_{T_1}, N_{T_2} \rangle \\
&\quad m = n \\
&\quad m + k = n + l \\
&\quad k = l \\
&\quad N_{P_1} = N_{T_1} \\
&\quad N_{P_2} = N_{T_2}
\end{aligned} \tag{A.111}$$

which is nonzero, $\hat{a}_B^\dagger \hat{a}_B \hat{a}_{s_2}^\dagger \hat{a}_B$:

$$\begin{aligned}
&\langle m, m+k, k, N_P | \hat{a}_B^\dagger \hat{a}_B \hat{a}_{s_2}^\dagger \hat{a}_B | n, n+l, l, N_{T_1}, N_{T_2} \rangle \\
&= N_{T_1} \sqrt{N_{T_2}(l+1)} \langle m, m+k, k, N_P | n, n+l, l+1, N_{T_1}, N_{T_2} - 1 \rangle \\
&\quad m = n \\
&\quad m + k = n + l \\
&\quad k = l + 1 \\
&\quad N_{P_1} = N_{T_1} \\
&\quad N_{P_2} = N_{T_2} - 1
\end{aligned} \tag{A.112}$$

which is zero, $\hat{a}_B^\dagger \hat{a}_B \hat{a}_B^\dagger \hat{a}_{s_2}$:

$$\begin{aligned}
& \langle m, m+k, k, N_P | \hat{a}_B^\dagger \hat{a}_B \hat{a}_B^\dagger \hat{a}_{s_2} | n, n+l, l, N_{T_1}, N_{T_2} \rangle \\
&= N_{T_1} \sqrt{l(N_{T_2} + 1)} \langle m, m+k, k, N_P | n, n+l, l-1, N_{T_1}, N_{T_2} + 1 \rangle \\
&\quad m = n \\
&\quad m+k = n+l \\
&\quad k = l-1 \\
&\quad N_{P_1} = N_{T_1} \\
&\quad N_{P_2} = N_{T_2} + 1
\end{aligned} \tag{A.113}$$

which is zero, $\hat{a}_B^\dagger \hat{a}_B \hat{a}_B^\dagger \hat{a}_B$:

$$\begin{aligned}
& \langle m, m+k, k, N_P | \hat{a}_B^\dagger \hat{a}_B \hat{a}_B^\dagger \hat{a}_B | n, n+l, l, N_{T_1}, N_{T_2} \rangle \\
&= N_{T_2} N_{T_1} \langle m, m+k, k, N_P | n, n+l, l, N_{T_1}, N_{T_2} \rangle \\
&\quad m = n-1 \\
&\quad m+k = n+l \\
&\quad k = l \\
&\quad N_{P_1} = N_{T_1} + 1 \\
&\quad N_{P_2} = N_{T_2}
\end{aligned} \tag{A.114}$$

which is nonzero.

Appendix B | MATLAB Code

B.1 Tripartite Electric Field Operator Simulation

```
clc
clearvars

rmin = 0.1;
rmax = 6;
countr1 = 0;
countr2 = 0;
%k=.7;
NB=100;
step = .01;
rr1 = rmin:step:rmax;
for k = 0:.1:1
for r1 = rmin:step:rmax
countr1 = countr1+1;
fprintf('%d out of %d\n', countr1,length(rr1));
for r2 = rmin:step:rmax
countr2 = countr2+1;
r = sqrt(r1^2+r2^2);
NS1(countr1,countr2) = sinh(r)^2 * r2^2/r^2;
NS2(countr1,countr2) = sinh(r)^2 * r1^2/r^2;
Ni(countr1,countr2) = sinh(r)^2;
a=1/sqrt(Ni(countr1,countr2)+1);
```

```

b=sqrt((Ni(countr1 , countr2)*NS1(countr1 , countr2)*r^2)/(Ni(
    countr1 , countr2)^2*r2^2+NS1(countr1 , countr2)*r^2));
II(countr1 , countr2)=(a^2*(1+b^2))/((-1+b^2)^2);

S1S1(countr1 , countr2)=(a^2*((1+b^2*(-1+k-2*NB)+2*NB)*r^2+b^2
    *k*(r1^2 - r2^2)))/((-1+b^2)^2 *r^2);

S2S2(countr1 , countr2)=(a^2*((1+b^2*(-1+k-2*NB)+2*NB)*r^2+b^2
    *k*(-r1^2 + r2^2)))/((-1+b^2)^2 *r^2);
sumIS1 = 0;
sumIS2 = 0;
sumS1S2 = 0;
for n=1:20
for l=1:40
sumIS1=sumIS1+k*a^2*b^(2*(n+1)) * (factorial(n+1)/(factorial
    (n)*factorial(1))) * ((r1^(2*n)*r2^(2*l))/(r^(2*(n+1))))
    *(sqrt(n*(n+1))+sqrt((n+1)*(n+1+1)));
sumIS2=sumIS1+k*a^2*b^(2*(n+1)) * (factorial(n+1)/(factorial
    (n)*factorial(1))) * ((r1^(2*n)*r2^(2*l))/(r^(2*(n+1))))
    *(sqrt(l*(l+n))+sqrt((l+1)*(n+1+1)));
sumS1S2=sumS1S2+k*a^2*b^(2*(n+1)) * (factorial(n+1)/(
    factorial(n)*factorial(1))) * ((r1^(2*n)*r2^(2*l))/(r
    ^2*(n+1)))*(sqrt(n*(l+1))+sqrt((l)*(n+1)));
end
end
IS1(countr1 , countr2)=sumIS1;
IS2(countr1 , countr2)=sumIS2;
S1S2(countr1 , countr2)=sumS1S2;
rhold(countr1 , countr2)=r;
end
countr2=0;
end
r1 = rmin:step:rmax;
r2 = rmin:step:rmax;
% imagesc(r1,r2,S1S2./sqrt(S1S1.*S2S2))

```

```

imagesc(r1(1,1:300),r2(1,1:300),S1S2(1:300,1:300)./sqrt(S1S1
    (1:300,1:300).*S2S2(1:300,1:300)));
colorbar;
caxis([0 .4])
%caxis([-1 1]);
title(sprintf('S1 and S2 correlation,  $\kappa = %d$ ', k))
xlabel('$r_1$')
ylabel('$r_2$')

fixfig
figure(2)
imagesc(r1(1,1:300),r2(1,1:300),IS1(1:300,1:300)./sqrt(S1S1
    (1:300,1:300).*II(1:300,1:300)));
colorbar;
caxis([0 .4])
%caxis([-1 1]);
title(sprintf('S1 and I correlation,  $\kappa = %d$ ', k))
xlabel('$r_1$')
ylabel('$r_2$')

fixfig
figure(3)
imagesc(r1(1,1:300),r2(1,1:300),IS2(1:300,1:300)./sqrt(S2S2
    (1:300,1:300).*II(1:300,1:300)));
colorbar;
caxis([0 .4])
%caxis([-1 1]);
xlabel('$r_1$')
ylabel('$r_2$')
title(sprintf('S2 and I correlation,  $\kappa = %d$ ', k))
fixfig

save(sprintf('data k= %d',k));

countr1 = 0;

```

```
end
```

B.2 Tripartite Number Operator Simulation

```
clc
clearvars

rmin = 0.1;
rmax = 1;
countr1 = 0;
countr2 = 0;
%k=.7;
NB=1;
step = .01;
rr1 = rmin:step:rmax;
for k = 0:.1:1
for r1 = rmin:step:rmax
countr1 = countr1+1;
fprintf('%d out of %d\n', countr1,length(rr1));
for r2 = rmin:step:rmax
countr2 = countr2+1;
r = sqrt(r1^2+r2^2);
NS1(countr1,countr2) = sinh(r)^2 * r2^2/r^2;
NS2(countr1,countr2) = sinh(r)^2 * r1^2/r^2;
Ni(countr1,countr2) = sinh(r)^2;
a=1/sqrt(Ni(countr1,countr2)+1);
b=sqrt((Ni(countr1,countr2)*NS1(countr1,countr2)*r^2)/(Ni(countr1,countr2)^2*r2^2+NS1(countr1,countr2)*r^2));

NumI2(countr1,countr2)=-(a^2*b^2*(1+b^2))/(b^2-1)^3;

NumR12(countr1,countr2)=-(a^2*((-1+b^2)^2*NB^2*r^4+b^2*k*r1^2*((k-2*(-1+b^2)*NB)*r^2+b^2*k*(r1^2-(r2^2)))))/((-1+b^2)^3 *r^4);
```

```

NumR22(countr1 , countr2)=(a^2*(-(-1+b^2)^2*NB^2*r^4+b^2*k*r2
^2*((k-2*(-1+b^2)*NB)*r^2+b^2*k*(-(r1^2)+r2^2))))/((-1+b
^2)^3 *r^4);

NumI(countr1 , countr2)=(a^2*b^2)/((b^2-1)^2);

NumR1(countr1 , countr2)=a^2*(((NB)/(1-b^2))+((b^2*k*r1^2)
/((-1+b^2)^2*r^2)));

NumR2(countr1 , countr2)=a^2*(((NB)/(1-b^2))+((b^2*k*r2^2)
/((-1+b^2)^2*r^2)));

NumR1R2(countr1 , countr2)=(a^2*(b^2*k*r1^2*(-1+b^2)*NB*r^2 -
2*b^2*k*r2^2)+(-1+b^2)*NB*r^2*((1-b^2)*NB*r^2+b^2*k*r2
^2)))/((-1+b^2)^3*r^4);

NumIR1(countr1 , countr2)=(a^2*b^2*((((-1+b^2)*NB)/(sqrt(1-k))
)-((1+b^2)*sqrt(k)*r1^2)/r^2)))/((-1+b^2)^3);

NumIR2(countr1 , countr2)=(a^2*b^2*((((-1+b^2)*NB)/(sqrt(1-k))
)-((1+b^2)*sqrt(k)*r2^2)/r^2)))/((-1+b^2)^3);

rhold(countr1 , countr2)=r;
end
countr2=0;
end

II=NumI2-(NumI.*NumI);

S1S1=NumR12-(NumR1.*NumR1);

S2S2=NumR22-(NumR2.*NumR2);

IS1=NumIR1-(NumI.*NumR1);

```

```
IS2=NumIR2-(NumI.*NumR2);
```

```
S1S2=NumR1R2-(NumR1.*NumR2);
```

B.3 Detector Function Simulation

```
clf
```

```
clear
```

```
load 'datak7B100.mat'
```

```
corr = (IS1+IS2)./sqrt((II.*(S1S1+S2S2+2.*S1S2)));
```

```
imagesc(r1(1:300),r2(1:300),corr(1:300,1:300));
```

```
colorbar;
```

```
caxis([0 .45])
```

```
title('Detector Function Correlation,  $\kappa = .4$ ')
```

```
xlabel('$r_1$')
```

```
ylabel('$r_2$')
```

```
fixfig
```

```
corrhold=zeros(length(r1),1);
```

```
r=rhold;
```

```
for i = 1:length(r1)
```

```
  rNew(i)=rhold(i,i);
```

```
  corrhold(i,1)=corr(i,i);
```

```
  Nshold = sinh(rNew).^2;
```

```
end
```

```
Ns=Nshold(1:225);
```

```
plot(Ns,2*sqrt(k*Ns.*(Ns+1))./sqrt((2*k*Ns+2*NB+1).*(2*Ns+1))  
      ), 'linewidth',2);
```

```
hold on
```

```
plot(Ns,corrhold(1:225), 'linewidth',2)
```

```
hold off

legend('Bipartite', 'Tripartite')
grid on
grid minor
ylabel('Correlation', 'FontSize', 15)
xlabel('$N_s$', 'FontSize', 15)
title('Correlation of Tripartite Quantum Radar,  $\kappa =$ 
      .7,  $N_B=100$ ', 'FontSize', 15)
fixfig
```

Bibliography

- [1] LLOYD, S. (2008), “Quantum Illumination,” .
URL <https://arxiv.org/abs/0803.2022>
- [2] LUONG, D., C. W. S. CHANG, A. M. VADIRAJ, A. DAMINI, C. M. WILSON, and B. BALAJI (2020) “Receiver Operating Characteristics for a Prototype Quantum Two-Mode Squeezing Radar,” *IEEE Transactions on Aerospace and Electronic Systems*, **56**(3), pp. 2041–2060.
URL <https://doi.org/10.1109%2Ftaes.2019.2951213>
- [3] BOWELL, R. A., M. J. BRANDSEMA, B. M. AHMED, R. M. NARAYANAN, S. W. HOWELL, and J. M. DILGER (2020) “Electric field correlations in quantum radar and the quantum advantage,” in *Radar Sensor Technology XXIV* (K. I. Ranney and A. M. Raynal, eds.), vol. 11408, International Society for Optics and Photonics, SPIE, p. 114080S.
URL <https://doi.org/10.1117/12.2562749>
- [4] BRANDSEMA, M. J., R. M. NARAYANAN, and M. LANZAGORTA (2020) “Correlation properties of single photon binary waveforms used in quantum radar/lidar,” in *Radar Sensor Technology XXIV* (K. I. Ranney and A. M. Raynal, eds.), vol. 11408, International Society for Optics and Photonics, SPIE, p. 114080Q.
URL <https://doi.org/10.1117/12.2560184>
- [5] CHANG, C. W. S., A. M. VADIRAJ, J. BOURASSA, B. BALAJI, and C. M. WILSON (2019) “Quantum-enhanced noise radar,” *Applied Physics Letters*, **114**(11), p. 112601, <https://doi.org/10.1063/1.5085002>.
URL <https://doi.org/10.1063/1.5085002>
- [6] LANZAGORTA, M. (2012) *Quantum Radar*, Springer International Publishing.
- [7] LOPAEVA, E. D., I. RUO BERCHERA, I. P. DEGIOVANNI, S. OLIVARES, G. BRIDA, and M. GENOVESE (2013) “Experimental Realization of Quantum Illumination,” *Phys. Rev. Lett.*, **110**, p. 153603.
URL <https://link.aps.org/doi/10.1103/PhysRevLett.110.153603>
- [8] BARZANJEH, S., S. GUHA, C. WEEDBROOK, D. VITALI, J. H. SHAPIRO, and S. PIRANDOLA (2015) “Microwave Quantum Illumination,” *Phys. Rev. Lett.*, **114**,

- p. 080503.
 URL <https://link.aps.org/doi/10.1103/PhysRevLett.114.080503>
- [9] SHAPIRO, J. H. (2019), “The Quantum Illumination Story,” .
 URL <https://arxiv.org/abs/1910.12277>
- [10] BOWELL, R. A., M. J. BRANDSEMA, R. M. NARAYANAN, S. W. HOWELL, and J. M. DILGER (2021) “Tripartite correlation performance for use in quantum radar systems,” in *Radar Sensor Technology XXV* (K. I. Ranney and A. M. Raynal, eds.), vol. 11742, International Society for Optics and Photonics, SPIE, p. 117420I.
 URL <https://doi.org/10.1117/12.2588308>
- [11] BRANDEMA, M. and X. SZIGETHY (2023) “Quantum radar: a brief review of current progress and new methods of understanding and signal processing, validated by experimental results,” in *Radar Sensor Technology XXVII*, International Society for Optics and Photonics, SPIE.
- [12] GUHA, S. (2009) “Receiver design to harness quantum illumination advantage,” in *2009 IEEE International Symposium on Information Theory*, pp. 963–967.
- [13] LUONG, D., S. RAJAN, and B. BALAJI (2020) “Quantum Two-Mode Squeezing Radar and Noise Radar: Correlation Coefficients for Target Detection,” *IEEE Sensors Journal*, **20**(10), pp. 5221–5228.
 URL <https://doi.org/10.1109%2Fjsen.2020.2971851>
- [14] ZHANG, W. and R. T. GLASSER (2020), “Coupled Three-Mode Squeezed Vacuum,” .
 URL <https://arxiv.org/abs/2002.00323>
- [15] ZHANG, Z., S. MOURADIAN, F. N. C. WONG, and J. H. SHAPIRO (2015) “Entanglement-Enhanced Sensing in a Lossy and Noisy Environment,” *Physical Review Letters*, **114**(11).
 URL <https://doi.org/10.1103%2Fphysrevlett.114.110506>
- [16] LUONG, D., B. BALAJI, and S. RAJAN (2021) “Biomedical Sensing Using Quantum Radars Based on Josephson Parametric Amplifiers,” in *2021 International Applied Computational Electromagnetics Society Symposium (ACES)*, pp. 1–4.
- [17] HAO, S., H. SHI, C. N. GAGATSOS, M. MISHRA, B. BASH, I. DJORDJEVIC, S. GUHA, Q. ZHUANG, and Z. ZHANG (2022) “Demonstration of Entanglement-Enhanced Covert Sensing,” *Physical Review Letters*, **129**(1).
 URL <https://doi.org/10.1103%2Fphysrevlett.129.010501>
- [18] GUHA, S. and B. I. ERKMEN (2009) “Gaussian-state quantum-illumination receivers for target detection,” *Physical Review A*, **80**(5).
 URL <https://doi.org/10.1103%2Fphysreva.80.052310>

- [19] FOX, M. (2013) *Quantum Optics: An introduction*, Oxford University Press.
- [20] RUSSEK, J. A., M. WÜRTH, W. UTSCHICK, F. BISCHELTSRIEDER, and M. PEICHL (2021) “Performance Considerations for Quantum Radar,” in *2021 International Applied Computational Electromagnetics Society Symposium (ACES)*, pp. 1–4.
- [21] LIU, H., B. BALAJI, and A. S. HELMY (2020) “Target Detection Aided by Quantum Temporal Correlations: Theoretical Analysis and Experimental Validation,” *IEEE Transactions on Aerospace and Electronic Systems*, **56**(5), pp. 3529–3544.
- [22] DAWOOD, M. and R. NARAYANAN (2001) “Receiver operating characteristics for the coherent UWB random noise radar,” *IEEE Transactions on Aerospace and Electronic Systems*, **37**(2), pp. 586–594.
- [23] YANG, H., W. ROGA, J. D. PRITCHARD, and J. JEFFERS (2021) “Gaussian state-based quantum illumination with simple photodetection,” *Opt. Express*, **29**(6), pp. 8199–8215.
URL <https://opg.optica.org/oe/abstract.cfm?URI=oe-29-6-8199>
- [24] ENGLAND, D. G., B. BALAJI, and B. J. SUSSMAN (2019) “Quantum-enhanced standoff detection using correlated photon pairs,” *Physical Review A*, **99**(2).
URL <https://doi.org/10.1103/PhysRevA.99.023828>
- [25] SCULLY, M. O. and M. S. ZUBAIRY (1997) *Quantum Optics*, Cambridge University Press.
- [26] VOURDAS, A. (1989) “Optical signals with thermal noise,” *Phys. Rev. A*, **39**, pp. 206–213.
URL <https://link.aps.org/doi/10.1103/PhysRevA.39.206>
- [27] HELSTROM, C. W. (1969) “Quantum detection and estimation theory,” *Journal of Statistical Physics*.
- [28] GRIFFITHS, D. J. and D. F. SCHROETER (2020) *Introduction to quantum mechanics*, Cambridge University Press.
- [29] ZHUANG, Q. and J. H. SHAPIRO (2022) “Ultimate Accuracy Limit of Quantum Pulse-Compression Ranging,” *Physical Review Letters*, **128**(1).
URL <https://doi.org/10.1103/PhysRevLett.128.010501>
- [30] AHMED, B. M., M. J. BRANDSEMA, R. A. BOWELL, R. M. NARAYANAN, S. W. HOWELL, and J. M. DILGER (2020) “Remote sensing performance enhancement due to quantum + classical cooperative sensor,” in *Radar Sensor Technology XXIV* (K. I. Ranney and A. M. Raynal, eds.), vol. 11408, International Society for Optics and Photonics, SPIE, p. 114080R.
URL <https://doi.org/10.1117/12.2562739>

- [31] BLAKELY, J. N. (2020) “Bounds on Probability of Detection Error in Quantum-Enhanced Noise Radar,” *Quantum Reports*, **2**(3), pp. 400–413.
URL <https://www.mdpi.com/2624-960X/2/3/28>
- [32] TAN, S.-H., B. I. ERKMEN, V. GIOVANNETTI, S. GUHA, S. LLOYD, L. MACCONE, S. PIRANDOLA, and J. H. SHAPIRO (2008) “Quantum Illumination with Gaussian States,” *Physical Review Letters*, **101**(25).
URL <https://doi.org/10.1103/PhysRevLett.101.253601>
- [33] BOWELL, R., M. BRANDSEMA, R. NARAYANAN, S. HOWELL, and J. DILGER (2022) “Comparison of Correlation Performance for Various Measurement Schemes in Quantum Bipartite Radar and Communication Systems,” *Progress In Electromagnetics Research*, **174**, pp. 43–53.

Vita

Rory Howell

Education

Ph.D., Electrical Engineering, The Pennsylvania State University	May 2023
M.S., Electrical Engineering, The Pennsylvania State University	May 2022
B.S., Electrical Engineering, Kansas State University	May 2019

Field of interests and Specialties

My main interest is in optical sensing and design, but I am interested in a variety of other topics also. I have been educated in quantum optics, radar, machine learning, and computer vision with my greatest specialization coming in quantum optics and quantum sensing.

Publications

- Rory A. Howell, Matthew J. Brandsema, Ram M. Narayanan, Stephen W. Howell, Jonathan M. Dilger, "Comparison of Correlation Performance for Various Measurement Schemes in Quantum Bipartite Radar and Communication Systems," Progress In Electromagnetics Research, Vol. 174, 43-53, 2022.
- Rory A. Howell, Matthew J. Brandsema, Bilal M. Ahmed, Ram M. Narayanan, Stephen W. Howell, Jonathan M. Dilger, "Electric field correlations in quantum radar and the quantum advantage," Proc. SPIE 11408, Radar Sensor Technology XXIV, 114080S (23 April 2020); <https://doi.org/10.1117/12.2562749>
- Bilal M. Ahmed, Matthew J. Brandsema, Rory A. Howell, Ram M. Narayanan, Stephen W. Howell, Jonathan M. Dilger, "Remote sensing performance enhancement due to quantum + classical cooperative sensor," Proc. SPIE 11408, Radar Sensor Technology XXIV, 114080R (23 April 2020); <https://doi.org/10.1117/12.2562739>
- Rory A. Howell, Matthew J. Brandsema, Ram M. Narayanan, Stephen W. Howell, Jonathan M. Dilger, "Tripartite correlation performance for use in quantum radar systems," Proc. SPIE 11742, Radar Sensor Technology XXV, 117420I (12 April 2021); <https://doi.org/10.1117/12.2588308>